

https://dspace.org/

Investigation of hydrochemistry and uranium radioactivity in the groundwater of Namaqualand, Northern Cape, South Africa

Leshomo, Joyce Tryphina

2012-06-21
http://hdl.handle.net/10539/11563

Downloaded from a DSpace repository. https://dspace.org/

INVESTIGATION OF HYDROCHEMISTRY AND URANIUM RADIOACTIVITY IN THE GROUNDWATER OF NAMAQUALAND, NORTHERN CAPE, SOUTH AFRICA

By

Joyce Tryphina Leshomo

Student Number: 385927

Degree of Master of Science by research only:

'A dissertation submitted to the School of Geosciences, Faculty of Science, University of the Witwatersrand, Johannesburg, in fulfilment of the requirement for the degree of Master of Science'

Supervisor: Prof Tamiru Abiye

School of Geosciences

Johannesburg, 2011

DECLARATION

I declare that “Investigation of hydrochemistry and Uranium radioactivity in the groundwater of Namaqualand, Northern Cape, South Africa”, is my own, unaided work. It is being submitted for the Degree of Master of Science in the University of the Witwatersrand, Johannesburg. It has not been submitted before for any degree or examination in any other University.

NAME: Joyce T. Leshomo

_____

Signature of Candidate

_____ day of _____ 20____

ACKNOWLEDGEMENT

I would like to thank the Council for Geoscience (CGS) for giving me an opportunity to further my studies and mostly for funding this research.

I also thank the Employees at CGS who made it possible to finish the research by providing assistance and resources when it was needed the most. Especially, Leslie Strachan (for all the support and encouragement), Robert Hansen (for teaching me the geochemical modelling software), Dirk Grobbelaar (for your GIS expertise) to mention but few, your help is highly appreciated.

To Alf Lewin and Frans Minnaar a heartfelt thanks for assisting me with sampling in both extreme hot and cold weather of Namaqualand.

My colleagues, the Water Geoscience Unit Team, I thank all of you for your support and being there for me always.

To the most special beings in my life, Judy, Boitumelo, Kabelo and my Husband (Dan Leshomo) thank you for your support, encouragement, patience and the time I stole from you while busy with the research. I am proud to have you as my family.

A special thank you to my Supervisor, Prof. Abiye who supported, encouraged, pushed and believed in me throughout the research. I am honored to have you as my Supervisor. Thank you!

Finally, to everyone who touched my life throughout the time I worked on this research project, thank you.

ABSTRACT

The demand for groundwater in South Africa has increased over the years, mainly in the arid, semi-arid and rural areas of the country. Groundwater is generally considered a safe and viable option to untreated surface water.

Groundwater samples analyzed were limited to inorganic chemicals, stable isotopes and radiological constituents. Dissolved inorganic constituents and parameters analyzed included major anions and cations, trace metals, and physico-chemical parameters. Inorganic constituents were analyzed to provide basic information pertaining to water chemistry.

The hydrochemistry of the area indicates that groundwater evolution is taking place and dissolution, ion exchange and mixing processes are the driving processes. Br^-/Cl^- ratio show that the salinity in the area is derived from seawater mixing, halite dissolution and atmospheric deposition/sea aerosol spray. Under excessive evaporative regimes, as experience in the study area some of the groundwater is heading towards hypersaline waters.

Isotopes analyses disclosed two groundwater flow types, deep and shallow groundwater flow. The data further revealed groundwater mixing within the aquifer where there is no direct infiltration (the samples have undergone fractionation due to evaporation before infiltration), recharge in the area results from regional flow from the neighboring catchments. . The age of the groundwater calculated from average tritium of the local rainfall of 28.32 TU, ranges from 87.01 to 174.02 years.

Gross alpha and beta emitters were detected in the water samples and are likely attributed to naturally occurring uranium isotopes present in the water. The radioactivity in the area is background activity, i.e. it is very low and is from the rock material.

Uranium occurs in high concentrations in the groundwater of the study area, ranges from 1 µg/l to 146 µg/l, which is above the WHO drinking water standard. Data analysis show that uranium occur as UO_2^+(c), UO_2OH^+, and $U(OH)_5^-$ complexes in the absence of other complexing agents. In the presents of carbonates uranium is found in solution as UO_2^+, UO_2CO_3 and $UO_2(CO_3)_2^{2-}$ and $UO_2(CO_3)_3^{4-}$ complexes.

TABLE OF CONTENTS

Content			Page No.
DECLARATION			ii
AKNOWLEDGEMENT			iii
ABSTRACT			iv-v
TABLE OF CONTESTS			vi-viii
LIST OF FIGURES			ix-xi
LIST OF TABLES			xii
LIST OF ABBREVIATIONS			xiii-xiv
1.	INTRODUCTION		1
	1.1.	Background	1-3
	1.2.	Aims and Objectives	3-4
	1.3.	Site Selection	4
2.	LITERATURE REVIEW		5
	2.1.	Introduction	5-6
	2.2.	Geochemistry of Uranium	7-9
	2.3.	Uranium solubility and mobility	9-12
	2.4.	Release Mechanisms of Uranium from the source rock	12-13
	2.5.	Uranium and Thorium occurrences in Namaqualand	13-14
	2.6.	Uranium aqueous speciation	14-20
	2.7.	Physico-Chemical properties groundwater	20-21
3.	METHODOLOGY		22
	3.1.	Introduction	22
	3.2.	Field Work	22-23
	3.2.1	Water sampling and handling procedure	23-24
	3.3.1.	Soil/Rock sample collection	24-25

TABLE OF CONTENTS

Content		Page No.
3.3.	Lab Analysis	25
3.3.1.	Analysis of anions in aqueous samples using dionex ion chromatograph	25
3.3.2.	Analysis of aqueous samples using (ICPMS)	26
3.3.3.	Analysis of rock samples using multi-acid digest and ICPMS	27
3.4.	Alkalinity test	28
3.5.	Radiological analysis	28-29
3.6.	Environmental isotope analysis	30-31
4.	CASE STUDY	32
4.1.	Introduction	32
4.2.	Location	32-35
4.3.	Climate	36
4.3.1.	General	36
4.3.2.	Precipitation	36-37
4.3.3.	Potential Evaporation	38
4.3.4.	Temperature	38-39
4.4.	Land Use	39-41
4.5.	Geology	41-46
4.6.	Hydrogeology of the area	47
4.6.1.	General	47
4.6.2.	Study Area	47-49
5.	ANALYTICAL RESULTS	50
5.1.	Introduction	50
5.2.	Physico-Chemical of groundwater	50-54
5.3.	Results for chemical parameters	54-65

TABLE OF CONTENTS

Content		Page No.
5.4.	Radiological results	66-69
5.5.	Environmental isotopes results	70-75
6.	DISCUSSION	75
6.1.	Hydrochemistry	75-89
6.2.	Stable Isotopes	89-93
6.3.	Tritium Data	93-95
6.4.	Salinity and recharge/discharge area delineation	95-100
6.5.	Uranium	100-103
7.	CONCLUSIONS	104-105
8.	RECOMMENTATIONS	106
9.	REFERENCES	107-120
	ANNEXTURE A: HYDROCHEMISTRY DATA	121-130

LIST OF FIGURES

Figure Number **Page No.**

Fig 2.1: The effect of chemical speciation on mobility and sorption processes 10

Fig 2.2: Eh–pH diagram showing uranium (IV) and (VI) hydrolytic species in the absence of other complexing ligands (i.e. in pure water). 16

Fig 2.3: Eh–pH diagram showing dominant uranium aqueous species 18

Fig 2.4: Uranium speciation in a system open to the atmosphere 19

Fig 4.1: Locality map of the study area 33

Fig 4.2: Hilly part of the study area, catchment F30A 34

Fig 4.3: Flat part of the study area, catchment D82B 34

Fig 4.4: Average rainfall of catchment F30A 37

Fig 4.5: Average rainfall of catchment D82B 37

Fig 4.6: Average temperature of catchment F30A 38

Fig 4.7: Average temperature of catchment D82B 39

Fig 4.8: Uranium deposits in South Africa showing uranium deposits and occurrence in the study area (Northern Cape Province) 40

Fig 4.9: Diamond workings at Bosluis se Pan and visible salt lying on the surface 43

Fig 4.10: Geology of the F30A Quarternary Catchment 45

Fig 4.11: Geology of the D82B Quarternary Catchment 46

Fig 4.12: Conceptual model of the study area showing groundwater flow between the two catchments 48

Fig 5.1: Salt pan in Bitterputs se Pan in D82B catchment 53

Fig 5.2: A diagram showing nitrate, phosphate and sulphate concentrations 55

Fig 5.3: Diagram illustrating Fluoride and Bromide anion concentration 56

Fig 5.4: Diagram showing uranium concentration in study area 57

LIST OF FIGURES

Figure Number **Page No.**

Fig 5.5: Uranium concentration analysed from the soil of the study area (F30A and D82B Catchments) 58

Fig 5.6: Eh-pH diagram of Chromium in water. 59

Fig 5.7: Eh-pH diagram of Iron in water. 60

Fig 5.8: Eh-pH diagram of Sulphate in water. 61

Fig 5.9: Eh-pH diagram of Uranium in water. 62

Fig 5.10: Eh-pH diagram showing Uranium and Carbonate speciation. 63

Fig 5.11: Activity diagram showing Fe^{++} vs. Sulphate. 65

Fig. 5.12: Distribution map showing tritium sampling points and values in both catchment D82B and F30A. 73

Fig. 5.13: Distribution map showing ^{18}O and ^{2}H sampling points and values in both catchment D82B and F30A. 74

Fig 6.1: Piper diagram for groundwater chemistry in the F30A and D82B Catchments and the control samples 76

Fig 6.2: A Durov plot of the groundwater samples showing geochemical evolution trend 78

Fig 6.3: Na/Cl relationship in the study area 80

Fig 6.4: The control of ions over EC 81-82

Fig 6.5a: Nitrate vs. sulphate diagram 84

Fig. 6.5b: Nitrate vs. chloride diagram 84

Fig. 6.5c: Sulphate vs. chloride diagram 85

Fig 6.6: Plot that depicts processes controlling water chemistry 86

Fig 6.7a: Br^- vs. Cl^- diagram 87

Fig 6.7b: Br^-/Cl ratio vs. $1/Cl^-$ diagram 88

Fig 6.8: Stable isotope plot relative to GMWL (Craig, 1961) and WLMWL 90

Fig 6.9a: $\delta^{18}O$ vs. Sulphate 91

Fig. 6.9b: $\delta^{18}O$ vs. NO_3 91

Fig.6.9c: $\delta^{18}O$ vs. Chloride 92

LIST OF FIGURES

Fig 6.10: TDS vs. $\delta^{18}O$ 93

Fig 6.11: Tritium vs. Chloride 94

Fig 6.12: Salt found on the surface in the Bitterputs se Pan 96

Fig 6.13: Spatial distribution of the Sodium (Na) 97

Fig 6.14: Spatial distribution of the Total Dissolved Solids (TDS) 98

Fig 6.15: Spatial distribution of the Electrical Conductivity (EC) 99

Fig 6.17: Spatial distribution of uranium 103

LIST OF TABLES

Table Number **Page No.**

Table 2.1: Uranium U^{+6} Aqueous Species 15

Table 4.1: Selected Quaternary Catchment properties 35

Table 4.2: Classification of major geological provinces 44

Table 5.1: Physico-chemical water chemistry data 51-52

Table 5.2: Constituents that occur in high concentration in the area 54

Table 5.3: Gross Alpha and Beta Activity of the Filter Residuals 67

Table 5.4: Gross Alpha and Beta Activity of the Liquid Residuals 68

Table 5.5: Results for Environmental Isotopes 75

Table 6.1 Groundwater type presentation of the study area 79

LIST OF ABBREVIATIONS

Aβ-Activity	–	Alpha-Beta-Activity
°C	–	Degrees Celsius
DWAF	–	Department of Water Affairs
EC	–	Electrical Conductivity
Eh	–	Redox Potantial
EPA	–	Environmental Protection Agency
g/l	–	Grams per litre
GMWL	–	Global Meteoric Water Line
^{1}H	–	Hydrogen-1 (Isotope of hydrogen)
^{2}H/ D	–	Hydrogen-2/ Deuterium (Isotope of hydrogen)
^{3}H	–	Hydrogen-3 (Isotope of hydrogen)
He	–	Helium (Isotope of helium)
HDPE	–	High density polyethylene
ICP-MS	–	Inductively Coupled Plasma Mass Spectrometry
KPA	–	Kinetic Phosphorescence Analysis
MDA	–	Minimum detectable activity
mBq/l	–	Millibecquerel per litre
mg/l	–	Milligrams per litre
mS/cm	–	Millisiemens per centimetre
MΩ	–	Milliohms - SI unit for electrical resistance equal to 10^{-3} ohms
NECSA	–	South African Nuclear Energy Cooperation
^{16}O	–	Oxygen-16 (Isotope of oxygen)
^{18}O	–	Oxygen-18 (Isotope of oxygen)
SMOW	–	Standard Mean Oceanic Water
TDS	–	Total Dissolved Solids
TU	–	Tritium Unit
U	–	Uranium
WHO	–	World Health Organisation
WLMWL	–	Windhoek Local Meteoric Water Line

LIST OF ABBREVIATIONS

µg	–	Micrograms per litre
$\delta^{18}O$	–	Oxygen Isotope value (‰)
δ H	–	Oxygen Isotope value (‰)
‰	–	Per Mil

1. INTRODUCTION

1.1 Background

The demand for groundwater in South Africa has increased over the years, mainly in the arid, semi-arid and rural areas of the country (Titus et al, 2009). Groundwater is generally considered a safe and viable option to untreated surface water. However, this is not always the case, as hazardous trace and radioactive constituents can contaminate the groundwater resource. This study will focus on the relationship between groundwater chemistry and the radioactive element (Uranium) occurrences, impacting on groundwater reserves in Namaqualand.

There are many ways in which these elements are introduced into the groundwater namely: geological source (parent rock characteristics), anthropogenic activities, climate, organic and inorganic compounds, redox potential of the soil/water, and pH of the water (Grenthe et al., 1992).

Uranium presents both chemical and radiological hazards in humans (EPA Report, 1999a). Relative to other radioactive elements, natural uranium has a low level of radioactivity because of its extremely long half-life (4.5 billion years). The chemical form of uranium determines its solubility and, thus, transportability in the body fluids as well as retention in the body and various organs. Chemical toxicity of uranium is the principal health concern, because soluble uranium compounds cause damage to renal tissues (WHO, 2006). Water quality has different types of effects on users. These effects range between chronic to acute; reversible to irreversible, and recoverable and irrecoverable conditions (Jordana and Batista, 2004).

Namaqualand area has a population of ± 300 000 dominantly living in villages (Titus, Pers.comm.). They depend on groundwater resource except the ones that

live in major towns and mining towns. The major towns receive their water from the Orange River System. The groundwater in the area is of poor quality with an electrical conductivity of about ± 250 mS/m, which is brackish water.

Toens et al. (1998) published a report which raised some concerns about the radiological quality of drinking water supplied in the Northern Cape region. The study focusing on the Poffadder area in the Northern Cape, found that the uranium concentrations at some boreholes are very high. The hydrochemical analysis also indicated that the groundwater contains high concentrations of arsenic and fluoride as well as elevated levels of radioactivity.

The most important controls of the speciation and mobility of trace or radioactive elements include, amongst others, pH, redox potential (Eh), temperature, surface properties of solids, the abundance and speciation of potential ligands, major cations and anions, the presence or absence of dissolved and/or particulate organic matter, and (micro)biological activity (Langmuir, 1997). Along the flow path if temperature or pH changes, some phases become unstable, solids dissolve and/or the solution may become over saturated on some elements and lead to newly formed minerals. These chemical reactions results in the change of chemical composition of groundwater along the flow path (Fig. 2.1). According to Jordana and Batista (2004), in general, under conditions of high pH, anions and oxy-anions are more mobile whereas most cations are less mobile, while at low pH this tendency reverses.

The occurrence and distribution of radionuclides in groundwater differs due to a number of factors (Langmuir, 1997). Each radioactive element has its own unique chemical characteristics, solubility, mobility and half-life, which may vary from those of the parent isotope (Senior, 1998). This means that the parent and daughter radionuclides in ground water are not usually found together in similar or equal amounts (Zapecza and Szabo, 1986; Senior, 1998; Reynolds et al.,

2003). In addition, they do not decay at a similar rate or produce the same level of radioactivity (Senior, 1998).

The movement of many radionuclides is dependent upon the particular radionuclide's solubility in water (Jordana and Batista, 2004). Hydrolysis reactions can limit the concentration of free radionuclide ions in solution, which means that such situations can lead to precipitation/adsorption, and/or complexation by other ligands (CO_3^{2-}, Cl^-, SO_4^{2-}, NO_3^{2-}, etc., Fig 2.1). Uranium must be oxidized before it is transported into groundwater but once in solution, it can travel great distances (Zapecza and Szabo, 1986).

1.2. Aims and Objectives

The aim of this project is to investigate the relationship of groundwater chemistry and the uranium and their health impact on the groundwater of the two quaternary catchments (F30A and D86B), in Namaqualand.

The specific objectives of this project are to study:

- Trace element occurrences,
- Physico-chemical behaviour of radioactive elements in groundwater,
- Characteristics of groundwater chemistry and radioactive element in different aquifers,
- To identify possible high-risk boreholes in the area, which might pose health risk as a result of consumption of ground water
- To give more information on the macro-chemical quality of selected water resources in the study area.

The following strategy has been used to achieve the aims of this project:

- Desk-top study
- Collection of water and rock or soil samples and analyses for major ions (cations and anions), trace element, uranium and environmental isotopes.

1.3. Site Selection

The selection of the study area was limited by hydrological unit, which is a catchment (quaternary catchment), of the Lower Orange Water Management Area. In selecting the study area certain criteria were of paramount importance. The criteria were:

- Two quaternary catchments were selected where there is sufficient data (number of boreholes samples) to allow for meaningful statistical analysis.
- One of the groundwater uses should be the supply of water for domestic use.
- The catchments selected also have relatively heterogeneous geology for uranium occurrence representative.

The second criterion takes into consideration the groundwater users that are fully dependant on it for basic needs due to low rainfall and arid climatic condition. The last criterion highlights any trend of the groundwater quality that might be worth studying further. For example if there is any noticeable high concentration of a certain element or uranium that associated with a particular rock type.

2. LITERATURE REVIEW

2.1. Introduction

Uranium is a naturally occurring radioactive element found in virtually all rocks, soil, and water. Significant concentration of uranium occur in phosphate rock deposits (Jerden and Sinha, 2003), granite, pegmatites, felsic rocks and minerals such as uraninite in uranium-rich ores (EPA Report, 1999a; Robertson et al., 2003). It also occurs in a variety of minerals, mainly quartz and feldspars (Guthrie and Kleeman, 1986). Uranium has a tendency to increase in abundance towards the more silicic varieties of igneous rocks, this result from the magmatic differentiation series process, a process explained by Bowen reaction series (Allard et al., 1999).

The abundance of uranium has been determined in a number of metamorphic rocks. Uraninite significantly occurs in aluminium rich metamorphic rocks. Quadrivalent uranium (U^{4+}) can occur in hydrothermal veins, but also crystallizes in mesothermal veins at high temperatures (EPA Report, 1999a).

Organic matter is an important reducing agent for uranium. Since organic matter is of biological origin, it exists in sedimentary rocks as fossils, coal, oil and a number of organic minerals and waxes. Also in sedimentary rocks, uranium is deposited by weathering and erosion of the parent rock. Uraninite generally occurs together with coffinite in sedimentary deposits (sandstone, limestone, lignite, etc.). It is also strongly enriched in carbonate-rich rocks (Langmuir, 1978). Uranium has also been found to strongly bind with ligands/humic and fluvic acids. Lenhart et al. (2000) proved that both humic and fluvic acids have strong affinity for uranium, with humic acid forming stronger complexes with slightly greater pH dependence.

The focus of this project will be on igneous and metamorphic rocks of the Namaqualand. An initial study has been done on a number of issues related to fluoride (Motalane and Strydom, 2004; Ncube and Schutte, 2005). Fluoride problems highlighted include bone deformation, stunted growth, etc., to mention but few.

Toens et al. (1998) conducted a study in Namaqualand in the Pofadder area (an area located north-east of the study area). The same study has investigated a relationship between hydrogeological parameters and the high relevance of haematological abnormalities (leukaemia related disease) of long-term residents in the area. The results showed a positive correlation between the elevated levels of uranium and arsenic in groundwater and atypical lymphocyte counts (a proxy of Haematological abnormality).

Andreoli et al. (2006) conducted a study on correlation between U, Th content and metamorphic grade in the western Namaqualand belt. They found out different concentrations of U and Th on different metamorphic terrains (facies). A maximum concentration of 52 ppm of U and 400 ppm of Th was determined from charnokites rocks.

The South African Nuclear Energy Corporation (NECSA) conducted a water-sampling programme in the Northern Cape area in the early 1980's. From the range of elements, uranium was chosen for further analysis because of its high value of up to 297 µg/l in some places.

Raith et al. (2003) found uranium and thorium concentration of up to 1633ppm U and 622ppm Th from the cores and rims of the Leucocratic orthogneiss; in the Namaqualand area.

2.2. Geochemistry of Uranium

Uranium and thorium occur naturally in the environment, as it is found in all rock types in different amounts and forms. The occurrence of uranium and other trace metals in groundwater typically results from natural, physical and chemical processes. Physical processes include those associated with the mineral composition and origin, transport, and deposition of the aquifer material. Chemical processes include the action of water, oxygen, carbon dioxide, and other acidic components that cause the chemical breakdown or dissolution of minerals containing uranium (Brickler and Jones, 1995).

The geochemical behaviour and mobility of Uranium has received extensive study. Uranium is found in U^{2+}, U^{3+}, U^{4+}, U^{5+} and U^{6+} redox state, but only uranium U^{4+} and U^{6+} are stable in all geological environments (Meinrath, 1998; EPA, 1999b). As U^{2+}, U^{3+} easily oxidize to U^{4+} under most reducing environment and U^{5+} easily change to U^{4+} and U^{6+} under certain conditions. Uranium is found in U^{4+} states (immobile state) in a rock and in a more reducing environment. Once released in the presence of oxygen uranium changes to U^{6+} oxidation state (the mobile state). In the presence of oxygen uranium will oxidize (corrode) to U^{4+}, this oxidation is shown by the following reaction, where U is elemental uranium and UO2 is U^{4+}:

$U + O_2 \rightarrow UO_2$

Depending on environmental conditions, further oxidation may form U^{6+}, shown here as UO_2^{2+}:

$UO_2 + 2\ H+ + ½\ O_2 \rightarrow UO_2^{2+} + H_2O$

In the absence of oxygen, uranium can be oxidized by water, releasing hydrogen gas, as shown by the following reactions:

$U + 2\ H_2O \rightarrow UO_2 + 2\ H_2$

$U + 3\ H_2O \rightarrow UO_2^{2+} + 3\ H_2$

The oxidation rate of uranium depends on several factors including fragment size, pH, humidity, soil moisture content, soil chemistry and oxygen content.

Uranium is present as U^{6+} and U^{4+} in typical subsurface environments. Once oxidized, an enormous variety of uranyl phases can precipitate from groundwater solutions, including phosphates, silicates, oxyhydroxides, sulphates, arsenates, vanadates and carbonates (Allard et al., 1995).

Generally, the occurrence and chemical speciation of uranium in groundwater are determined by:

- hydrogen ion availability (defined by pH),
- the presence and concentrations of inorganic ligands such as carbonate, sulphate, sulphide, and chloride,
- the presence and concentrations of organic complexing agents (primarily humic and fulvic acids),
- free electron availability, and
- the ionic strength and cation distribution of the water (Allard et al., 1995).

The chemical composition of groundwater is the combined results of water that infiltrates through to the aquifer and reactions with minerals present in the soil or rock that may modify the water composition (Jordana and Batista, 2004). The chemical constituent of groundwater primarily depends on the hydrochemical processes and mineral composition of infiltrating water and host rock.

The concentrations of contaminants in sediment pore water and groundwater are controlled primarily by the amount of contaminant present at the source; rate of release from the source; hydrologic factors such as dispersion, advection, and dilution; and a number of geochemical processes including oxidation/reduction, aqueous speciation, adsorption/desorption, and precipitation/dissolution (Raith et al., 2003).

In the year 1999, an extensive compilation of detailed reviews on the mineralogical, geochemical, and environmental behaviour of uranium was published in Burns and Finch (1999). The review by Langmuir (1978) and an

updated discussion in Langmuir (1997) are particularly noteworthy. Grenthe et al. (1992) and Grenthe et al. (1995) have published an extensive, critical review of the thermodynamics of uranium.

Hsi and Langmuir (1985) gave surface properties of amorphous iron oxyhydroxide, goethite and haematite, providing sorption constants for uranium hydroxide and carbonate species onto goethite. The authors noted that the adsorption process is not entirely reversible, desorption kinetics tending to be slower. The constants derived from their work are often quoted, particularly in the waste disposal literature (Waite et al., 1994).

Uranium can be removed very effectively from solution by organic matter. Although the processes are not fully understood, it is generally believed that U(VI) species are initially complexed by carboxylic groups on the organic molecule (Grenthe et al. 1995). The reversibility of the process was studied by Read et al. (1993) who demonstrated that release to solution could only be affected by lowering the pH.

2.3. Uranium Solubility and Mobility

Given the inhomogeneous and highly complex chemical, biological, and physical properties of soil, rocks, groundwater, and surface water, it has been found that predicting the mobility of radionuclides is far complicated (Langmuir, 1997). In real systems there may be chemical and biological processes that will occur which affect the mobility of contaminants. These processes may themselves be changing over space and time, which would further complicate efforts to predict radionuclide transport. Modeling has shown that processes such as adsorption, precipitation, dissolution and desorption can affect mobility of radionuclides (Reynolds et al., 2003).

There may also be more pathways by which the radionuclides can move than can be expected Lekhov and Shvarov, 2002). For example, some actinides and

other transuranics can adsorb onto very small particles known as colloids. These particles are so small that they can move with the groundwater or surface water and thus mobilize contaminants that would otherwise have been considered to be insoluble and tightly held by the soil or sediments. The rate at which the radionuclides move depends on the soil or rock pore spaces and the groundwater velocity (Lekhov and Shvarov, 2002).
Contrary to the case of groundwater, the amount of natural radioactivity in surface water is typically low (EPA Report, 1999b).

Fig 2.1 shows the effect of chemical speciation of uranium on mobility and sorption processes.

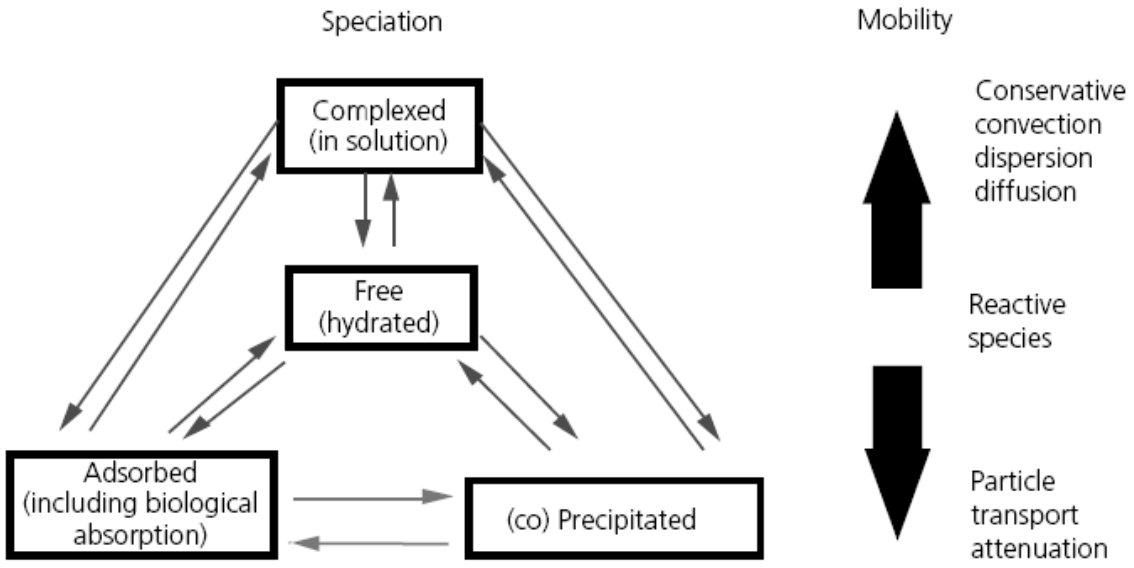


Figure 2.1: The effect of chemical speciation on mobility and sorption processes adapted from Bourg (1988). In the case of uranium, complexed species are often particularly mobile due to the formation of oxy-anion complexes with zero or negative charges.

Uranium migration in natural aqueous systems is an ongoing concern in environmental research. Sorption interactions with soils, sediments and rocks are important mechanisms for understanding uranium mobility in the environment.

Uranium immobilization is possible due to reduction of U (VI) to U (IV), adsorption or co-precipitation. Under oxidizing environmental conditions, uranium typically occurs in the hexavalent form as the mobile, aqueous uranyl ion (UO_2^{2+}) (Langmuir, 1978).

Uranium is most soluble in carbonate / bicarbonate-rich oxidizing groundwater with low total dissolved solids (TDS) content (EPA, 2000b). Uranium sorption to aquifer and soil materials decreases with increasing carbonates/bicarbonates concentration in solution (Hsi and Langmuir, 1985). This results from the formation of negatively charged uranium-carbonate complexes.

Uranium is easily dissolved and transported in oxidizing groundwater due to the presence of oxygen; hence, it can be transported far away from its original emplacement (Bucur et al., 2006). In addition, in phosphate- and fluoride-rich waters uranium solubility is enhanced as it becomes more soluble and gets into solution. Contrary to above, it is immobile in reducing groundwater and it tends to adsorb strongly onto humic substances in the aquifer or colloids (Crançon and van der Lee, 2003; Křepelová et al., 2006).

In deeper environments, mobility and attenuation of uranium are controlled by the composition of fracture coatings and water chemistry. Where uranium is highly mobile, water resources may be more vulnerable to contamination. The mobility of depleted uranium (DU), a by-product of the nuclear power generation process, in the near-surface environment will be controlled by the local environment of the penetrator which may lead to corrosion and dissolution, and factors such as the pH of soil minerals and water, and the sorption potential of soil minerals
Uranium is present as a positively charged uranyl ion UO_2^{2+} in low pH conditions and is very mobile (Hsi and Langmuir, 1985).

Radionuclides can also be transported by diffusion and advection (Bucur et al., 2006). By diffusion the radionuclide move from the areas of higher concentration

to the areas of lower concentration in the aquifer, this process will continue as long as the concentration gradient exists. Convection process occurs when flowing groundwater carries dissolved solutes with it along a flow path at different rate due to the difference in the aquifer media. This result in a contaminant plume which spreads along the direction of the flow path typically referred to longitudinal dispersion (Bucur et al., 2006).

2.4. Release Mechanisms of Uranium from the Source Rock

Physical characteristics of the host rock and the contained minerals help to determine the weathering of the mineral from the rock (e.g. grain size, growth habit and mineral association). Uranium is found in three ways in the source rock (Guthrie and Kleeman, 1986; Gueniot et al., 1988) namely: background, resistate and interstitial modes.

- Background uranium is found in minerals which are very unstable, these are; fine fractures in quartz, hornblende, feldspar, biotite, amphibole, etc.;
- Resistate uranium is found in minerals which are more resistant to weathering, these are; zircon, sphene, allanite, monazite, apatite, magnetite, ilmenite, fluorite (with zircon being the predominant uranium carrier); and
- Interstitial uranium is found in grain boundaries, along cleavages and fractures, in the crystal lattice and along the grain boundaries of clay minerals, amorphous Fe, Ti, Mn-oxides and hydroxides (Gueniot et al., 1988; Yeliseyeva and Omel'yanenko 1988).

Weathering (mainly chemical weathering) and erosion processes as well as topographic and hydromorphic factors are very crucial for the leaching, distribution and dispersion of uranium from the source rock (Gueniot et al., 1988; and Allard, et al, 1999). The concentration of uranium in the environment is

determined by its chemical mobility during the integration of the rock (Tieh et al., 1980).

The interstitial uranium will then further be weathered through ion-exchange and adsorption processes during intense leaching of the host rock. Furthermore, interstitial uranium is more susceptible to oxidation and hydration and will readily be mobilized as disintegration of the rock starts (Frick, 1986).

The release of heavy minerals such as zircon, sphene, etc. due to weathering of the source rock does not mean that the resistate uranium is released from such minerals. Uranium found in accessory minerals is mainly immobile during in-situ weathering and initial erosion of the rock, and then it is released or leached with time (Guthrie and Kleeman, 1986).

Once uranium is released from the source rock, it may occur in the soil profiles depending on the local Eh and pH conditions, it may be further leached into aqueous environment.

2.5. Uranium and Thorium Occurrences in Namaqualand

According to Cole (1998), there are two principal types of uranium deposits in the Northern Cape Province.

- The one associated with granites and pegmatites of the Namaqualand Metamorphic Complex, and,
- Surficial deposit which occur in the form of tertiary to recent fluvial and pedogenic sediments.

The same work also noted that the granite, leucogranites and gneiss of the Namaqualand Metamorphic complex shows anomalously high uranium concentrations.

Pegmatitic and aplitic rocks show near surface secondary enrichment, where uraniferous thorianite ($ThSiO_4$) is a major thorium and uranium-bearing mineral (Cole, 1998). Uranium-bearing pegmatites are found mainly intruding granitic gneiss in the Namaqualand Metamorphic Complex with values of up to 2660 ppm (Cole, 1998). Pegmatites also host a variety of minerals containing thorium together with other base minerals of economic importance (e.g. beryl, colombinte-tantalite lithium and bismuth-bearing minerals, mica, feldspars, etc.) (Frick, 1986).

The Concordia granite hosts higher average uranium content (35 to 70 ppm) as compared to other granites in the area (Cole, 1998). Alaskites has even higher uranium content which is between 20 and 450 ppm (Cole, 1998). The prime uranium-bearing minerals are quartz and alkali feldspar and the other minerals where uranium was found are biotite, zircon, magnetite, monazite, gadolinite, and niobium-tantalum oxide phases (Cole, 1998).

The lacustrine deposits provide uraninite and urano-organic complexes with carnotite being the main uranium mineral (Cole, 1998). The carnotite mineral is said to be derived from the gneiss of the Namaqua Metamorphic Province (Agenbacht, 2007). Other anomalies are associated with the Dwyka Group with uranium values of up to 210 ppm (Cole, 1998). “The uranium is apparently incorporated in apatite crystals within nodules of calcareous mudrock that shows concentrations of up to 950 ppm U” (Cole, 1998). Andreoli et al. (2006) noted an even higher concentration of U and Th from charnokites rocks, 52 ppm and 400 ppm respectively.

2.6. Uranium Aqueous Speciation

Both uranium (U^{4+}) and uranium (U^{6+}) hydrolyze readily with U^{4+} hydrolyzing more than U^{6+}, due to its higher ionic charge (EPA, 1999a). As a result U^{4+} forms strong hydrolytic complexes and sparingly soluble precipitates, which control its

concentrations in groundwater. Dissolution, precipitation and co-precipitation processes are very effective in controlling the concentration of U^{4+} in groundwater under reducing condition (EPA, 1999a).

The group classification in Table 2.1 shows aqueous speciation of uranium at varying pH and Eh conditions. The uranium species are grouped in order of decreasing dominance and stability.

Table 2.1: Uranium U^{+6} Aqueous Species (Adopted and modified from EPA, 1999a)

Groups	Aqueous Species
1	UO_2^{2+}, UO_2OH^+, $UO_2(OH)^o_2$ (aq), $UO_2(OH)^-_3$, $UO_2(OH)^{2-}_4$, $(UO_2)_2OH^{3+}$, $(UO_2)_2(OH)^{2+}_2$, $(UO_2)_3(OH)^{2+}_4$, $(UO_2)_3(OH)^+_5$, $(UO_2)_3(OH)^-_7$, $(UO_2)_4(OH)^+_7$, $U_6(OH)^{9+}_{15}$
2	$UO_2CO^o_3$ (aq), $UO_2(CO_3)^{2-}_2$, $UO_2(CO_3)^{4-}_3$, $UO_2(CO_3)^{5-}_3$, $(UO_2)_3(CO_3)^{6-}_6$, $(UO_2)_{11}(CO_3)_6(OH)^{2-}_{12}$, $UO_2)_{11}(CO_3)_6(OH)^{2-}_{12}$, $(UO_2)2CO_3(OH)^-_3$
3	$UO_2PO^-_4$, $UO_2HPO^o_4$(aq), $UO_2H_2PO^+_4$, $UO_2H_3PO2^+_4$, $UO_2(H_2PO_4)^o_2$(aq), $UO_2(H_2PO_4)(H_3PO_4)^+$
4	UO_2SOo_4(aq), $UO_2(SO_4)2\text{-}_2$
5	UO_2NO+_3
6	UO_2Cl^+, UO_2Clo_2(aq)
7	UO_2F^+, $UO_2F^o_2$(aq), $UO_2F^-_3$, $UO_2F^{2-}_4$
8	$UO_2SiO(OH)^+_3$

The uranyl hydro complexes (group 1), Uranyl carbonate complexes (group 2) and the uranyl phosphate complexes (group 3) occur in a wide pH ranges, with group 1 and 2 being the most common and stable complexes in water depending on the water composition. The uranium sulphate (group 4), nitrate (group 5), chloride (group 6), fluoride (group 7) and silicate (group 8) complexes mainly occur in low pH values (acidic conditions) and are less stable in aqueous solutions.

In the absence of other ligands complexes other than hydroxide, uranium hydrolyses to form mono- and polynuclear complexes. Fig. 2.2 shows that tetravalent uranium (U^{4+}) is stable under reducing conditions and slightly oxidizing conditions at very low pH (< pH 1). Above pH 2, the hydrolysis of U^{4+} is dominated by the neutral species $U(OH)_4^0$(aq). This species occur in a wide pH range in slightly oxidizing to more reducing conditions.

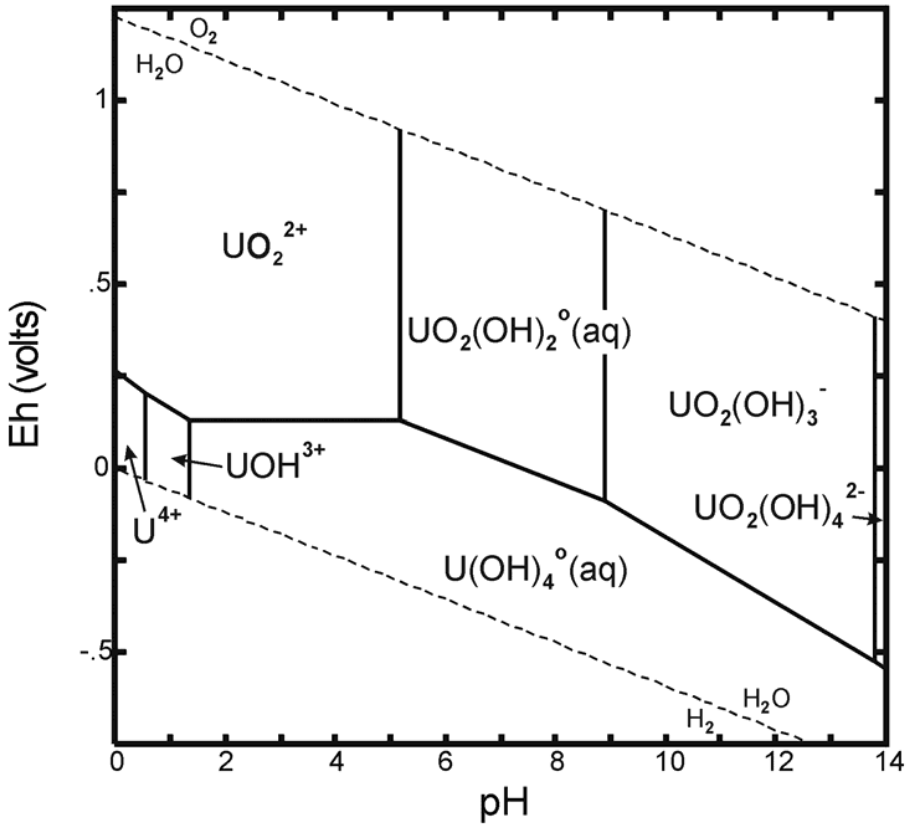


Fig. 2.2: Eh–pH diagram showing uranium (IV) and (VI) hydrolytic species in the absence of other complexing ligands (i.e. in pure water). Diagram was calculated at 25˚C and a concentration of 10-7 mol/L total dissolved uranium (Krupka and Serne, 2002)

In water, at low pH solutions, U^{6+} exists as the uranyl cation (UO_2^{2+}), also at pH less than 5, UOH^{3+} dominates in both slightly reducing and oxidizing waters. Above pH 5, U^{6+} hydrolyses to form hydroxy complexes such as: $UO_2(OH)^+$, $UO_2(OH)_2^0$ (aq), $(UO_2)_3(OH)^{+5}$, etc. (Figure 2.2 and Table 2.1). In more

basic/alkaline environment at pH greater than 8, $UO_2(OH)_3^-$ and $UO_2(OH)_4^{2-}$ is the dominant species (Krupka and Serne, 2002). Figure 2.2 shows the $UO_2(OH)_2^0$ (aq) complex as an expected dominant species at normal groundwater pH ranges of between 7 and 8.

The speciation in Fig 2.3 indicates that $UO_2(CO_3)_2^{2-}$ complex as an expected dominant species at normal groundwater pH ranges of between 7 and 8 (Table 2.1). At pH greater than 3, carbonate complexes dominates other uranium species. In pH 3–5.5 $UO_2CO_3^0$ is the dominant species, in slightly alkaline conditions pH 5.5–8 $UO_2(CO_3)_2^{2-}$ dominates, and in more alkaline environments above pH 8, the polycarbonate $UO_2(CO_3)_3^{4-}$ is the dominant species (Krupka and Serne, 2002). These carbonate complexes are responsible for the mobility of uranium in oxidizing waters.

Fig. 2.3 shows the uranium sulphate complexes.

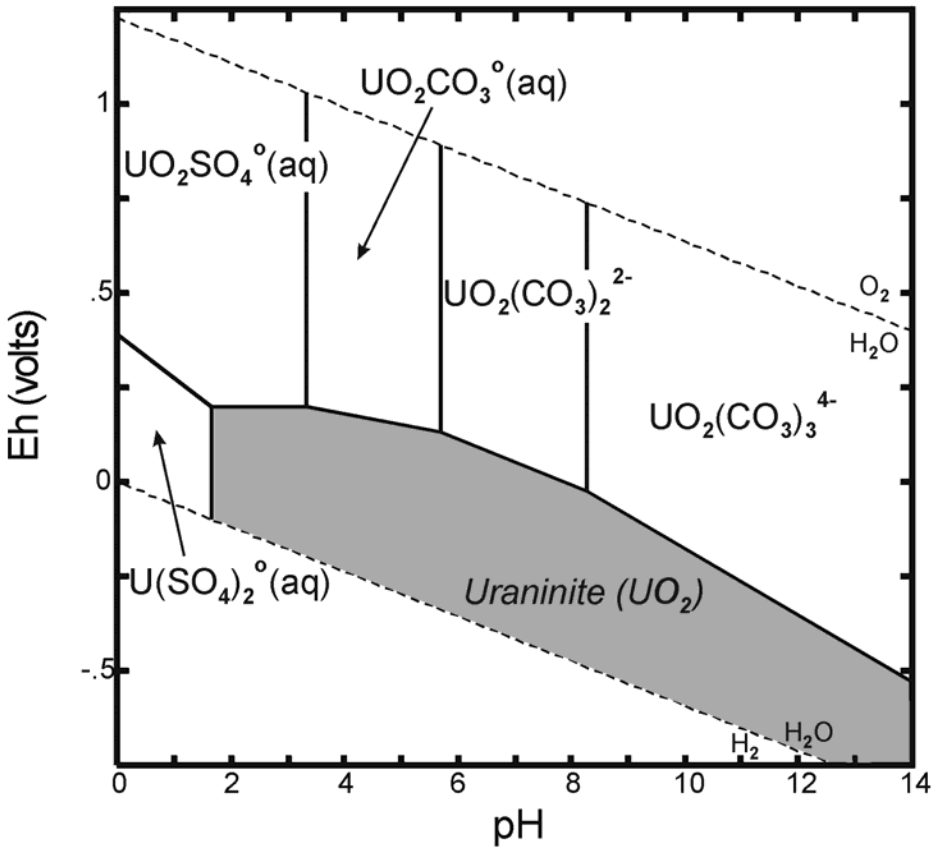


Fig. 2.3: Eh–pH diagram showing dominant uranium aqueous species and the SHADED AREA shows that the solubility of Uraninite has been exceeded. Diagram was calculated at 25˚C and a concentration of 10-7 mol/L total dissolved uranium in the presence of dissolved chloride, nitrate, carbonate, and sulphate (Krupka and Serne, 2002)

At pH lower than 2, the $UO_2SO_4^0$ species dominates. In oxidizing conditions at pH lower than 3, the $UO_2(SO_4)_2^{2-}$ dominates. The shaded area in Fig. 2.3 represent solid uranium mineral (uraninite) which resulted from the precipitation of U^{4+} and/or U^{6+} from oversaturated solution (Krupka and Serne 2002).

Uranium mobility is affected by a number of factors, Fig. 2.4 show uranium mobility in a wide pH range interacting/ mixing with water, phosphate and carbonates.

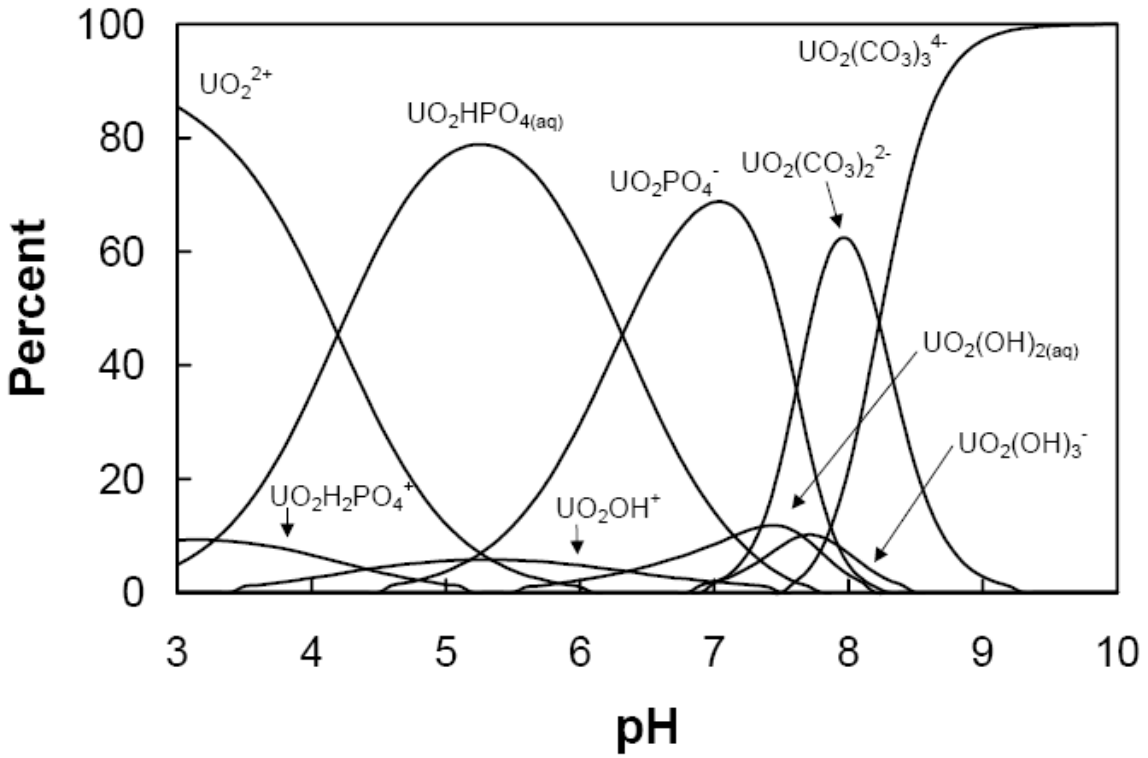


Fig. 2.4: Uranium speciation in a system open to the atmosphere (Pco_2 = 10-3.5 atm), at 0.01 M ionic strength, and with an excess of phosphate ([P]diss = 100 µM) over uranium ([U]diss = 1 µM). No solid phases were considered in the calculation, and species that are never greater than 5% of total uranium are not included (Adopted from Giammar, 2001)

Uranium also forms phosphate complexes in slightly acidic to basic waters from pH 6 to 9 (Fig. 2.4) (EPA, 1999b; Giammar, 2001; Robertson et al., 2003). Under alkaline condition U^{6+} is highly soluble and form stable aqueous carbonate complexes (Siegel and Bryan, 2004). Uranium also forms complexes with the fluoride ions under low pH values (Fig. 2.3). Uranium-fluoride forms several species ranging from UF^{3+} to UF_6^{2+} (EPA, 1999b) (Table 2.1 and Fig. 2.4). In Fig. 2.4 other U^{6+} complexes are plotted as other species between the pH ranges of 3 and 6.4.

Adsorption of natural uranium by chlorite appears to be a kinetically controlled process. Milton and Brown (1987) conducted an experiment on chlorite and

uranium uptake, which showed that uranium reaction with chlorite, was very slow; this may result from the very low cation exchange capacity of the chlorite relative to the amount of uranium originally present in the solution (Siegel and Bryan, 2004).

2.7. Physico-Chemical Properties of Groundwater

The occurrence of natural constituents in groundwater varies greatly depending on the nature of the parent rock and geochemical processes. In arid and semi-arid regions such as the study area, evapotranspiration rates are much higher than other hydrological parameters, low recharge rates, the flow paths take longer to circulate through the geological formations to reach the aquifers and when it does, residence times are much greater (Jordana and Batista, 2004). This culminates to much longer times for natural rock-water interaction. Thus, the major cations and anions composition, spatial distribution and TDS of the groundwater are often variable in such climatic zones. The properties of both the water and the material are, therefore, important and natural groundwater quality varies within aquifers along a groundwater flow path. Groundwater in weathered basement aquifers and alluvial deposits have low pH, and the reducing conditions which can promote the mobilisation of metals and other species of hazardous nature such as uranium (Reynolds et al., 2003). This could be due to shallow groundwater circulation depth in the interstitial pore spaces. Jordana and Batista (2004) outlined climate, topography and geology as three components of the hydrogeological environment that control the parameters of the groundwater flow regime.

Jordana and Batista (2004) stated that:

- Climate controls the amount of water received by a particular area/region
- Topography controls the amount of rain water that infiltrate through and the driving energy for the groundwater flow

- Geology controls the flow path within the system and the geochemistry of water.
- Rock material is predominantly inorganic in nature and contact of flowing groundwater with the rock may dissolve inorganic ions into that water, i.e. dissolution of the rock occurs.

Changes in natural groundwater quality start in the soil, where infiltrating rainfall dissolves carbon dioxide from biological activity in the soil to produce weak carbonic acid that may assist removal of soluble minerals from the underlying rocks. At the same time, soil organisms consume some of the oxygen that was dissolved in the rainfall. In temperate and humid climates with significant recharge, groundwater moves relatively quickly through the aquifer. Contact time with the rock matrix is short and only readily soluble minerals will be involved in reactions. Groundwater in the recharge areas is likely to be low in overall chemical content, i.e. have low major ion contents and low TDS, with igneous rocks usually having less dissolved constituents than sedimentary rocks (Hem, 1989). Based on the composition of the aquifer, for example, in carbonate rocks groundwater has pH above 7 with a mineral contents usually dominated by bicarbonate and calcium.

The biogeochemical behaviour of radionuclides is influenced by both their own physico-chemical properties and by those of the soil or rock with which they interact. The mobility of the radionuclides changes in physico-chemical characteristics during transport and deposition. During mobilization along a pathway further reactions can occur as the radionuclides equilibrate (Hem, 1989). These include immobilization by ion exchange and precipitation/adsorption and remobilization by complexing and dissolution.

3. METHODOLOGY

3.1. Introduction

This project mainly focuses on characterizing the groundwater resource of two quaternary catchments (F30A and D82B) in Namaqualand, Northern Cape with special emphasis to Uranium concentration and transport. The investigation begin with detail background information on theoretical aspects of Uranium genesis, geochemistry and transport, brief overview of local Scio-economy and introducing local site condition including geology, topography, climate, hydrogeology and surface water conditions. The methodologies applied in the investigation include assessment of analytical, radiological and stable isotope data and relating the information with local site information. A number of commercial software codes (ArcGIS®, Aquachem®, GeochemWorkbench®) were used to present the data and make the interpretation easy. The thesis also incorporate discussion of the result and summary of the results including recommendations to show how the current information can be developed to benefit local communities with additional information in future.

3.2. Field Work

Field data collection was conducted in the quaternary two catchments selected for the study, in Namaqualand. Boreholes were randomly selected for water sampling using borehole information from the Atomic Energy Board data of the early eighties. Fifty-seven samples were collected from boreholes fit with pumps and wind pump taps in Namaqualand. Water samples were collected from the boreholes currently used for human and animal consumption, as there is more than one borehole per farm. The other boreholes are used for livestock.

In the Kalkvlei (JL 07/01) and Vaalkoie (JL 07/04) Farms water samples were collected from the base of the tap – directly from the borehole. In Bitterputs3 (JL

07/02) Farm water samples were collected from a tank, 2.5 meters from the borehole. In Koppieskraal (JL 07/03) Farm and other farms water samples were collected from a tap directly from the borehole (see farm location in Fig 4.11). Rock or soil sample was collected around each borehole, with one soil sample collected from a newly dug borehole in order to establish the U distribution at shallow depth within the weathering profile.

3.2.1 Water Sampling and Handling Procedures

Before the samples were collected the sample bottles and the physical properties testing equipment were rinsed with a mixture of water and disinfectant solution, then with the borehole water only. This process was practiced before sampling in each borehole.

Alkalinity test: The sampling procedure was performed based on the specific purpose of the analyses. Briefly the sampling used is shown as follows: a 100ml, *HDPE, brown, plastic bottle was used. The bottles were filled to the top to prevent introducing oxygen into the water. Original samples were not being filtered or acidified, in order to keep the alkalinity as constant as possible. Filtering could cause possible de-gassing. The samples were kept cooled in the dark place.

Cations Analysis: a 100ml, glass bottle was used. The samples were filtered on site with 0.45µ filters. The samples were acidified immediately with HNO_3 acid to keep the metals dissolve and prevent precipitation. They were also kept cool in a dark place.

Anions Analysis: a 100ml, *HDPE, brown, plastic bottle was used. The samples were filtered on site with 0.45µ filters and kept cool in the dark place. Samples were not acidified. The above sampling procedure was carried out as outline by Weaver et al, (2007).

Isotopes Analysis: The sampling procedure was carried out as per the Lab's (iThenba Lab) requirement. 5l, *HDPE plastic bottles were used. After sampling the bottles were kept in the cool, dark place. The Maximum holding time for the samples was approximately one week.

- HDPE = High density polyethylene

Uranium Analysis by KPA Method: The sampling procedure was carried out as per the Lab's (NECSA) requirement. 2.5l, *HDPE plastic bottles were used. After sampling the bottles were kept in the cool, dark place. The Maximum holding time for the samples was approximately one week.

The physical properties: (pH, EC, Temperature, TDS, Redox, and Salinity) were measured on site. For each sample, a form was filled out in the field. Sample bottles were properly labelled to identify each specific sample.

Immediately after sample collection, samples were placed in a refrigerator and transported for temporary storage. The samples were sent to Pretoria where it was kept safely in the refrigerator at the Council for Geoscience over the weekend. The following week the samples were sent to the Council for Geoscience Geochemical Lab for major cations and trace element, anions and rock and soil samples analysis. The 5l bottle samples were sent to NECSA (South African Nuclear Energy Cooperation) Nuclear Technology and Services Lab for radioactivity analysis. The 2.5l bottles were sent to iThemba Labs for environmental isotope analysis.

3.2.2. Soil/Rock Sample Collection

A total of 57 rock/soil samples were collected next to the borehole for analysis. In case where there were no rocks where the area is flat and completely covered by soil, soil samples were collected instead. A small trench of 10-15 centimetres

was dug before collecting the soil sample. In some instances the soil samples were collected from a freshly drilled borehole. The soil or rock samples were collected to determine the chemical composition in order to compare it with the chemistry of the groundwater.

3.3. Lab Analysis

3.3.1. Analysis of anions in aqueous samples using dionex ion chromatograph

(a)Instrumentation

Anions were analysed using a Dionex QIC Ion Chromatograph, equipped with an automated sampler and an IonPac AG4A guard column and IonPac AS4A analytical column. A carbonate/bicarbonate eluant was used with a weak sulphuric acid regenerant solution.

(b) Sample Preparation and Analysis

The water samples were diluted with Ultra-pure water (18.2 MΩ) and analysed for the anions F, Cl, NO_2, Br, NO_3, PO_4 and SO_4. The dilution, which normally ranges between 7 and 100 times depends on the specific sample's concentration of analyses so that the conductivity peak heights fell within the detection range of the chromatograph.

Calibration standards were prepared using calculated amounts of ultra-pure salts (NaF, NaCl, $NaNO_2$, KBr, $NaNO_3$, KH_2PO_4 and K_2SO_4) that were oven-dried overnight, accurately weighed and dissolved in ultra-pure water (18.2 MΩ). Aliquots of these solutions were further diluted to obtain the required calibration solution that has 2 ppm F, 5 ppm Cl, 5 ppm NO_2, 20 ppm Br, 20 ppm NO_3, 30 ppm, PO_4 and 30 ppm SO_4.

3.3.2. Analysis of water samples using Merckvi calibration standard and inductively coupled plasma mass spectrometry (ICP-MS)

(a) Instrumentation

A Perkin Elmer ELAN® DRC II ICP-MS system, equipped with a Meinhard nebulizer and a Cyclonic quartz spray chamber, was used in the analyses. Samples were introduced via Tygon® peristaltic pump tubing on a Perkin Elmer AS93 Plus autosampler, using a Type F autosampler tray capable of holding 148 sample vials of 16 ml each.

The ICP-MS was optimized according to the manufacturer's recommendations (i.e. nebulizer gas flow, mass calibration, lens voltages, dual detector and Autolens TM optimization).

(b) Sample preparation and analysis

An aliquot of sample was diluted in 50ml polypropylene volumetric flasks with ultra-pure water (18.2 MΩ) and acidified with 2% HNO_3 (AR grade). 20ppb indium and 30ppb iridium were added as internal standards. A suitable dilution factor was chosen for the sample's expected TDS and to match the calibration range of the instrument (normally 50 times dilution is sufficient).

The calibration standards were prepared using the MerckVI multi-element standard (containing 30 elements) and single element standard solutions for the major elements. The standards were prepared in 2% (v/v) HNO_3 to match the sample matrix, with 20ppb indium and 30 ppb iridium added as internal standards.

3.3.3. Analysis of rock samples using multi-acid digest and inductively coupled plasma mass spectrometry

(a) Instrumentation

A PerkinElmer SCIEX (Concord, Ontario, Canada) ELAN® 6000 ICP-MS system, equipped with a standard cross-flow nebulizer and a Scott-type Ryton ® double-pass spray chamber, was used in this work. Samples were introduced via Tygon ® peristaltic pump tubing on a Perkin Elmer AS91 autosampler, using a Type F autosampler tray capable of holding 150 sample vials of 16 ml each.

The ICP-MS was regularly optimized according to the manufacturer's recommendations (i.e. nebulizer gas flow, mass calibration, lens voltages, dual detector and Autolens TM optimization).

(b) Sample preparation and analysis

A 0.20 gram portion of milled rock sample was weighed into a Savillex container, and digested with 3 ml HCl, 2ml HNO_3, 1 ml $HClO_4$ and 2 ml HF (all AR grade). The samples were heated on aluminium heating blocks at 110 °C to almost dry, and then at 160 °C until all acid evaporated (overnight). Another 1 ml of $HClO_4$ was added after 24 hours and again evaporated at 160 °C overnight. The residue was then dissolved with 1 ml HNO_3 and 2 drops H_2O_2. 19 ml of 1% HNO_3 was then added, the sample containers was capped and then heated in an oven at 100 °C for 30 minutes. The dissolved samples were diluted again 20 times in polypropylene tubes with Indium and Iridium added as internal standards, and analysed by ICP-MS.

3.4. Alkalinity Test

The alkalinities were analysed with a PC Multidirect photometer based on spectral conversion into concentration pattern of the colour of the solution after a buffer is added. 10 ml water is taken of a sample, and added to the sample analyses vial which must go into the photometer. The sample is then zeroed in the photometer. After zeroing, an Alka-M-photometer tablet is added into the sample and crushed using a clean stirring rod. Care is taken to ensure that the whole tablet is dissolved. The vial is placed in the sample chamber for measurement in mg/l.

3.5. Radiological Analysis

Four water samples were submitted for analysis of their radioactivity content. The radionuclides of interest are NORM's (Naturally Occurring Radioactive Materials) and typically include uranium (U^{238}, U^{235}, U^{234}), thorium (Th^{232}, Th^{230}, Th^{228}, Th^{227}), radium (^{226}Ra, ^{224}Ra, 223Ra), as well as ^{210}Pb and ^{210}Po. Besides the nuclide specific analyses, the samples were also analysed for their gross activity content. Dose calculations, based on the nuclide-specific activity content of the water, were also performed in order to calculate the dosage received by members of the public from this possible source of ingestion.

(a) Initial sample preparation

Filtration and acidification of water

Method: RA-WIN-121

The water sample is filtered and acidified according to the regulations laid down by the National Nuclear Regulator (NNR). Residual liquid fraction analysis.

Gross α-activity counting of liquids

Method: RA-WIN-161

Samples are evaporated to dryness and counted on a low-background gas flow-proportional counter for 5 to 6 hours per sample. A detailed analysis procedure of the above mentioned radionuclides is provided in Table 5.4.

(b) Analysis of the Gross Alpha/Beta-activity of residual liquids and filters

Twenty-two liquid were analysed for Gross Alpha/Beta-activity of residual liquids and filters. Two litres of each sample was filtered using 0.45µm membrane filters. An aliquot of 50ml of each sample was evaporated into a planchette and residues obtained were measured for gross Alpha/Beta.

The method used for analysis is:

RA-WIN-161: Measurement of the gross αβ-activity in evaporated water samples using the Oxford LB instrument

RA-WIN-168: Measurement of the gross αβ-activity of air particulates on filters using the Oxford LB instrument

(c) Analysis of Uranium by Kinetic Phosphorosence Analysis (KPA)

A 1 ml water sample aliquot is mixed with enhancing agent and injected into the KPA cell; Light emitted by uranium when excited by a laser is measured and converted to uranium concentration. Samples with high uranium concentrations are diluted before analysis. Samples containing high levels of interfering substances are either diluted or pre-treated with concentrated nitric acid and peroxide before analysis.

3.6. Environmental Isotope Analysis

Fourteen water samples were analysed for D/H ($^{2}H/^{1}H$), $^{18}O/^{16}O$ and tritium (^{3}H). Water D/H ($^{2}H/^{1}H$) and $^{18}O/^{16}O$ ratios were analysed in the laboratory of the Environmental Isotope Group (EIG) of iThemba Laboratories, Gauteng.

(a) Oxygen Isotopes analysis

The equipment used for stable isotope analysis consists of a PDZ Europa GEO 20-20 gas mass–spectrometer connected to peripheral sample preparation devices. A PDZ water equilibration system (WES), working in dual inlet mode is employed for hydrogen and oxygen isotope analysis of water. Equilibration time for the water sample with hydrogen is about one hour and CO_2 is equilibrated with a water sample in about eight hours. Laboratory standards, calibrated against international reference materials, are analysed with each batch of samples. The analytical precision is estimated at 0.1‰ for O and 0.5‰ for H.

Analytical results are presented in the common delta-notation:

$$\delta^{18}O\ ‰ = \left(\frac{(^{18}O/^{16}O)\ \text{sample}}{(^{18}O/^{16}O)\ \text{standard}} - 1\right) X1000$$

This applies to D/H (2H/1H), accordingly. These delta values are expressed as per mil deviation relative to known standard, in this case standard mean ocean water (SMOW) for $\delta^{18}O$ and δD.

(b) Tritium Analysis

A tritium analysis was conducted for age dating of the groundwater in the area. The samples were distilled and subsequently enriched by electrolysis. The electrolysis cells consist of two concentric metal tubes, which are insulated from

each other. The outer anode, which is also the container, is of stainless steel. The inner cathode is of mild steel with a special surface coating. Some 500 ml of the water sample, having first been distilled and containing sodium hydroxide, is introduced into the cell.

A direct current of some 10–20 ampere is then passed through the cell, which is cooled because of the heat generation. After several days, the electrolyte volume is reduced to some 20 ml. The volume reduction of some 25 times produces a corresponding tritium enrichment factor of about 20. Samples of standard known tritium concentration (spikes) are run in one cell of each batch to check on the enrichment attained.

For liquid scintillation counting samples are prepared by directly distilling the enriched water sample from the now highly concentrated electrolyte. 10 ml of the distilled water sample is mixed with 11 ml Ultima Gold and placed in a vial in the analyzer and counted 2 to 3 cycles of 4 hours. Detection limits are 0.2 TU for enriched samples.

4. CASE STUDY

4.1. Introduction

In Namaqualand, people depend entirely on groundwater except the major towns such as Springbok, Nababeep, Okiep and Kleinzee which have surface water supplies from the Orange River. State and privately owned farms also depend on groundwater for domestic, irrigation and live stock water supply.

Three physiographic regions according to topography, altitude and landforms classify the Namaqualand area (Tankard et al., 1982). These regions are the higher lying Bushmanland Plateau to the east, the Namaqualand highlands (which is the escarpment zone), and the lower lying coastal area to the west (Visser, 1989).

4.2. Location

The study area falls within the Bushmanland area. According to DWAF (2002) the two selected catchments fall in the western part of the Lower Orange Water Management: catchments D82B and F30A. These catchments are between -29˚00´– -30˚30´S latitude and between -18˚00´E and -19˚30´E longitude. The area is between Springbok and Pofadder, and just south of Aggeneys in the Northern Cape (Fig 4.1).

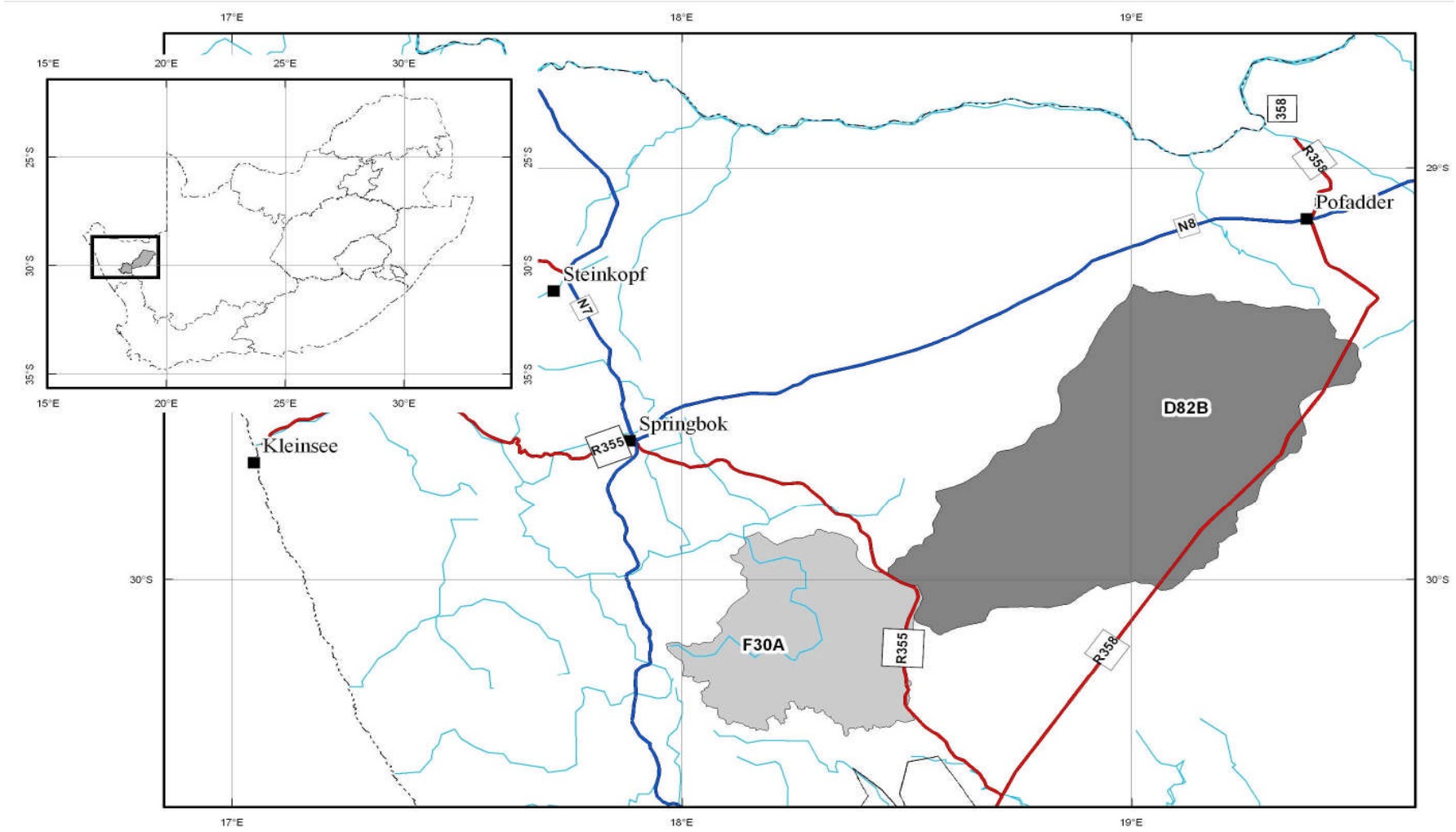


Fig. 4.1: Locality map of the study area.

The F30A catchment is 400–1400 m above sea level and is generally hilly whereas catchment D82B is 800–1200 m above sea level and is considered flat (DWAF, 2001). See Fig 4.2 and Fig 4.3.



Fig. 4.2: Hilly part of the study area, catchment F30A



Fig. 4.3: Flat part of the study area, catchment D82B.

The two catchments (F30A and D82B) covered in the current investigation have been studied by the Department of Water Affairs in the past whereby information regarding areal, aquifer hydraulics and population data are compiled (Table 4.1). The F30A catchment is characterised by a class C soil type (DWAF, 2003). The soil has a moderate depth and is predominantly sandy. Catchment D82B is entirely characterised by class P soil type, which is generally sandy and has a shallow depth with some exposed rocks (DWAF, 2002).

Table 4.1: Selected Quaternary Catchments Properties (From Groundwater Resource Direct Measures; DWAF, 2002)

Quaternary Catchments	D82B	F30A
Area (km^2)	4872.58	1950.89
Area (km^2) within SA	4872.58	1950.89
% Area within SA boundaries	100%	100%
Average Water level (m.bgl)	36.45	22.22
Average Thickness Saturated Weathered Zone (m)	65.37	20.68
Average Thickness Saturated Fractured Zone (m)	132.47	164.96
Average Specific Yield Weathered Zone	0.001076	0.001536
Average Fractured Zone Storativity	0.000021	0.000049
Average Aquifer Storativity	0.000448	0.000368
Volume Weathered Zone of Water (m^3)	301,850,000	75,564,400
Volume Fractured Zone of Water (m^3)	13,986,000	15,860,000
Total Volume Aquifer (m^3)	315,836,000	91,424,400
Recharge (mm)	19.49	5.8527
Population	Not given	2039

4.3. Climate

4.3.1. General

The study area falls in the arid, hot, tropical desert climatic region of South Africa. The F30A catchment area receives winter rainfall and summer rainfall falls at the D82B catchment. Altitude, topography and distance from the sea, and also the change in altitude play a major role in determining the climate of this area. This area is characterised by high evaporation rate caused by high summer temperatures.

4.3.2. Precipitation

The region can be classified as arid to semi-arid, with hilly settings having higher rainfall than the arid lowland which is due to orographic effects. The mean annual precipitation is highly seasonal and occurs dominantly during the winter months (F30A) and summer months (D82B). Rainfall data of 19 years (1990–2008) showing average rainfall in the study area is plotted in Figs 4.4 and 4.5. The data shows that catchment F30A receives slightly more rainfall than catchment D82B.

The average annual rainfall generally increases from west to east until it reaches the escarpment (catchment F30A), and decreases towards the inland (D82B). The area experiences the lowest rainfall in the country with large parts having a mean annual precipitation 200 mm or less. The higher lying areas within the study area receive higher rainfall than the surrounding lower lying areas and coastal plains. An example is part of the Kamiesberg, east of Kamieskroon which receives in excess of 400mm per annum (DWAF, 2002).

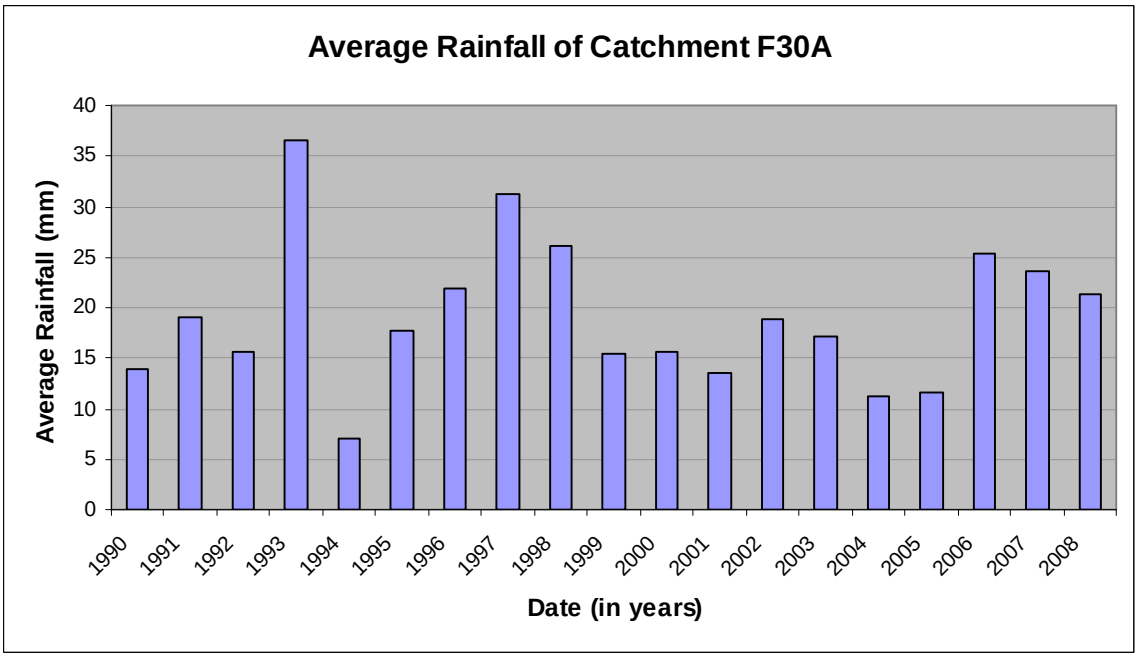


Figure 4.4: Average rainfall of catchment F30A.

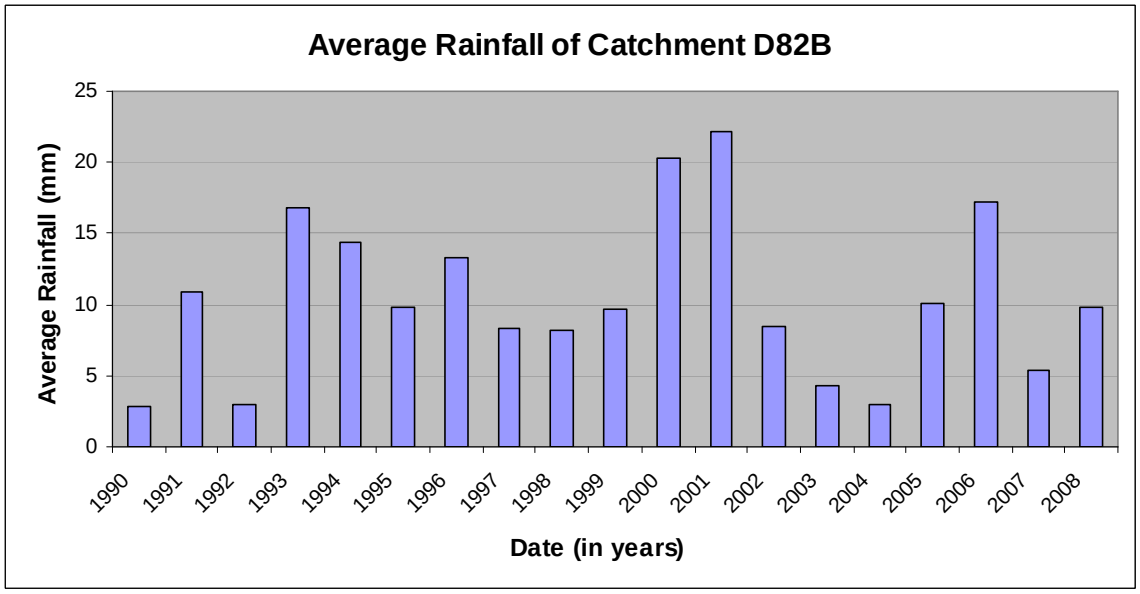


Figure 4.5: Average rainfall of catchment D82B.

4.3.3. Potantial Evaporation

Potantial evaporation can be as much as from 12 to 22 times the precipitation (Titus et al., 2007). Mean Annual Evaporation for both catchments (F30A and D82B) is between 2200-2400 mm/year (as measured by S-pan) (DWAF, 2002).

4.3.4. Temperature

Large variations between the maximum and minimum temperatures, as well as between daily and seasonal temperatures exist for the region (Fig 4.6 and 4.7).

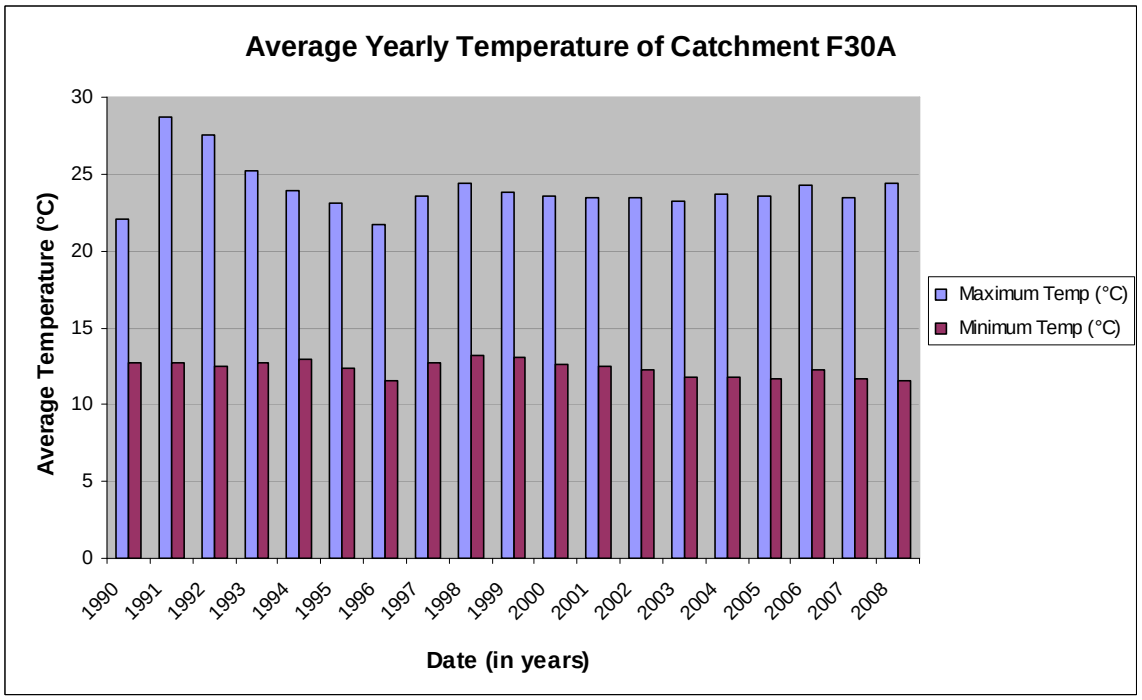


Figure 4.6: Average temperature of catchment F30A

The histograms show the variation between the maximum and minimum temperatures in each catchment and also between the two catchments (Figs 4.6 and 4.7). Catchment F30A has almost uniform maximum temperature of 23/24 °C/year except in 1991, 1992 and 1993 where the maximum temperatures were

higher, 28.7 °C, 27.5 °C and 25.2 °C respectively (Fig 4.6). The minimum temperatures were between 12 and 13 °C.

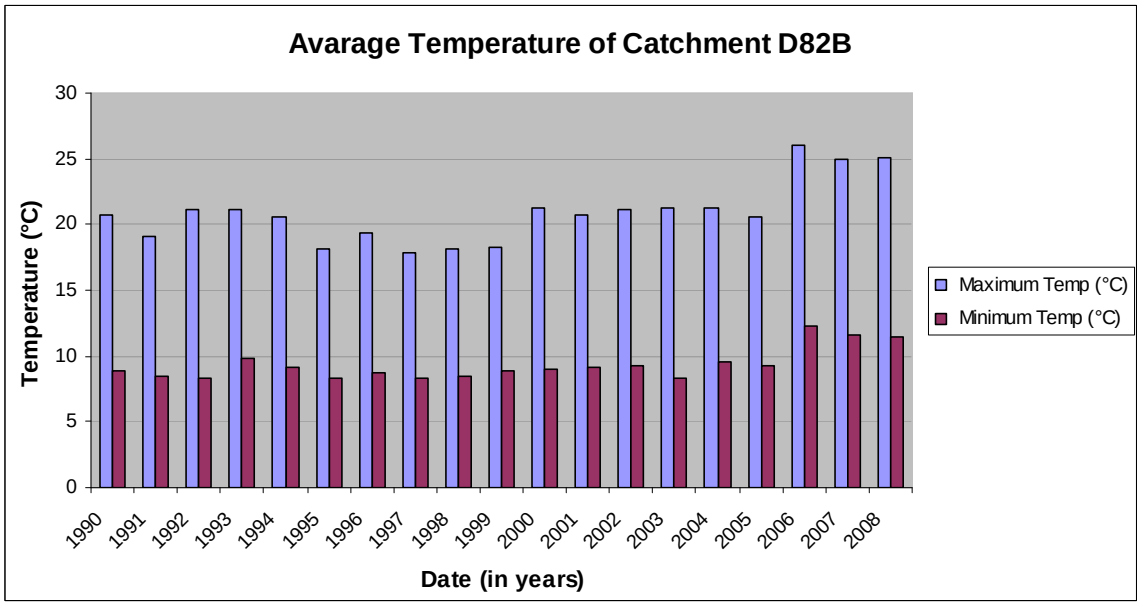


Figure 4.7: Average temperature of catchment D82B

The average maximum temperature in catchment D82B alternated between 21 °C and >20 °C/year from 1990 to 2005. There was an increase in the average maximum temperature in the last three years (2006, 2007 and 2008) to 26 °C, 24.9 °C and 25 °C respectively. This increase was also evident in the minimum average temperature from <10 °C to 12 °C, 11.6 °C, and 11.5 °C respectively.

4.4. Land Use

The study area is situated in the semi-arid area of Namaqualand in the Northern Cape Province, South Africa. In this area people sustain themselves through livestock farming or working on diamond and heavy-minerals mines that occupy most of the region. The area is known to have mining of diamonds, salt (Na) and heavy minerals deposits, some of which are mined in a small scale (Agenbacht, 2007).

Small scale mining observed in the study are concentrated mainly in natural pans shown as P1, P2, P3 and P4 (Fig 4.8) whereas large scale mining opperations occur in the Bosluis se Pan (P2), which is the largest pan in D82B catchment area (Fig 4.8). Minerals that are mined include diamonds which are concentrated in alluvial or “placer” deposits, sulphur, salts, molybdenum, vanadium, uranium, zinc, lead, copper, etc. (Agenbacht, 2007).

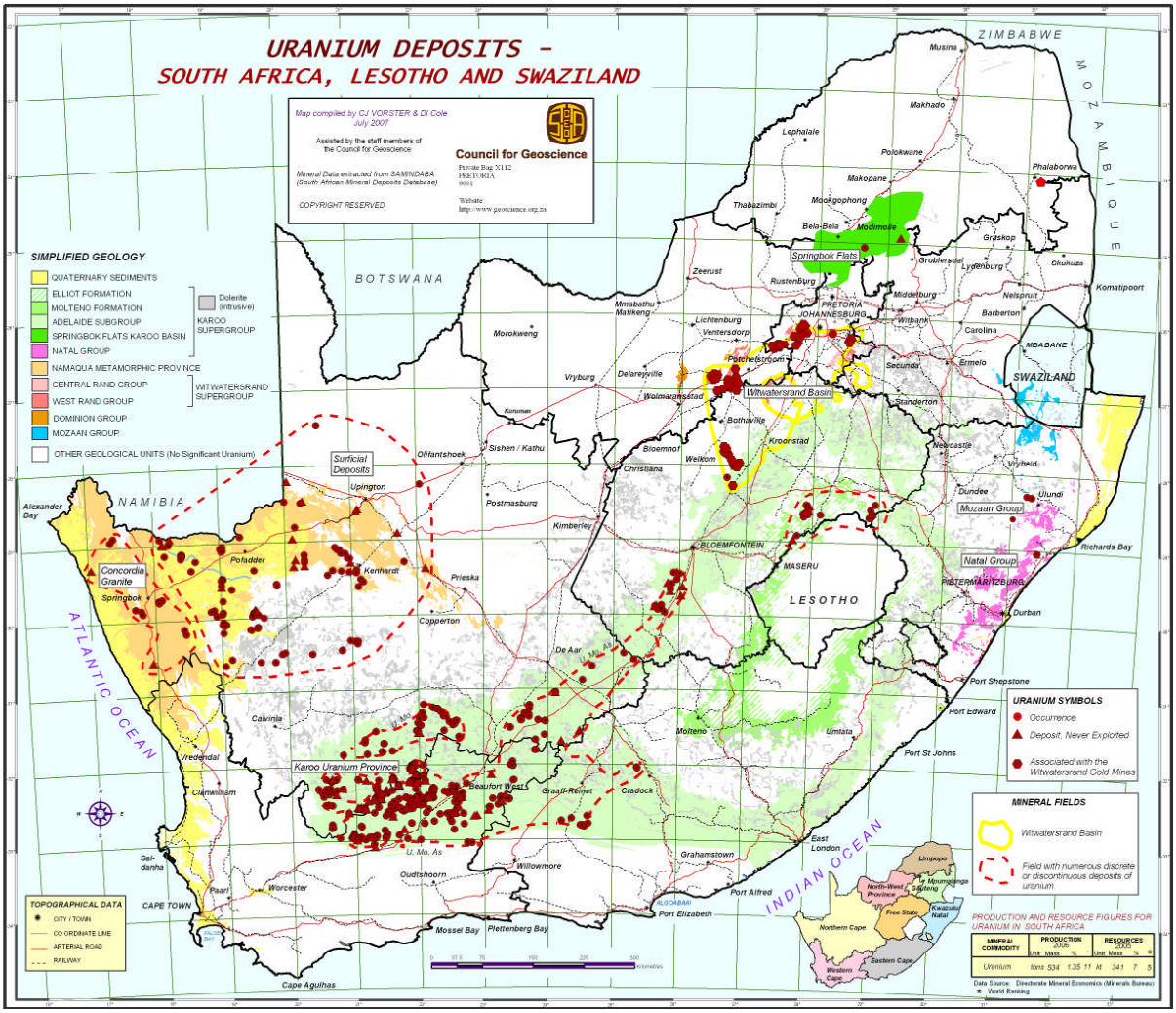


Figure 4.8: Uranium deposits in South Africa showing uranium occurrence and deposits in the study area (Northern Cape Province) (Vorster and Cole, 2007).

The above map Fig 4.8, show uranium occurrence and deposits in South Africa. In Namaqualand in the Northern Cape Province uranium is mined in a small scale because the deposits are discrete or discontinuous (Fig 4.8).

Observed livestock farming in the study area was mainly sheep followed by cattle and goat farming. Sheep farming is common in both catchments, while cattle and goat farming mainly concentrates in the hilly catchment (F30A).

4.5. Geology

The Northwestern Cape Province (i.e. Namaqualand) can be subdivided into three major geological provinces (Tankard et al., 1982). These are the basement rocks of the Namaqua Province (further subdivided into three zones), the volcano-sedimentary rocks of the Gariep Complex (Visser, 1989) in the northwest, and a Phanerozoic cratonic cover (Table 4.2).

The Namaqua Province (Table 4.2) represents most of the crystalline basement in the Northern Cape and southern Namibia (Tankard et al., 1982). In Namaqualand, the margins of the Namaqua Province are largely obscured by younger cover rocks of the Gariep, Nama and Karoo sequences, as well as with Cenozoic surficial sediments to the east and west. In the west and extreme north, rocks of the Namaqua Province and its correlatives are bordered by formations of the late Proterozoic Gariep Complex and in the East abut the Kaapvaal craton with marked structural discordance in both cases (Raith et al., 2003). In the south, rocks of the Nama Group, the Cape Supergroup and the lowermost units of the Karoo Supergroup cover the rocks of the Namaqua Province (Albat, 1984).

Rocks of the Central Zone (Table 4.2) cover most of central Namaqualand and Bushmanland (including parts of northern and eastern Bushmanland) as well as the southwestern parts of southern Namibia (Tankard et al., 1982). The Bushmanland Group consists of granitic gneisses and a metamorphosed

sequence of clastic shallow-water sediments, mafic to felsic volcanic rock, and exhalites (Raith et al., 2003).

The central zone of the Namaqua Province, a complex deformed heterogeneous group of gneisses and intrusions of medium to high grade metamorphism (Tankard et al., 1982) covers most of the Namaqua Province and comprises an assemblage of metasedimentary, metavolcanic and intrusive rocks (Figs 4.2 and 4.3).

Both Catchments are mainly characterised by the sedimentary, volcanic and intrusive rocks of the Kheisian and Namaquan age which is mainly granites and gneisses (Fig 4.10 and 4.11). These rocks are overlain by the intrusive rocks of the Jurassic age, which are covered by the cover rocks/sediments of the Tertiary and Quarternary age. The younger sediments are characterised by alluvium, pan sediments, calcareous and gypsiferous soil, red and grey aeolian sand, and superficial cover sand, rubble and soil in both Catchments with bolder gravel derived from dwyka tillite as an addition in Catchment D82B.



Fig. 4.9: Diamond workings at Bosluis se Pan and visible salt laying on the surface.

Table 4.2: Classification of major geological provinces (after Tankard et al, 1982 and Visser, 1989), taken from (Titus et al, 2009)

Geological Province		Group	Age	Locality	OROGENIES & Subprovinces
Cover Rocks		Sand, Alluvium and Calcrete Karoo Group 1. Prince AlbertForm 2. Dwyka Formation Nama Group 1. Kuibis Formation 2.Schwarzrand Formation	Late Phanerozoic (Cenozoic) Early Phanerozoic (Middle/Late Palaeozoic) Late Proterozoic (Late Namibian)	Along coast. Most of Western Bushmanland Southeastern corner of Namaqualand Isolated strip north of Springbok	
		Gariep Complex Six Formations	Late Proterozoic (Early/Middle Namibian)	Central and Western Richtersveld	PAN-AFRICAN Gariep Sub-province
Namaqua Province	Central Zone	Namaqua Metamorphic Complex, (or Province)	Middle Proterozoic (Middle Mokolian)	Most of Namaqualand and parts of Bushmanland	NAMAQUAN Bushmanland & Gordonia Subprovinces
	Western Zone	Vioolsdrif Intrusive Suite	Middle Proterozoic (Early Mokolian)	North-eastern and Eastern Richtersveld. Northern Namaqualand	EBURNIAN Richtersveld Subprovince
		Orange River Group	Middle Proterozoic (Early Mokolian)	North-eastern part of Richtersveld	
	Eastern Zone			Upington	

Fig. 4.10 and Fig.4.11 are a contribution of this work with the base map sourced from the Council for Geoscience database.

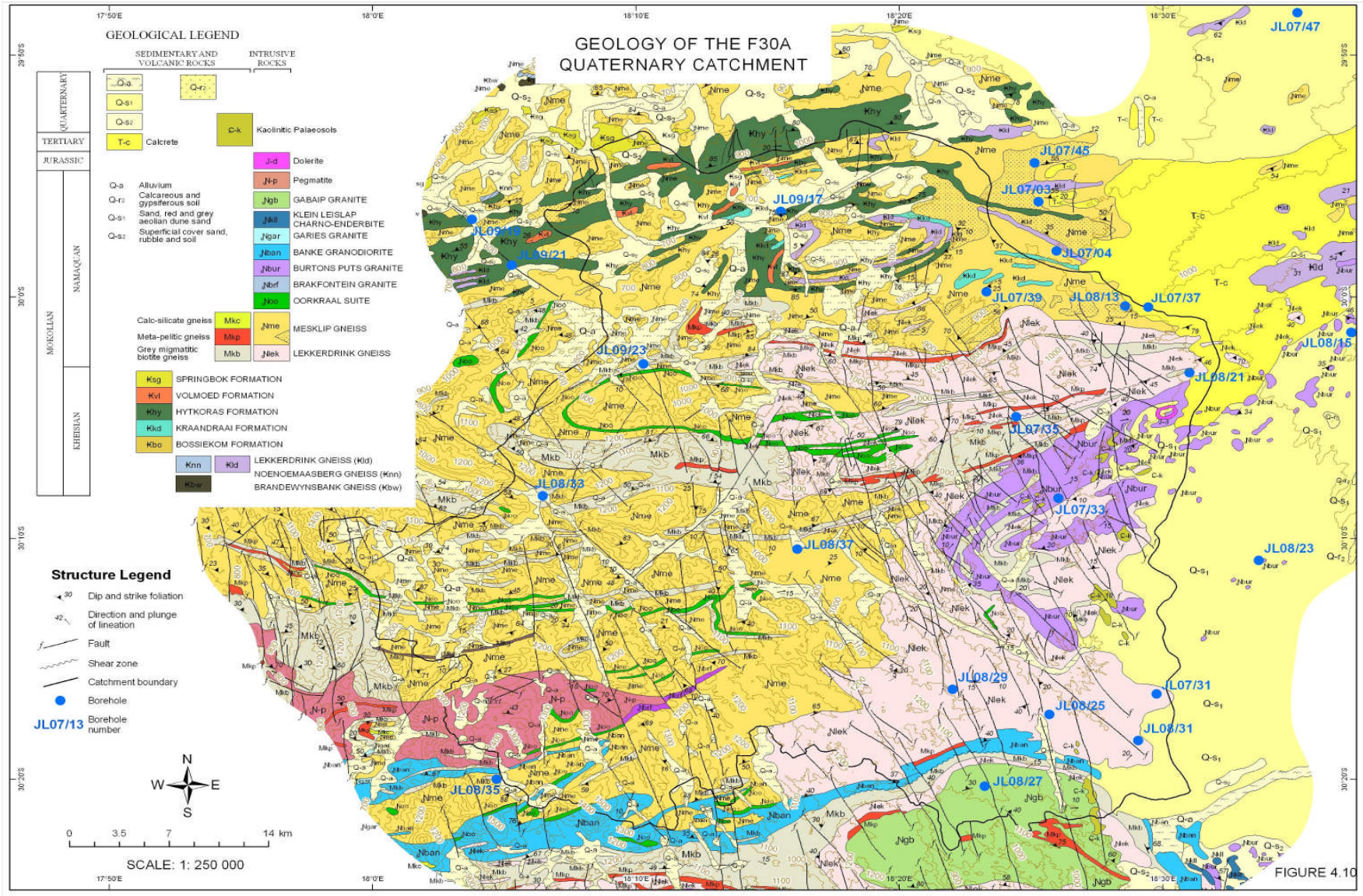
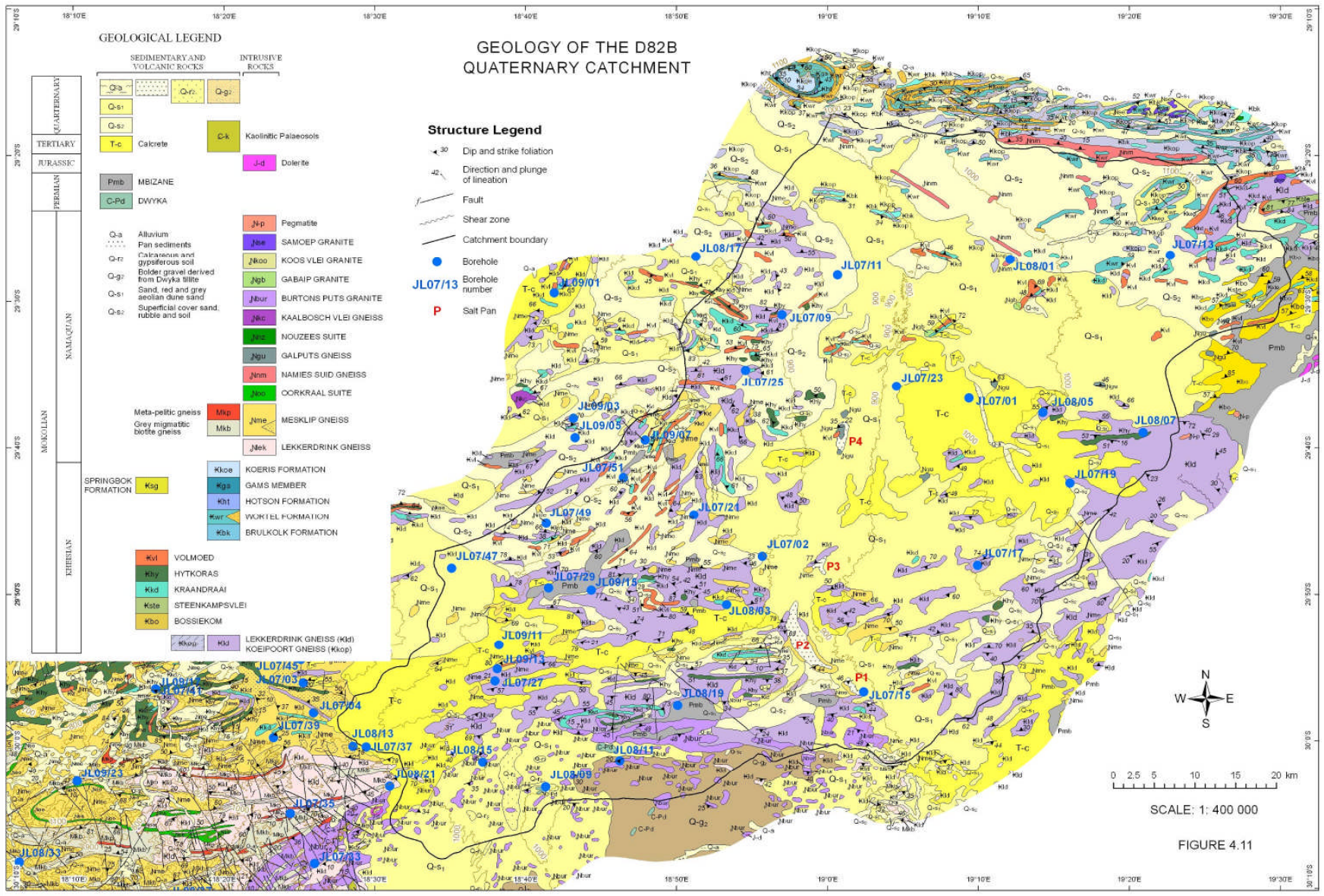

GEOLOGICAL LEGEND
SEDIMENTARY AND VOLCANIC ROCKS
INTRUSIVE ROCKS
QUARTERNARY
TERTIARY
JURASSIC
NAMAQUAN
KHEISIAN
MOKOLIAN
Q-a Alluvium
Q-r2 Calcareous and gypsiferous soil
Q-s1 Sand, red and grey aeolian dune sand
Q-s2 Superficial cover sand, rubble and soil
T-c Calcrete
C-k Kaolinitic Palaeosols
J-d Dolerite
N-p Pegmatite
Ngb GABAIP GRANITE
Nkll KLEIN LEISLAP CHARNO-ENDERBITE
Ngar GARIES GRANITE
Nban BANKE GRANODIORITE
Nbur BURTONS PUTS GRANITE
Nbrf BRAKFONTEIN GRANITE
Noo OORKRAAL SUITE
Mkc Calc-silicate gneiss
Mkp Meta-pelitic gneiss
Mkb Grey migmattitic biotite gneiss
Nme MESKLIP GNEISS
Nlek LEKKERDRINK GNEISS
Ksg SPRINGBOK FORMATION
Kvl VOLMOED FORMATION
Khy HYTKORAS FORMATION
Kkd KRAANDRAAI FORMATION
Kbo BOSSIEKOM FORMATION
Knn NOENOEMAASBERG GNEISS (Knn)
Kbw BRANDEWYNSBANK GNEISS (Kbw)
Structure Legend
Dip and strike foliation
Direction and plunge of lineation
Fault
Shear zone
Catchment boundary
Borehole
JL07/13 Borehole number
N
W
E
S
0 3.5 7 14 km
SCALE: 1: 250 000
GEOLOGY OF THE F30A
QUATERNARY CATCHMENT
JL07/47
JL07/45
JL07/03
JL09/17
JL09/19
JL09/21
JL07/04
JL07/39
JL08/13
JL07/37
JL08/15
JL09/23
JL08/21
JL07/35
JL08/33
JL07/33
JL08/37
JL08/23
JL08/29
JL07/31
JL08/25
JL08/31
JL08/27
JL08/35
17°50'E
18°0'E
18°10'E
18°20'E
18°30'E
29°50'S
30°0'S
30°10'S
30°20'S

FIGURE 4.10


GEOLOGICAL LEGEND
SEDIMENTARY AND VOLCANIC ROCKS
INTRUSIVE ROCKS
QUATERNARY
TERTIARY
JURASSIC
PERMIAN
NAMAQUAN
MOKOLIAN
EKHEIAN
Q-a Alluvium
Pan sediments
Q-r2 Calcareous and gypsiferous soil
Q-g2 Bolder gravel derived from Dwyka tillite
Q-s1 Sand, red and grey aeolian dune sand
Q-s2 Superficial cover sand, rubble and soil
T-c Calcrete
C-k Kaolinitic Palaeosols
J-d Dolerite
Pmb MBIZANE
C-Pd DWYKA
Jkp Pegmatite
Jkse SAMOEP GRANITE
Jkoo KOOS VLEI GRANITE
Jkgb GABAIP GRANITE
Jkbur BURTONS PUTS GRANITE
Jkkb KAALBOSCH VLEI GNEISS
Jkvz NOUZEES SUITE
Jkgu GALPUTS GNEISS
Jknm NAMIES SUID GNEISS
Jkoo OORKRAAL SUITE
Meta-pelitic gneiss Mkp
Grey migmatitic biotite gneiss Mkb
Jkme MESKLIP GNEISS
Jkek LEKKERDRINK GNEISS
SPRINGBOK FORMATION Ksg
Kkoe KOERIS FORMATION
Kgs GAMS MEMBER
Kht HOTSON FORMATION
Kwr WORTEL FORMATION
Kbk BRULKOLK FORMATION
Kvl VOLMOED
Khy HYTKORAS
Kkd KRAANDRAAI
Kste STEENKAMPSVLEI
Kbo BOSSIEKOM
Kkop Kkd LEKKERDRINK GNEISS (Kkd) KOEIPOORT GNEISS (Kkop)
GEOLOGY OF THE D82B QUATERNARY CATCHMENT
Structure Legend
Dip and strike foliation
Direction and plunge of lineation
Fault
Shear zone
Catchment boundary
Borehole
JL07/13 Borehole number
P Salt Pan
JL08/17
JL07/11
JL09/01
JL07/09
JL07/25
JL07/23
JL07/01
JL08/05
JL08/07
JL07/13
JL08/01
JL09/03
JL09/05
JL09/07
P4
JL07/51
JL07/19
JL07/21
JL07/49
JL07/47
JL07/02
JL07/17
P3
JL07/29
JL08/15
JL08/03
JL09/11
JL09/13
P2
JL07/27
JL08/19
P1
JL07/15
JL07/45
JL07/41
JL07/03
JL07/04
JL07/39
JL08/13
JL07/37
JL08/15
JL05/23
JL08/21
JL07/35
JL08/11
JL08/09
JL08/33
JL07/33
N
W
E
S
0 2.5 5 10 15 20 km
SCALE: 1: 400 000
FIGURE 4.11

4.6. Hydrogeology of the area

4.6.1 General

Crystalline rock aquifers as defined by Gustafson and Krásný (1994) are hard rock aquifers that comprise predominantly of fractured igneous and metamorphic rocks with negligible matrix porosity and permeability. The basal part of the regolith and the top of the weathered saprock (i.e. weathered bedrock) has sufficient permeability to support successful boreholes for small-scale village water-supply (Wright and Burgess, 1992; Rebouças, 1993; Chilton and Foster, 1995). The aquifer systems are mostly limited to fault-controlled valleys occurring throughout the study area. Groundwater, within the lower most unweathered basement rocks, is stored in interconnected systems of fractures, joints and fissures associated with regional tectonism (Rebouças, 1993). In fractured rocks, water is stored in vertical, lateral and sub-horizontal faults, weathered joints, whereas in some areas it can be found along lithological contacts (Ainslie, 2003). The fractured bedrock is characterized by high transmissivity and low storativity values.

4.6.2 Study area

The study area is located in the arid to semi-arid western part of South Africa where low amount of precipitation has impact on net recharge into the local aquifer. The study area is characterised by fractured basement aquifers. Basement aquifers which are usually fractured Precambrian crystalline rocks are found extensively in sub-Saharan Africa where the resource supplies many rural communities.

There are no surface water resources in the study area and the supply is mainly derived from groundwater resources. The geometry of the aquifer systems in the area is largely controlled and influenced by the underlying geology of igneous

and metamorphic rocks (such as granites and gneisses), geomorphic development including weathering and its deformation history or structural evolution (Conrad and Adams, 2003).

In the study area, groundwater occurs in three different aquifer systems:

- The sandy/alluvial aquifers
- The weathered zone , and
- Fractured bedrock

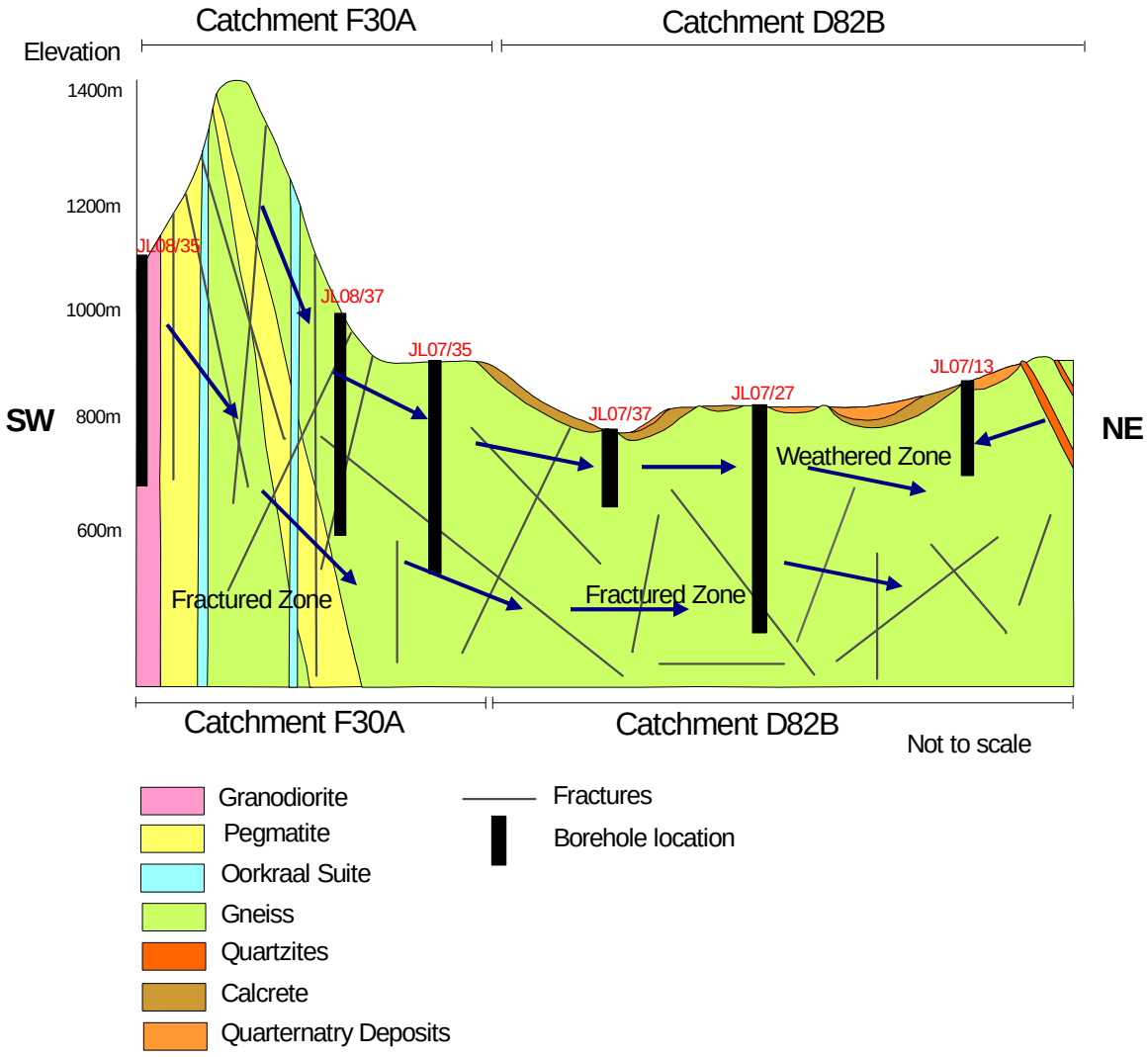


Fig. 4.12: Conceptual model of the study area showing groundwater flow between the two catchments.

The fractured bedrock and weathered zone aquifers are hydraulically linked; the weathered zone acts as a reservoir that is able to recharge the bedrock aquifers (Fig. 4.12). This process may be minimal where extensive clay or calcrete layers exist between the two aquifers. Fig. 4.12 also shows an interaction between the groundwater systems in the area, where groundwaters flow is from F30A catchment to D82B Catchment. Groundwater flow between the two catchments show two flow paths, shallow and deep flow (shown by arrows in Fig. 4.12).

5. ANALYTICAL RESULTS

5.1. Introduction

The groundwater quality samples were collected from 57 domestic boreholes in Namaqualand and were analysed in situ for pH, Redox potential, Electrical conductivity (EC), Temperature, Salinity and Total Dissolved Solids (TDS). The results for these physico-chemical constituents are shown in Table 5.1. All 57 samples were sent to the laboratory for major, minor, trace elements and gross alpha and beta count analyses, 24 samples were analysed for environmental isotopes (oxygen-18, deuterium and tritium), and 4 samples were analysed for radioactivity. The samples were randomly selected but, carefully to cover the whole area. More samples could have been collected for analysis but due to financial constraints only the above was collected.

5.2. Physico-chemical parameters

The results of the physico–chemical parameters from two catchments (D82B and F30A) and the control samples are presented in Table 5.1 below. Most of the samples were colourless with only three samples showing yellowish colour.

As regards to the pH, groundwater in the study area is near neutral to slightly alkaline (pH 6.72–8.84), however, one sample (sample JL07/09 of the D82B catchment) has acidic water with pH 4.90. The water ranges from fresh (TDS <1000 mg/l) to brackish (TDS ranging from 1000 to 6430 mg/l).

Adams et al., (2001) stated that pH ranges between 6.3 and 8.5 is an indication that the dissolved carbonates are predominantly in the HCO_3 form. This water is inline with the South African water quality guideline of pH 6-9, except sample number JL07-09 with pH 4.90.

Table 5.1: Physico-Chemical water chemistry data

Sample ID	Date	pH	EC (mS/cm)	TDS (mg/l)	Salinity (g/l)	Temperature (˚C)	Eh (Volts)
JL07/01	20.03.2007	7.29	3.36	1678	1.8	22.3	+0.00
JL07/02	20.03.2007	7.91	3.73	1879	2.0	23.6	-0.04
JL07/03	22.03.2007	7.45	1.51	752	0.7	33.4	-0.01
JL07/04	22.03.2007	7.28	1.36	682	0.7	24.8	+0.00
JL07/09	26.09.2007	4.90	3.60	1814	1.9	23.2	+0.12
JL07/11	26.09.2007	6.72	5.82	2920	3.2	20.9	+0.00
JL07/13	26.09.2007	7.11	2.75	1375	1.4	21.5	+0.00
JL07/15	27.09.2007	7.64	12.13	6070	6.9	17.2	+0.04
JL07/17	27.09.2007	7.78	1.49	746	0.8	19.1	+0.03
JL07/19	27.09.2007	7.20	4.58	2290	2.4	22.7	+0.00
JL07/21	28.09.2007	7.22	3.72	1863	2.0	17.0	+0.00
JL07/23	28.09.2007	7.17	6.41	3180	3.4	31.7	-0.01
JL07/25	28.09.2007	7.37	10.29	5150	5.8	18.4	-0.01
JL07/27	29.09.2007	7.92	4.62	2320	2.5	16.8	-0.05
JL07/29	29.09.2007	7.42	3.33	1667	1.7	23.5	-0.02
JL07/31	01.10.2007	7.75	1.86	932	0.9	19.2	-0.03
JL07/33	01.10.2007	7.77	2.28	1144	1.2	19.9	-0.04
JL07/35	01.10.2007	7.62	4.23	2110	2.2	28.0	-0.03
JL07/37	01.10.2007	8.84	2.32	1156	1.2	18.6	-0.10
JL07/39	02.10.2007	7.27	2.02	1009	1.0	23.4	+0.00
JL07/41	02.10.2007	7.27	1.17	585	0.6	33.2	-0.02
JL07/43	02.10.2007	7.40	1.57	786	0.8	21.7	-0.01
JL07/45	02.10.2007	7.49	2.05	1027	1.0	23.8	-0.02
JL07/47	03.10.2007	7.42	5.64	2820	3.0	19.8	-0.01
JL07/49	03.10.2007	7.10	12.88	6430	7.4	20.2	+0.00
JL07/51	03.10.2007	7.22	10.62	5310	6.0	20.7	+0.00
JL08/01	08.10.2008	6.39	1.71	856	0.9	19.1	+0.05
JL08/03	09.10.2008	5.75	6.57	3270	2.1	21.2	+0.09
JL08/05	09.10.2008	6.27	1.38	689	0.7	26.6	+0.07
JL08/07	09.10.2008	6.22	2.06	1032	1.1	22.8	+0.08
JL08/09	11.10.2008	5.75	3.41	1694	1.8	27.2	+0.08
JL08/11	11.10.2008	6.18	8.22	4150	4.6	23.6	+0.07
JL08/13	13.10.2008	5.87	1.76	601	0.6	24.5	+0.05
JL08/15	13.10.2008	6.40	5.30	2640	2.8	23.6	+0.06
JL08/17	13.10.2008	6.80	4.09	2050	2.2	25.0	+0.04
JL08/19	13.10.2008	6.74	7.74	3920	1.6	24.9	+0.04
JL08/21	14.10.2008	6.63	1.30	646	0.6	17.6	+0.04
JL08/23	14.10.2008	6.42	6.50	3240	3.5	18.8	+0.01
JL08/25	14.10.2008	7.11	2.26	1136	1.2	20.4	+0.02
JL08/27	14.10.2008	6.86	1.70	854	0.9	27.1	+0.04
JL08/29	14.10.2008	6.39	1.29	643	0.6	24.4	+0.07
JL08/31	14.10.2008	6.38	2.64	1316	1.4	26.6	+0.06
JL08/33	15.10.2008	6.42	1.45	721	0.8	19.2	+0.06
JL08/35	15.10.2008	6.42	3.68	161.6	0.2	19.4	+0.07
JL08/37	15.10.2008	6.01	2.81	1385	0.0	25.1	+0.09

Sample ID	Date	pH	EC (mS/cm)	TDS (mg/l)	Salinity (g/l)	Temperature (˚C)	Eh (Volts)
JL09/01	27.07.2009	7.33	5.60	2800	3	15.3	+0.01
JL09/03	27.07.2009	6.92	6.86	3430	3.7	11.1	+0.03
JL09/05	27.07.2009	6.45	6.87	3430	3.7	11.4	+0.04
JL09/07	27.07.2009	6.04	7.89	3960	1.3	13.7	-0.06
JL09/09	27.07.2009	6.84	11.54	5780	6.6	20.7	+0.03
JL09/11	28.07.2009	7.42	4.33	2160	2.3	11.9	+0.02
JL09/13	28.07.2009	7.20	5.98	2990	3.2	18.1	+0.01
JL09/15	28.07.2009	7.08	6.55	3250	3.6	19.2	+0.02
JL09/17	29.07.2009	7.94	0.99	497	0.5	12.5	-0.02
JL09/19	29.07.2009	7.84	2.80	1403	1.4	14.9	-0.02
JL09/21	29.07.2009	7.32	11.75	5870	6.6	15.9	+0.01
JL09/23	29.07.2009	8.17	1.62	811	0.8	13.9	-0.03

The Total Dissolved Solids (TDS) varies between 585 mg/l and 6430 mg/l in the D82B catchment, and from 497 mg/l and 2110 mg/l in F30A catchment. It ranges from 162 mg/l to 580 mg/l in the control samples. Most of the TDS values of the two catchments (F30A and D82B) and the control samples are above the South African water quality guideline of 450 mg/l (DWAF, 1996). The maximum salinity values of 6.07 g/l and 6.43 g/l are observed from two boreholes found in the D82B catchment. Salinity in the water samples varies from as low as 0.6 g/l to the highest salinity of 7.4 g/l (Table 5.1). These results reveal that in some places the borehole tap has groundwater with high salt content. This may results either from the lithology of the aquifer or excessive evaporation (Fig. 5.1). This figure portrays a salt pan with salt all over the low lying area (the white patches in the picture below).

The EC values of the groundwater range from 1.49 mS/cm to 12.88 mS/cm in the D82B catchment, and from 1.29 mS/cm to 4.23 mS/cm in catchment F30A. It ranges from 1.36 mS/cm to 11.75 mS/cm in the control samples. The EC values of the groundwater tend to increase with the decreasing elevation.

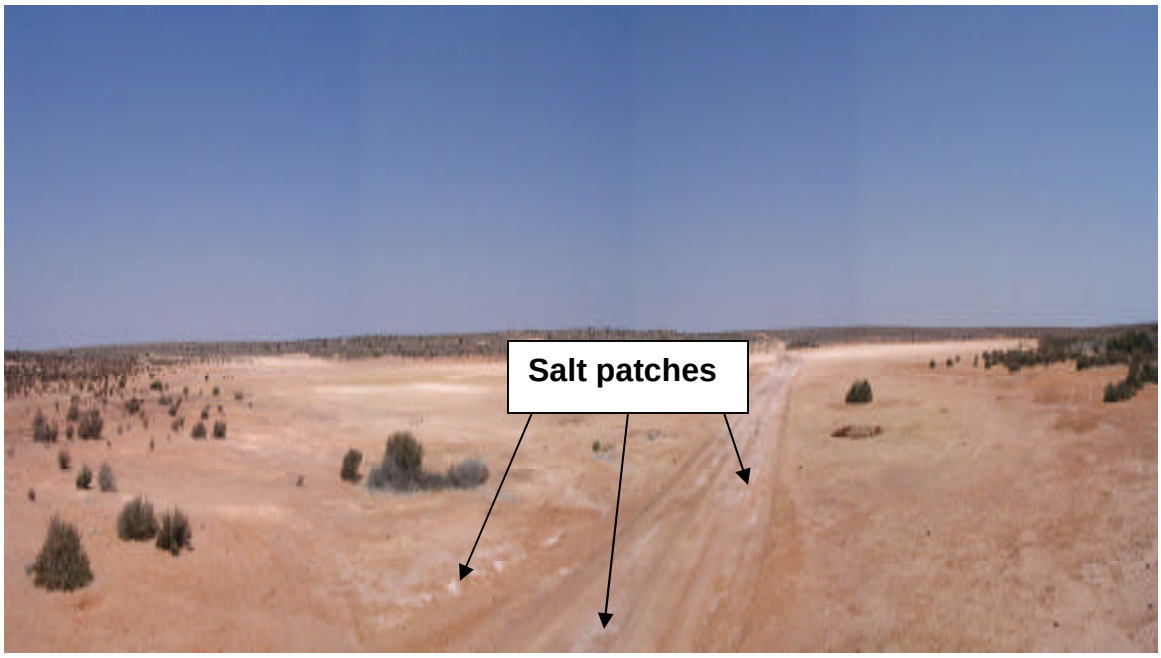


Figure 5.1: Salt pan found in Bitterputs se Pan in D82B catchment (P3 in Fig 4.11) showing salt patches found on the surface.

The temperature of the groundwater in the area is within the acceptable range of 25˚C or less with the exception of four boreholes of higher temperature 28˚C, 31.7˚C, 33.2˚C and 33.4˚C (Table 5.1). Low or cool temperature generally plays a major role in regulating water chemicals and inorganic constituents to acceptable levels, thereby, keeping water in portable condition. High water temperature enhances the growth of microorganisms and may increase taste, odour, colour and corrosion problems (WHO, 2006).

Alkalinity and pH are properties of water that are related, but are different. Alkalinity is the measure of the pH buffering capacity of the water, while, pH is the acidity of water. Alkalinity is expressed as the amount of calcium carbonate ($CaCO_3$) in water, although other substances can contribute to alkalinity as well. The Total Alkalinity of the samples ranges from 111 mg/l to 290 mg/l in the D82B catchment, 73 mg/l to 310 mg/l in the F30A catchment and from 64 mg/l to 310 mg/l in the control samples (Table 5.1). The total alkalinity is above the South African water quality guidelines of 50–100 mg/l.

The Alkalinity is derived from dissolved rocks, particularly limestone ($CaCO_3$) and CO_2 in soil.

5.3. Chemical Parameters

Most trace elements such as aluminium, cobalt, zinc, antimony, barium, beryllium, cadmium, lead, silver, gallium, arsenic and thallium were rarely detected in the groundwater of the area. Lithium, vanadium, boron, chromium, iron, manganese, copper, nickel, selenium, rubidium, strontium, molybdenum and uranium were the only trace elements detected at the sites. Sodium, Strontium, Uranium, Chloride, Fluoride, Nitrate, Sulphate, Iron and Chromium occur in higher concentrations (Table 5.2).

Table 5.2: Constituents that occur in high concentration in the area

Element	Catchment D82B	Catchment F30A	Control Samples
Na (in mg/l)	111.99–1960	117.01–587	27.92–1539.73
Sr (in µg/l)	645.17–8307.77	273.05–910.58	68.84–4953.01
U (in µg/l)	2.84–145.99	3.14–31.81	3.21–76.74
Cr (in µg/l)	6.09–470.72	4.74–212.13	2.27–222.52
Cl (in mg/l)	240.23–4104.57	209.72–1206.78	62.08–4715.76
F (in mg/l)	1.12–31.80	1.18–5.91	1.49–4.34
NO_3 (in mg/l)	41.76–448.86	4.37–123.18	6.36–223.58
SO_4 (in mg/l)	83.63–1187.61	54.74–242.23	43.29–769.77
Fe (in µg/l)	282.56–1113.74	316.64–881.06	364.60–53893.58

The concentrations of major anions were plotted to assess and clearly describe the water composition (Fig. 5.2).

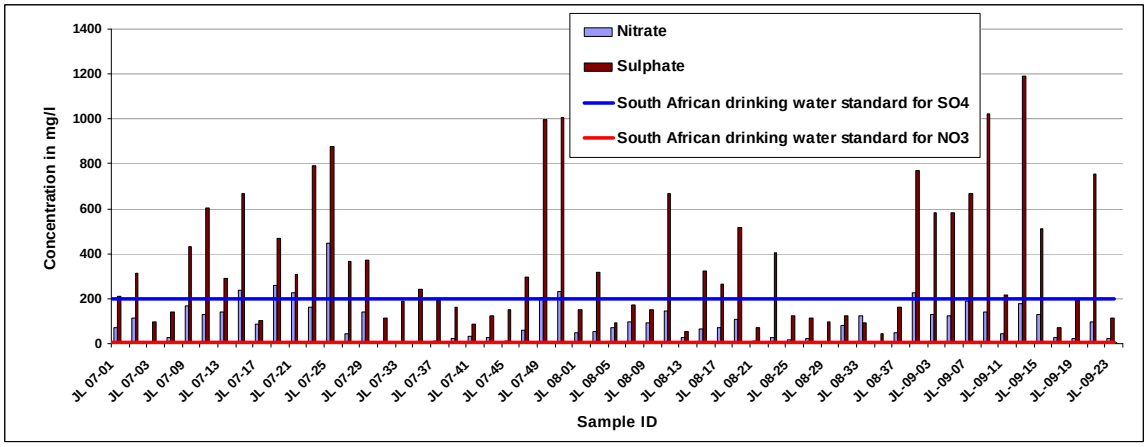


Fig. 5.2: A diagram showing nitrate and sulphate concentration. South African water quality guidelines for Sulphate 200 mg/l and Nitrate 6 mg/l.

The plot on Fig. 5.2 shows that sulphate, in the area, occurs in high concentration (long bars). It is the second abundant anion following chloride. Phosphate occurs in lower concentration in all the water samples except in sample JL07-01 where it is higher than both nitrate and sulphate (Fig. 5.2). The concentrations of sulphate and nitrate generally exceed the South African water quality guidelines of 200 mg/l and 6 mg/l, respectively (DWAF, 1996).

The concentrations of fluoride and bromine were plotted to assess and describe the water composition (Fig. 5.3).

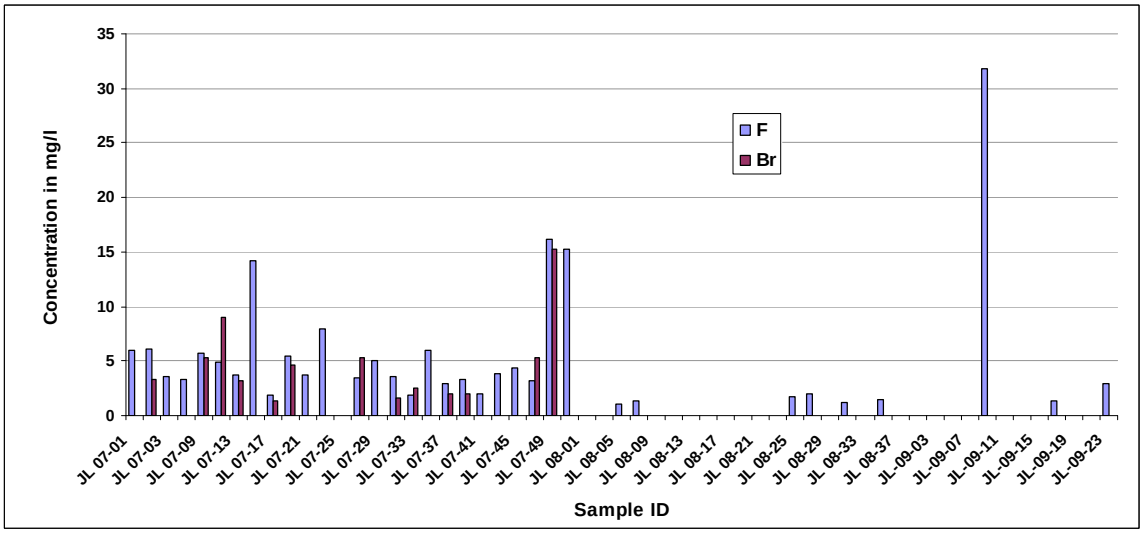


Fig. 5.3: A Diagram illustrating Fluoride (1 mg/l, DWAF, 1996) and Bromide (0.01 mg/l, WHO, 2006) anion concentration.

Fig. 5.3 demonstrates a low concentration of fluoride and no bromide in the samples that are collected in 2008. This may result from the difference in lithology of the two catchments as most of the samples that are collected in 2008 are from catchment F30A. The previous samples were collected mainly from catchment D82B.

Uranium concentrations were plotted to assess the results from two different methods used to determine uranium in the water samples (Fig. 5.4).

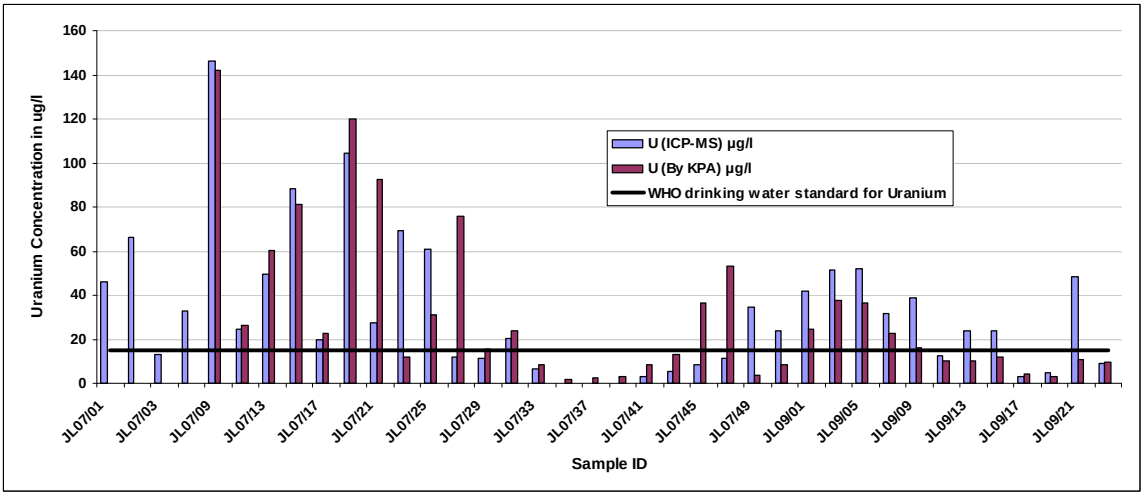


Figure 5.4: Diagram showing uranium concentration in the study area. WHO (2006) proposed drinking water quality of 15µg/l shown in a horizontal line.

Metallic uranium concentrations have been determined using KPA and ICP-MS methods. The uranium values are above the WHO (2006) proposed drinking water quality of 0.015 mg/l, which is equal to 15µg/l (Fig. 5.4). The uranium values measured by KPA show some difference from the ones measured by ICP-MS (Fig. 5.4). The KPA methods seemed to pick more uranium than the ICP-MS method while in some boreholes the ICP-MS methods picked up more uranium than the KPA method (Fig. 5.4).

Uranium was also analysed from the soil and/or rock samples collected around the groundwater sampling points to understand the source of uranium in the water samples. The uranium concentrations in the soils/rocks were plotted (Fig. 5.5) to assess the concentration in soils/rocks.

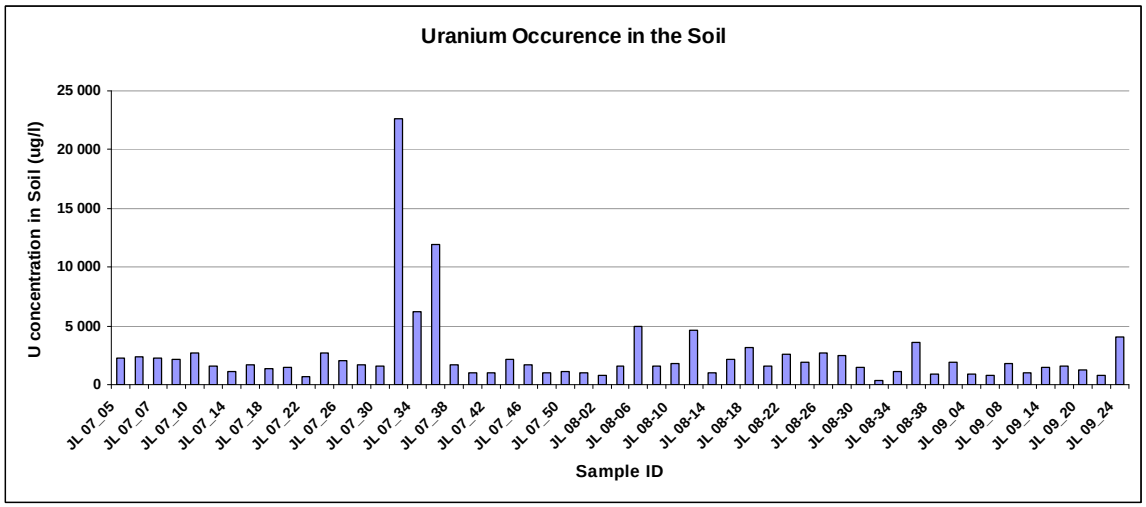


Fig. 5.5: Uranium concentration analysed from the soil of the study area (F30A and D82B Catchments).

The uranium content of the soils varies widely in the area with high concentration in some localities (Fig. 5.5).

Uranium concentrations in the borehole waters range from 3µg/l to 146µg/l, by ICP-MS method and range from 1.15 µg/l to 142 µg/l, by KPA method. In the soil samples uranium ranges from 402 µg/l to 22625 µg/l. Soil samples were collected from a trench of 15–20 cm closer to the borehole.

The concentrations of Cr in the water samples are found to be high, therefore, an Eh-pH diagram is plotted below to assess the form in which it occurs in the groundwater (Fig 5.6). If ingested, Cr^{6+} is considered to be carcinogenic in the human body (Jordana and Batista, 2004).

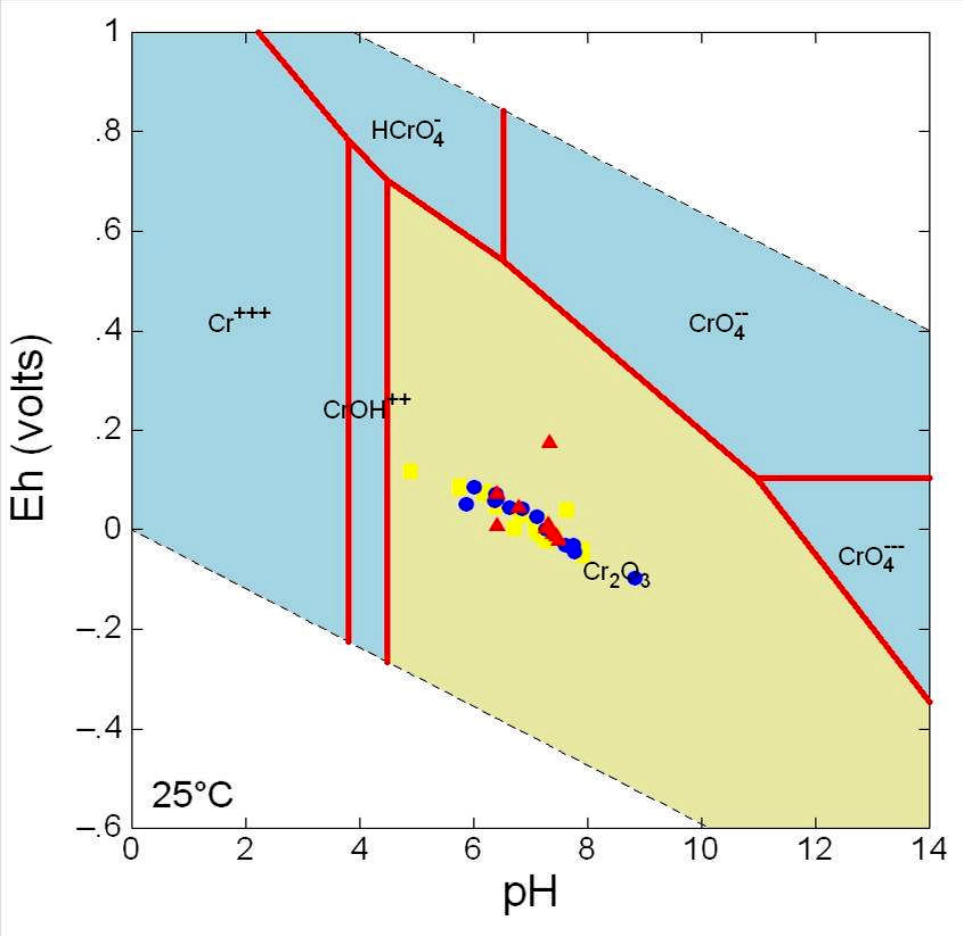


Fig. 5.6: Eh-pH diagram for Chromium in water. Diagram Cr^{3+}, T= 25 °C, P= 1.013 bars, a [main] = $10^{-9.041}$, a [H_2O] = 1

Cr^{3+} and Cr^{6+} are the most abundant species in solution, with Cr^{6+} being the most mobile and most easily absorbed by the human body. Chromium dissolved in groundwater occurs naturally in the environment and the predominant species depends on the pH/Eh of the environment (Mukhopadhyay et al., 2007). Cr(VI) is reduced to Cr(III) because of the ferrous iron (Fe-II) and/or manganese (Mn-II) that are present in the groundwater. Chromium (total Cr) concentration in the water samples ranges between 2 µg/l to 471 µg/l, which is above the drinking water limit of 50 µg/l of total Chromium (WHO, 2006).

The diagram (Fig. 5.6) show that all the samples from the two quaternary catchments including the control samples plots in the same field of Cr_2O_3. This

field covers a wide range of pH from 4.8 to 14 and ranges from oxidation (positive Eh values) to reducing (negative Eh values); it gets more reducing with increasing pH (Fig. 5.6). These results show that Chromium III Oxide (Cr_2O_3) is the major form of Cr in the sample solution.

Eh-pH diagram for iron was plotted in a similar way to understand which major form of Fe is dominant in the water samples of the area (Fig. 5.7)

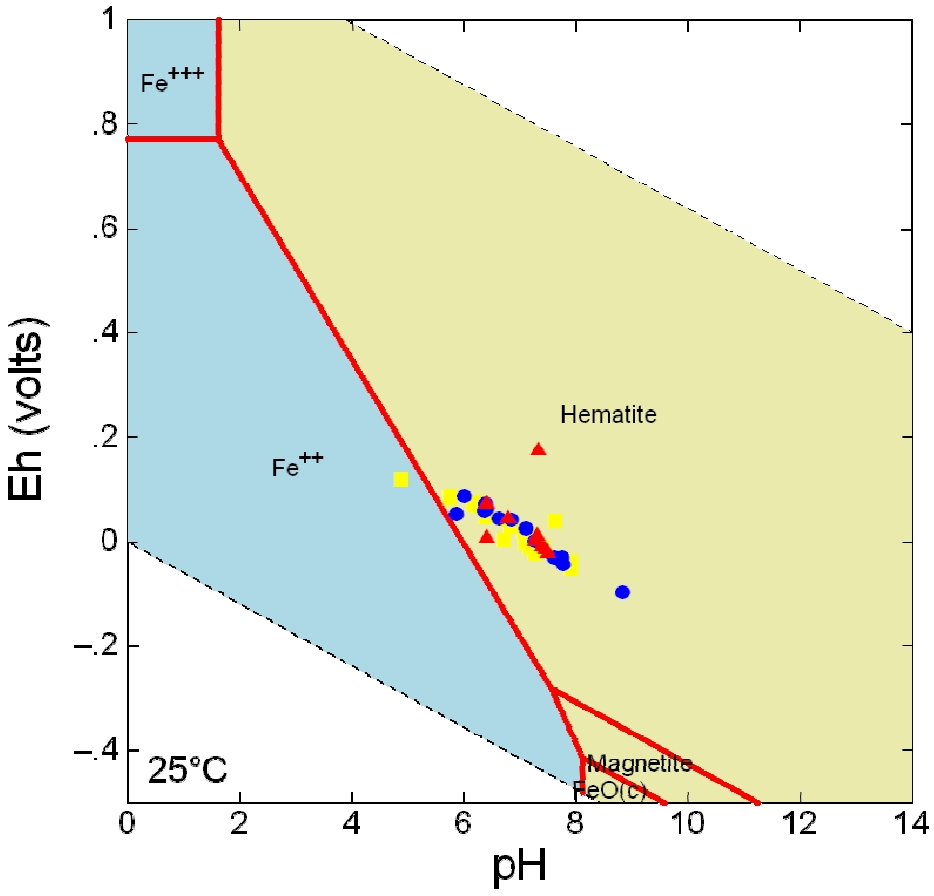


Fig. 5.7: Eh-pH diagram of Iron in water. Diagram Fe^{2+}, T= 25 °C, P= 1.013 bars, a [main] = $10^{-4.863}$, a [H_2O] = 1

The above diagram (Fig. 5.7) shows that all samples of the two quaternary catchments including the control samples plot in the same field of hematite and only two samples plot in the stability field of Fe^{2+}. These results in the above diagram show that iron is present in the groundwater as Fe_2O_3 and Fe^{2+} (Fig.

5.7). Fe_2O_3 is solid, therefore, the iron in the water occur as ferric iron hydroxide ($Fe(OH)_3$). The diagram is in line with the high concentrations of iron in the water samples as it ranges from 0.28 mg/l to 53.9 mg/l.

In order to assess the form in which sulphate occur in the water samples of the area an Eh-pH diagram was plotted (Fig. 5.8).

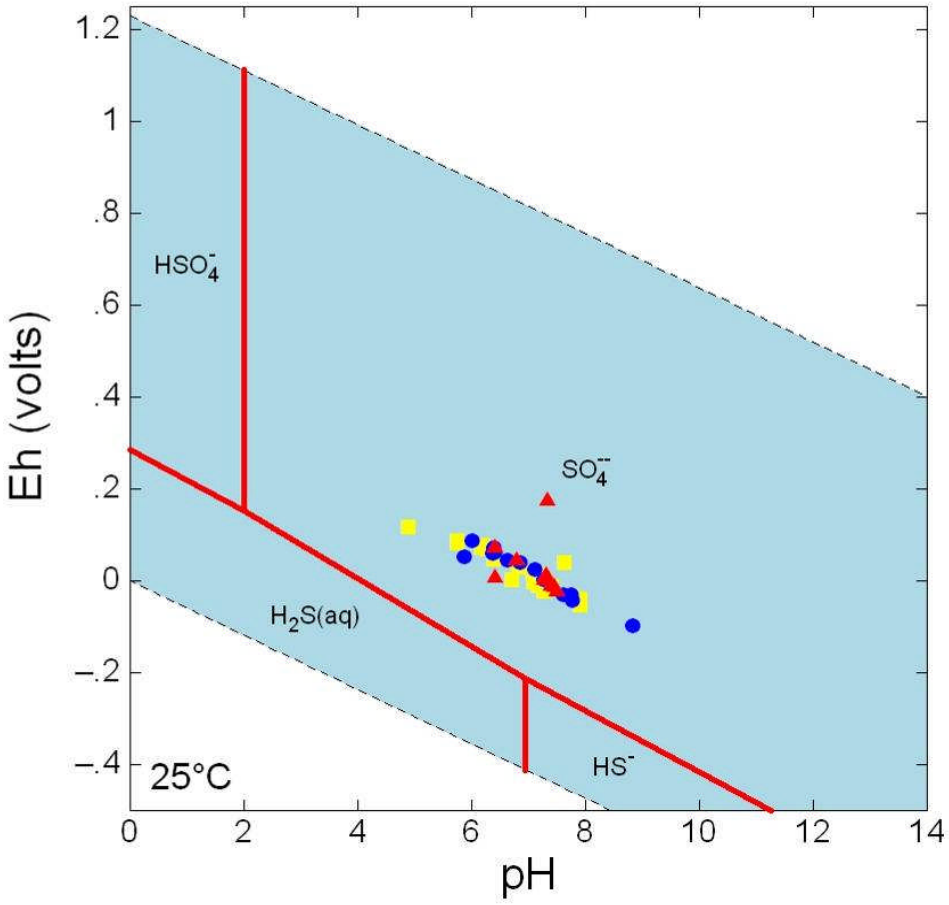


Fig. 5.8: Eh-pH diagram of Sulphate in water. Diagram SO_4^{2-}, T= 25 °C, P= 1.013 bars, a [main] = $10^{-5.298}$, a [H_2O] = 1

The above diagram (Fig 5.8) shows that all the samples of the two quaternary catchments including the control samples plot in the same field of SO_4^{2-}. This field covers a wide range of pH from pH 2 to 14 and ranges from oxidation (positive Eh values) to reducing (negative Eh values); it gets more reducing with

increasing pH (Fig. 5.8). The results show that sulphate occur as SO_4^{2-} in the groundwater of the area; which is consistent with elevated concentration of SO_4^{2-} in the water samples.

Eh-pH diagram for U^{6+} was plotted in a similar way to understand which major form of uranium is dominant in the water samples of the area (Fig. 5.9)

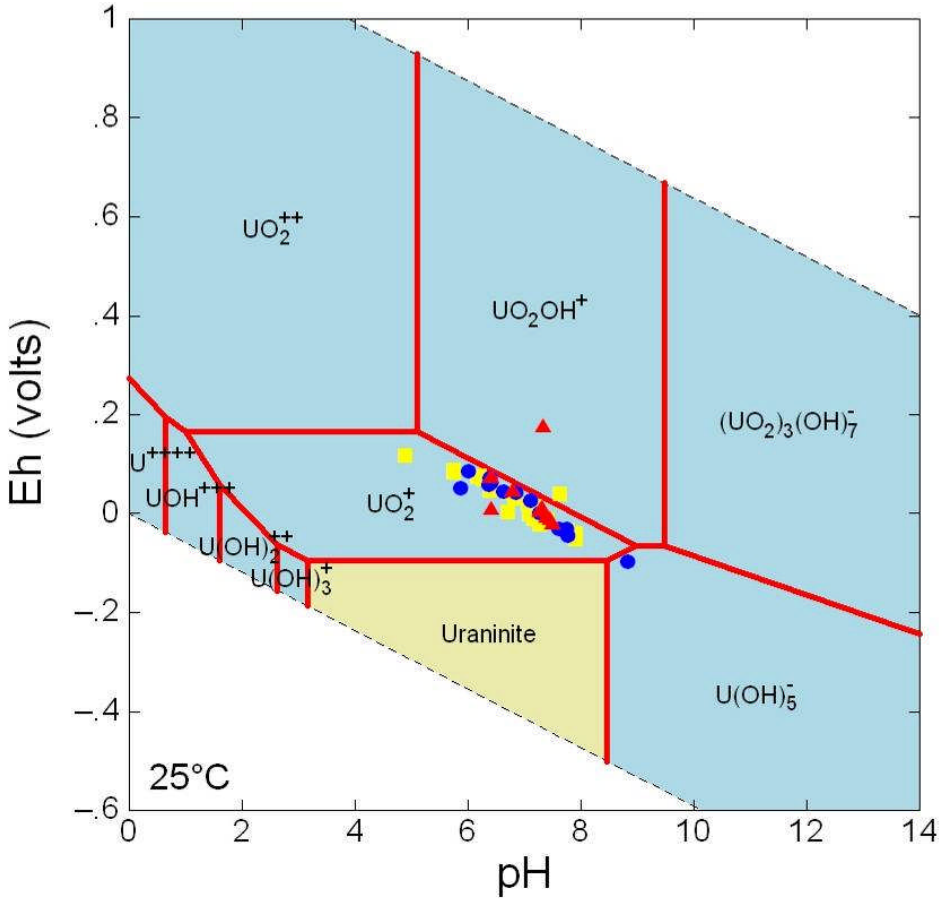


Fig. 5.9: Eh-pH diagram of Uranium in water. Diagram U^{6+}, T= 25 °C, P= 1.013 bars, a [main] = $10^{-12.67}$, a [H_2O] = 1

The above diagram (Fig. 5.9) shows that all the samples of the two quaternary catchments including the control samples plot in three stability fields. The data plots in the UO_2^+(c), two samples UO_2OH^+, and one sample plot in the $U(OH)_5^-$ fields (Fig. 5.9). The majority of the groundwater samples fall on the transition

line between Uraninite and U_4O_9 (c). Most of the water sample in the study area plot on the deep groundwater with minimal recharge zone, which is from Eh 0.1 Volts downwards (Grainger, 1958).

Eh-pH diagram was plotted to understand the dominant species of uranium and carbonates in the water samples of the area (Fig. 5.10)

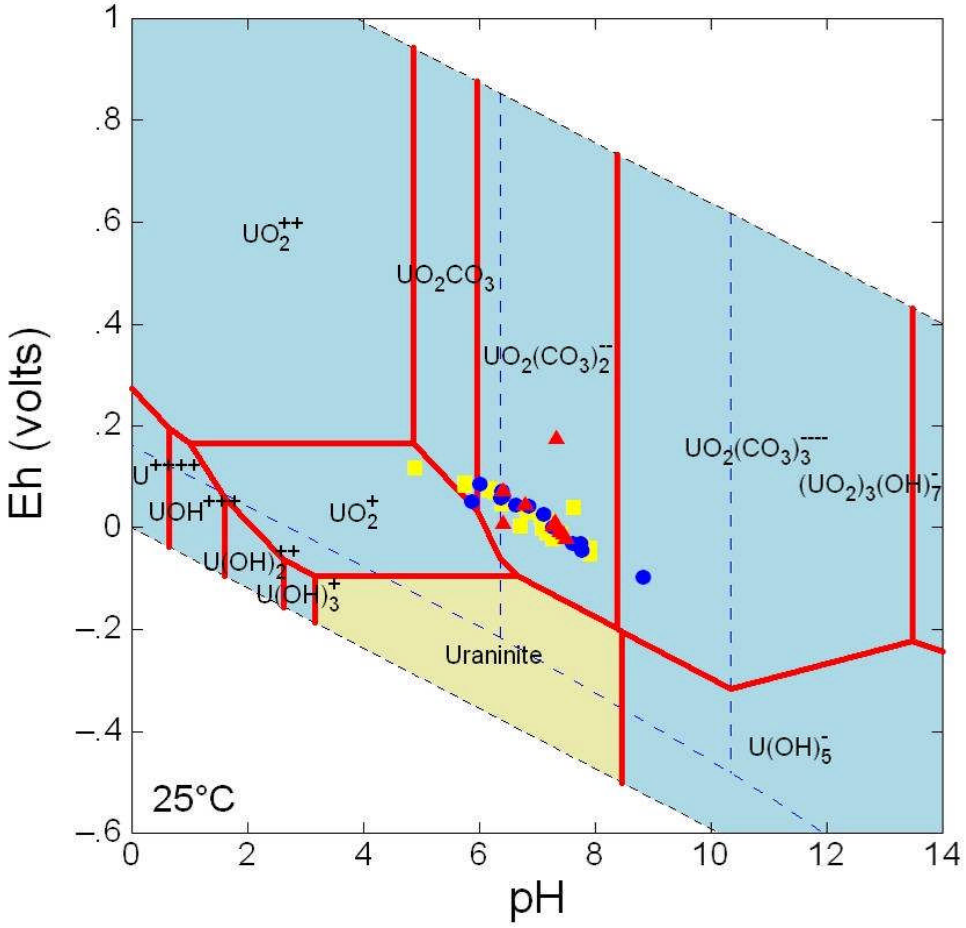


Fig. 5.10: Eh-pH diagram showing Uranium and Carbonate speciation. Diagram U^{6+}, T= 25 °C, P= 1.013 bars, a [main] = $10^{-12.67}$, a [H_2O] = 1, a [HCO_3] = $10^{-2.658}$

The high uranium concentrations at almost neutral pH are related to the strong complexation of uranyl ion with aqueous carbonate. Other strong complexants of uranyl ion include phosphate and fluoride. This can be seen in Fig. 5.10; the

presence of carbonates shifted/changed the stability lines. This diagram gives a prediction trends in uranium concentrations in the presence of complexing ions.

It should be noted that it is not always possible to accurately predict absolute concentrations of uranium in solution, due to the variable solubility of uranium mineral phases. Even the stability of the most common uranium ore mineral, uraninite, is strongly influenced by impurities (Meinrath et al., 1999). The rest of the data plots in the $UO_2(CO_3)_2^{2-}$ field, three samples straddle in the transition line between UO_2^{+}, UO_2CO_3 and $UO_2(CO_3)_2^{2-}$ fields. One sample from F30A catchment plots in the $UO_2(CO_3)_3^{4-}$ field and one from catchment D82B plot in the UO_2^{+} field (Fig. 5.10).

Activity diagram of Fe and SO_4^{2-} was plotted to determine if iron and sulphate resulted from natural water-rock interaction, weathering or acid mine drainage in the water samples of the area (Fig. 5.11)

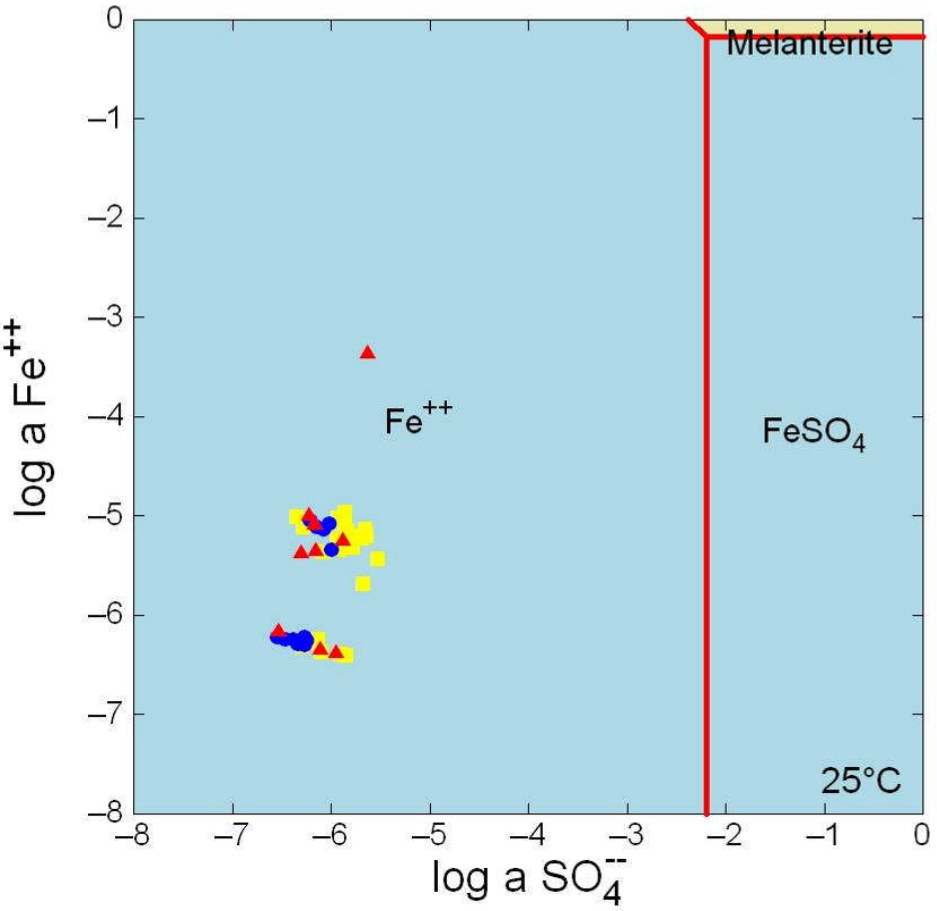


Fig. 5.11: Activity diagram showing Fe^{2+} vs. Sulphate. Fe^{2+}, T= 25 °C, P= 1.013 bars, a [H2O] = 1

From Fig. 5.11, it can be deduced that the iron and sulphate in the groundwater of the area are from geogenic sources (possibly dissolution of gypsum and pyrite oxidation) and not pollution from anthropogenic influence. Iron occurs as Fe^{++} in the groundwater of the area (Fig. 5.11).

5.4. Radiological Results

Natural waters contain a number of both alpha and beta radionuclides in widely varying concentrations. Measurement of the gross alpha emissions is used to establish the potential for high concentrations of certain radionuclides in a given water supply. A gross alpha analysis yields an estimate of the total alpha emissions from all decaying radionuclides in a sample, but does not speciate radiological constituents (Ainslie, 2003).

An important mechanism for the migration of actinides might be the transport by colloids Tricca et al. (2001), who showed that a large fraction of uranium and thorium may be associated with colloid. In groundwater, colloids may consist of bacteria, precipitates, organic matter, rock and/or mineral fragments. For these reasons the samples were analysed for gross alpha and beta from both liquid and filtered solids (colloids).

The present results show that in the groundwater of the two catchments, the actinides are present in remarkable amount in solution than in solid form (Tables 5.3 and 5.4).

Gross alpha and Gross beta emitters were detected in the water samples and are also likely attributed to naturally occurring uranium isotopes present in the water.

Table 5.3: Gross Alpha and Beta Activity of the Filter Residuals

Necsa Code	Sample ID	Filters Residuals in mBq/l					
		Gross Alpha-activity			Gross Beta-activity		
		Value	Unc.	MDA	Value	Unc.	MDA
RA-08555X001	JL 07/09	0.5	±14.8	12	31	±17.4	13
RA-08555X002	JL 07/11	-6.7	±14.6	12	4	±17.1	13
RA-08555X003	JL 07/13	-4.7	±14.7	12	4.9	±17.1	13
RA-08555X004	JL 07/15	-3.4	±14.7	12	8.6	±17.2	13
RA-08555X005	JL 07/17	5.2	±14.9	12	24.9	±17.4	13
RA-08555X006	JL 07/19	-6.6	±14.6	12	-1.4	±17.1	13
RA-08555X007	JL 07/23	-6.7	±14.6	12	7.8	±17.2	13
RA-08555X008	JL 07/27	-2	±14.7	12	8.4	±17.2	13
RA-08555X009	JL 07/21	-6	±14.6	12	7.7	±17.2	13
RA-08555X010	JL 07/25	-6	±14.6	12	8.1	±17.2	13
RA-08555X011	JL 07/29	-3.3	±14.7	12	5.1	±17.1	13
RA-08555X012	JL 07/31	-2	±14.7	12	8.4	±17.2	13
RA-08555X013	JL 07/33	-10.7	±14.5	12	8.5	±17.2	13
RA-08555X014	JL 07/35	1.2	±14.8	12	19.5	±17.3	13
RA-08555X015	JL 07/37	-6.6	±14.6	12	1.3	±17.1	13
RA-08555X016	JL 07/39	2.6	±14.8	12	4.2	±17.1	13
RA-08555X017	JL 07/43	-10.6	±14.5	12	6.6	±17.2	13
RA-08555X018	JL 07/47	-4	±14.7	12	10.2	±17.2	13
RA-08555X019	JL 07/49	-4	±14.7	12	6.4	±17.2	13
RA-08555X020	JL 07/51	-4.7	±14.7	12	4.5	±17.1	13
RA-08555X021	JL 07/41	0.6	±14.8	12	4.8	±17.1	13
RA-08555X022	JL 07/45	0	±14.8	12	10.5	±17.2	13

Table 5.4: Gross Alpha and Beta Activity of the Liquid Residuals

Liquid Residuals in Bq/l							
Necsa Code	**Sample ID**	**Gross Alpha-activity**			**Gross Beta-activity**		
		Value	**Unc.**	**MDA**	**Value**	**Unc.**	**MDA**
RA-08555X001	JL 07/09	2.25	±0.39	1.2	1.69	±0.12	0.21
RA-08555X002	JL 07/11	0.573	±0.561	1.9	1.52	±0.12	0.22
RA-08555X003	JL 07/13	1.67	±0.33	1	1.14	±0.1	0.21
RA-08555X004	JL 07/15	2.2	±0.61	1.9	2.14	±0.15	0.22
RA-08555X005	JL 07/17	0.721	±0.266	0.86	0.893	±0.086	0.21
RA-08555X006	JL 07/19	4.84	±0.52	1.3	1.51	±0.11	0.22
RA-08555X007	JL 07/23	2.56	±0.55	1.7	1.7	±0.13	0.22
RA-08555X008	JL 07/27	0.334	±0.446	1.5	1.1	±0.1	0.22
RA-08555X009	JL 07/21	0.135	±0.172	0.57	0.0874	±0.063	0.2
RA-08555X010	JL 07/25	1.13	±0.45	1.5	2.15	±0.14	0.22
RA-08555X011	JL 07/29	0.269	±0.261	0.86	0.512	±0.076	0.21
RA-08555X012	JL 07/31	0.868	±0.236	0.75	0.731	±0.081	0.21
RA-08555X013	JL 07/33	0.259	±0.227	0.75	0.617	±0.077	0.21
RA-08555X014	JL 07/35	0.0753	±0.3544	1.2	1.49	±0.11	0.21
RA-08555X015	JL 07/37	-0.0026	±0.2553	0.86	0.975	±0.087	0.21
RA-08555X016	JL 07/39	-0.0431	±0.2481	0.84	0.263	±0.069	0.21
RA-08555X017	JL 07/43	0.136	±0.255	0.85	0.285	±0.07	0.21
RA-08555X018	JL 07/47	0.303	±0.454	1.5	0.903	±0.093	0.22
RA-08555X019	JL 07/49	0.327	±0.439	1.5	1.68	±0.12	0.22
RA-08555X020	JL 07/51	0.579	±0.449	1.5	2.19	±0.14	0.22
RA-08555X021	JL 07/41	0.0634	±0.2053	0.69	0.229	±0.067	0.2
RA-08555X022	JL 07/45	0.281	±0.315	1	0.547	±0.078	0.21
RA-09616X001	JL 08/01	0.39	0.38	1.3	0.6	0.34	1.1
RA-09616X009	JL 08/03	-0.28	1.02	3.4	2.01	0.39	1.2
RA-09616X019	JL08/05	1.2	0.4	1.3	17.5	0.7	1.1
RA-09616X010	JL 08/07	1.2	0.5	1.7	3.01	0.37	1.1
RA-09616X012	JL 08/09	1.2	0.6	2	1.1	0.4	1.2
RA-09616X013	JL 08/11	2.4	0.8	2.5	37.4	1.6	1.2
RA-09616X004	JL 08/13	-0.082	0.32	1.1	0.65	0.34	1.1
RA-09616X003	JL 08/15	1	0.6	2.1	2.39	0.37	1.2
RA-09616X007	JL 08/17	1.4	0.8	2.6	1.22	0.37	1.2
RA-09616X016	JL 08/19	0.3	1.31	4.4	7.32	0.63	1.6
RA-09616X017	JL 08/21	1.25	0.38	1.2	0.63	0.34	1.1
RA-09616X015	JL 08/23	12.7	0.9	2.1	283	10	1.2
RA-09616X018	JL 08/25	18.2	1	1.7	590	20	1.1
RA-09616X002	JL 08/27	-0.22	0.35	1.2	0.15	0.34	1.1
RA-09616X008	JL 08/29	-0.22	0.36	1.2	0.37	0.34	1.1
RA-09616X006	JL 08/31	-0.36	0.53	1.8	0.33	0.35	1.1
RA-09616X005	JL 08/33	0	0.37	1.3	0.52	0.34	1.1
RA-09616X014	JL 08/35	0.12	0.23	0.77	18.6	0.7	1.1
RA-09616X011	JL 08/37	-0.38	0.57	1.9	0.83	0.35	1.2

Notes:

1. If a measured value (**Value** column) was recorded, it is reported regardless if the value is less than the minimum detectable activity concentration (**MDA**

column) or even if the value is negative. In the case where a value could not be obtained, a less than MDA ("< MDA") will be indicated.

2. The reported uncertainty (**Unc.** column) is quoted at 1 sigma (or coverage factor k = 1). The uncertainty is calculated mainly from counting statistics and it is not the standard deviation obtained from replicate measurements. No uncertainty value is reported of a less than MDA ("< MDA") is indicated in the **Value** column.
3. The minimum detectable activity concentration (**MDA** column) is calculated at a confidence level of 95%.
4. A value is reported with 3 significant digits if it is greater than the MDA value and the associated uncertainty will be reported the same precision. If a value is less than the MDA, the value and its associated uncertainty are reported with 2 significant digits regardless their respective magnitudes. A MDA value is always reported with 2 significant digits.

An important aspect of the geology of the Namaqualand region is the presence of widespread radiometric anomalies. It is expected that the groundwaters would be similarly enriched in uranium and thorium and/or their daughter isotopes. In the study area, groundwater is the main pathway for the transport of radioactivity to the human population by direct ingestion of water as drinking water from boreholes.

Studies have been carried out in the radiometric anomalies in Namaqualand (Andreoli et al., 2004 and Andreoli et al., 2006). Andreoli et al. 2006 concluded that the K, U and Th values for rocks of the metamorphic complex are sufficient to explain the elevated airborne radiometric anomalies in Namaqualand. It was also noted that U and Th are largely hosted by primary igneous or high-grade metamorphic minerals, mainly zircon and monazite (Andreoli et al. 2006). According to Andreoli et al. (2004) the radiometric anomalies in the area are related to the emplacement history of the igneous host rocks or to metamorphic processes in the granulite-facies.

5.5. Environmental Isotopes Results

δ^2H and $\delta^{18}O$ values in groundwater are representative of values in precipitation that recharge the groundwater, unless some process after the water reaches the earth's surface as precipitation causes isotopic fractionation, and consequently, deviation from meteoric water lines. Some processes that cause fractionation are evaporation, exchange with the aquifer matrix, or recharge that occurred at a different temperature or under a different climate (Tantawi et al., 1998; Ghomshei and Allen, 2000).

Oxygen-18 (^{18}O) and deuterium (D, or ^2H) are routinely used in hydrologic, climatologic and geothermal studies. In hydrology, stable isotopes provide information on the type and topology (altitude and latitude) of the recharge waters and the historical effects on water, related to such physical processes as evaporation (in ponds), melting (of snow or ice), condensation, evapotranspiration and mixing (Ghomshei and Allen, 2000; Yuan and Miyamoto, 2008).

Twenty-four samples were analyzed for stable isotopes and tritium in the two catchments (D82B and F30A) and the control samples. Ten samples were analyzed for stable isotopes for each catchment and four for the control samples. Stable isotopes are typically used in hydrogeology as "tracers of water, carbon, nutrient, and solute cycling" (Clark and Fritz, 1997,) whereas radioactive isotopes are typically used "to estimate the age or circulation of groundwater" (Clark and Fritz, 1997,). Both radioactive and stable isotopes were examined during this study.

δD and $\delta^{18}O$ concentrations in groundwater are used to examine sources of water, flow patterns and mixing processes in the groundwater flow system of the area. The stable isotope analyses for all samples data were reproduced within the expected analytical error limits. The isotopic contents of sampled

groundwater vary from -2.22‰ to -6.24‰ for $\delta^{18}O$ and from -21.1‰ to -41.0‰ for δD (Table 5.3).

Tritium is produced by cosmic radiation naturally in the upper atmosphere at very low concentrations and is incorporated into precipitation. Tritium in ground water is primarily from precipitation that infiltrated downward to the aquifer (ground-water recharge) (Bajjali et. al. 1997; Boronina et al., 2005). Concentrations detected in the water samples discussed in this study are discussed below.

Tritium (^3H) is the radioactive isotope of hydrogen having 12.43 years of half-life and can be measured in tritium unit. 1 TU is defined as one atom of ^3H in 10^{18} atoms of ^1H and 7.1 disintegrations per minute per gram of water (Katz et. al., 1998). Tritium is derived:

- Naturally from the atmosphere by cosmic-ray radiation involving the interaction of nucleons with nitrogen, oxygen and argon,
- Artificially from the testing of thermonuclear devices in the period of 1952–1962.

As a result of thermonuclear tests the tritium values increased dramatically reaching a peak of several thousands TU around 1963, and since then the levels have decreased steadily to several tens TU. The attraction of tritium as a hydrological tool is its use in distinguishing between recent water (recharged after 1950's) and older water (recharged before 1950's) (Ghomshei and Allen, 2000).

Significant ^3H activity (>1 TU) signifies a hydraulic connection with the surface which may be connected fractures and faults or at least one of its components consists of a mixture of old and young water <50 years old (Mook, 2006). Tritium is used to identify the age of waters as post and pre 1963 and as evidence of groundwater mixing (Bajjali et. al. 1997).

Clark and Fritz (1997), describes water containing ^{3}H of <0.8 TU as sub-modern waters recharged prior to recent recharge; and between 0.8 to 4TU as a mixture between sub-modern and recent recharge (Tantawi et al., 1998; Salameh, 2004). Groundwater ages determined by tritium are not necessarily the true age of the groundwater, therefore considered apparent ages (Price et al., 2003).
The groundwater from the two catchments F30A and D82B and the control samples show that the groundwater have consistently low tritium concentrations, with the majority having ^{3}H concentrations less than the analytical limit (0.6 TU) (Table 5.5). The measurable ^{3}H in 75% of the samples from the area is attributed to contributions from groundwater mixing from different sources.

Similarly, mixing occurs in both catchments water where tritium levels ranging between < 1 and 2.0 TU have been recorded. In 25% of the samples tritium concentration of 0.0 TU have been recorded, this shows that the groundwater is essentially tritium-free and recharged prior to the era of thermonuclear bomb testing. The analytical results are presented in Table 5.5. Tritium values in the study area ranges from 0–2 TU (Table 5.5)

Fig 5.12 and 5.13 show the distribution of tritium (^{3}H), deuterium (^{2}H) and ^{18}O in the study area.

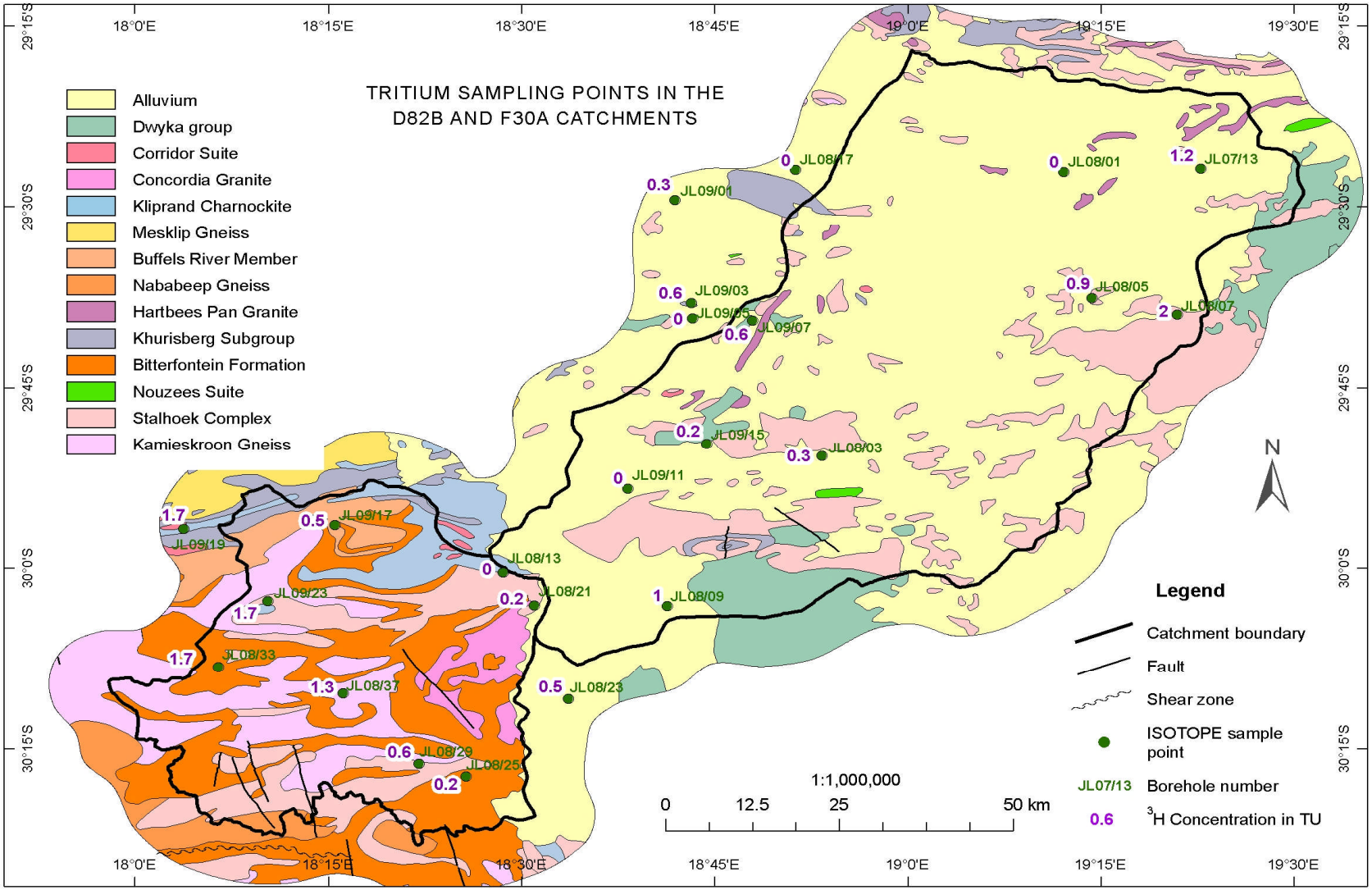


Fig. 5.12: Distribution map showing tritium sampling points and values in both catchment D82B and F30A.

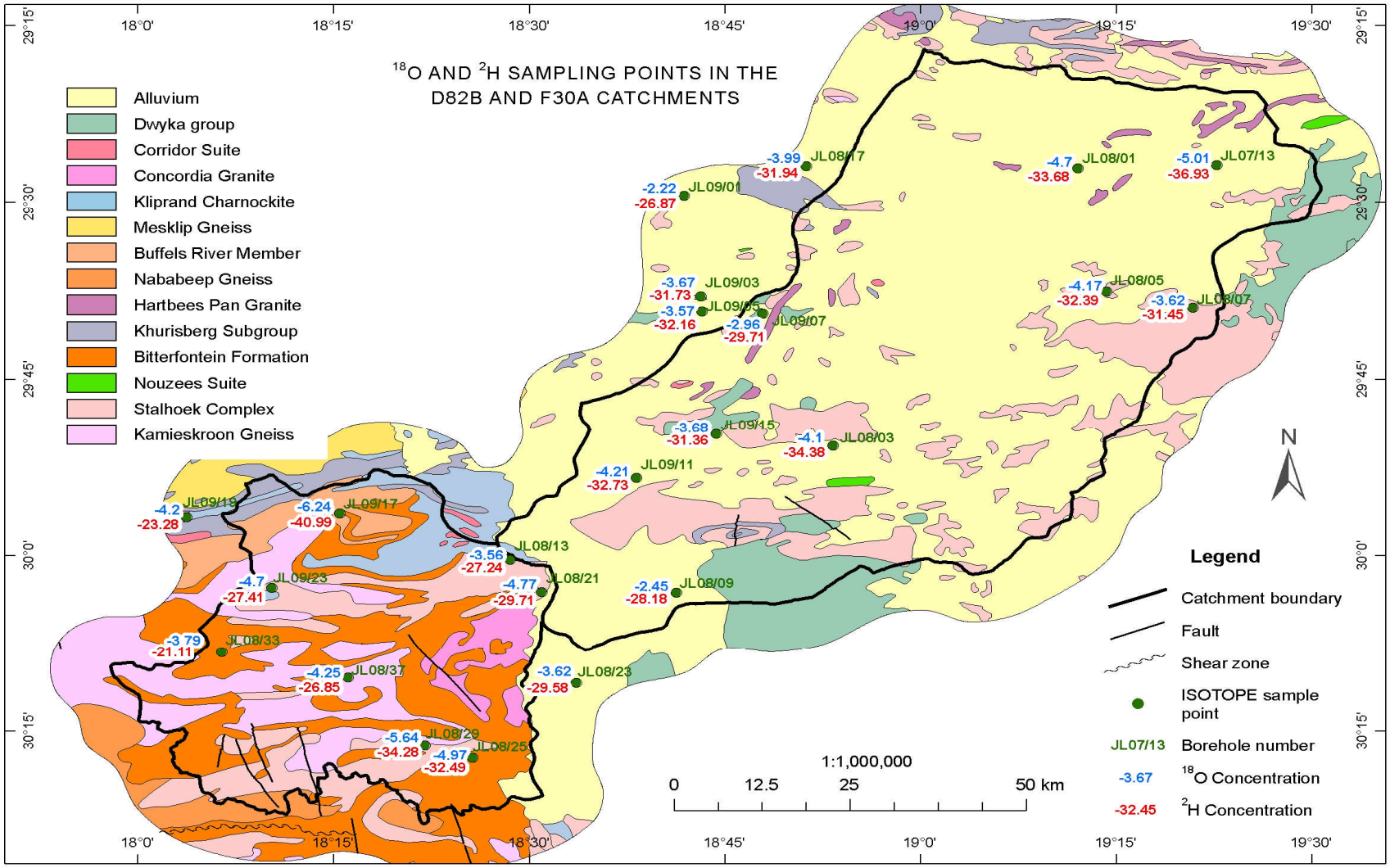


Fig. 5.13: Distribution map showing ^{18}O and ^{2}H sampling points and values in both catchment D82B and F30A.

Table 5.5: Results for Environmental Isotopes

Number	Identification	δD (‰)	δO^{18} (‰)	^{3}H(T.U.)	
CGS 495	JL 07/13 Neelsvlei	-36.9	-5.01	1.2	±0.3
CGS 496	JL 08/01 Oubip Farm	-33.7	-4.70	0.0	±0.2
CGS 497	JL 08/03 Bosluis	-34.4	-4.10	0.3	±0.2
CGS 498	JL 08/05 Naroegas	-32.4	-4.17	0.9	±0.2
CGS 499	JL 08/07 Heuningvlei	-31.5	-3.62	2.0	±0.3
CGS 500	JL08/09 Frummel Bakkies	-28.2	-2.45	1.0	±0.3
CGS 501	JL 08/13 Wolfkraal	-27.2	-3.56	0.0	±0.2
CGS 502	JL 08/17 Driehoek	-31.9	-3.99	0.0	±0.2
CGS 503	JL 08/21 Kamiebees	-29.7	-4.77	0.2	±0.2
CGS 504	JL 08/23 Bokseputs	-29.6	-3.62	0.5	±0.2
CGS 505	JL 08/25 Kaams	-32.5	-4.97	0.2	±0.2
CGS 506	JL 08/29 Riet	-34.3	-5.64	0.6	±0.2
CGS 507	JL 08/33 Pedro's Kloof	-21.1	-3.79	1.7	±0.3
CGS 508	JL08/37 Couragie Fontein	-26.9	-4.25	1.3	±0.3
CGS 526	JL 09/01 Spioenkop	-26.9	-2.22	0.3	±0.2
CGS 527	JL 09/03 Rooiduin 1	-31.7	-3.67	0.6	±0.2
CGS 528	JL 09/05 Rooiduin 2	-32.2	-3.57	0.0	±0.2
CGS 529	JL 09/07 Diepvlei	-29.7	-2.96	0.6	±0.2
CGS 530	JL 09/09 Uitkyk	-29.8	-2.98	0.0	±0.2
CGS 531	JL 09/11 Katvlei 2	-32.7	-4.21	0.0	±0.2
CGS 532	JL 09/15 Mannsepan	-31.4	-3.68	0.2	±0.2
CGS 533	JL 09/17 Tweefontein	-41.0	-6.24	0.5	±0.2
CGS 534	JL 09/19 Nuwedam	-23.3	-4.20	1.7	±0.3
CGS 535	JL 09/23 Stofkraal	-27.4	-4.70	1.7	±0.3

6. DISCUSSION

6.1. Hydrochemistry

Based on the major cations and anions a piper diagram was constructed, which shows the groundwater evolution in the study area (Fig. 6.1). Accordingly, the most common water types in the analysed samples are Na-Cl, Na-Ca-Cl, Na-Ca-Cl-HCO_3, Ca-Na-Cl, Na-Ca-Cl-SO_4 and Na-Ca-SO_4 amongst others (Table 5.2).

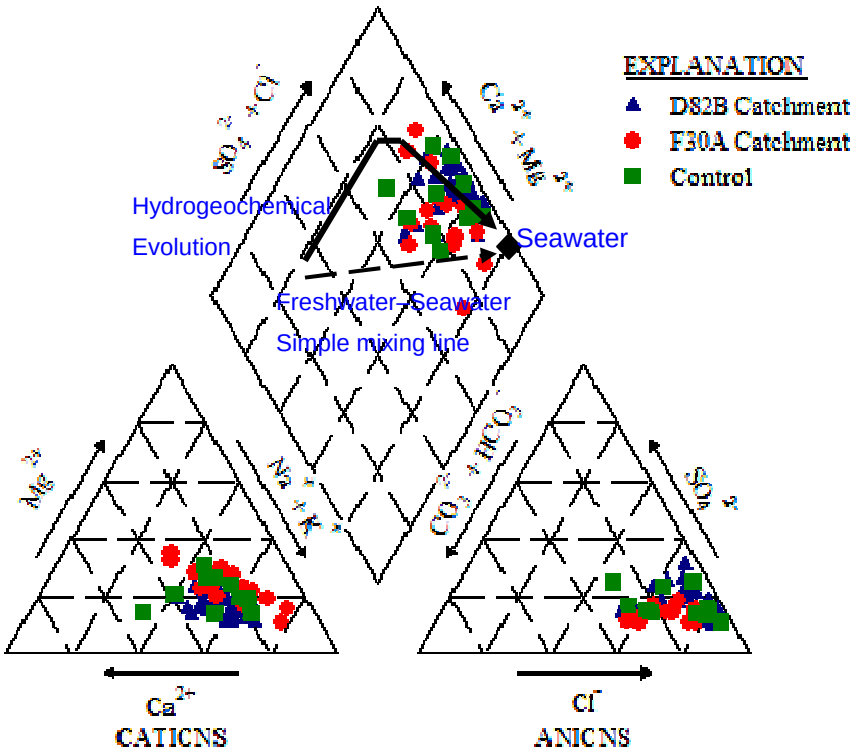


Fig. 6.1: Piper diagram for groundwater chemistry in the F30A, D82B catchments and the control Samples.

In the cationic triangle of Piper diagram, most samples are plotted on Na-dominant area. In the anionic triangle, the values are almost plotted near the seawater composition because of the predominance of chloride. In the diamond field, water samples are plotted in the Na-Cl dominant field, some samples are

plotted on the transition line between Na-Cl field and Ca-Mg-SO_4 field and the rest plots in the Ca-Mg-SO_4 field.

The samples show that the groundwater in the area is evolving. The geochemical evolution is shown by the wide range of sample distribution in the diamond-shaped field (Fig. 6.1). The evolution is caused by the different rock types within the lithology of the area. As groundwater flow through the fractured basement aquifer geochemical processes such as ion exchange, adsorption, mixing/dissolution, etc. take place. Also long residence time of groundwater within the aquifer promotes rock-water interaction which results in the alteration of the groundwater chemistry. Catchment F30A has low Cl and TDS while catchment D82B has high Cl and TDS which shows mixing and evolution from F30A to D82B.

The samples are widely distributed between 20–70% Ca+Mg, 30–80% Na+K and between 50–100% SO_4+Cl in the diamond-shaped field (Fig 6.1). The shift of the samples to the far right in the diamond-shape field depict the presence of salt (NaCl) in the groundwater samples (Allen and Suchy, 2001; Sayko, et al., 2004).

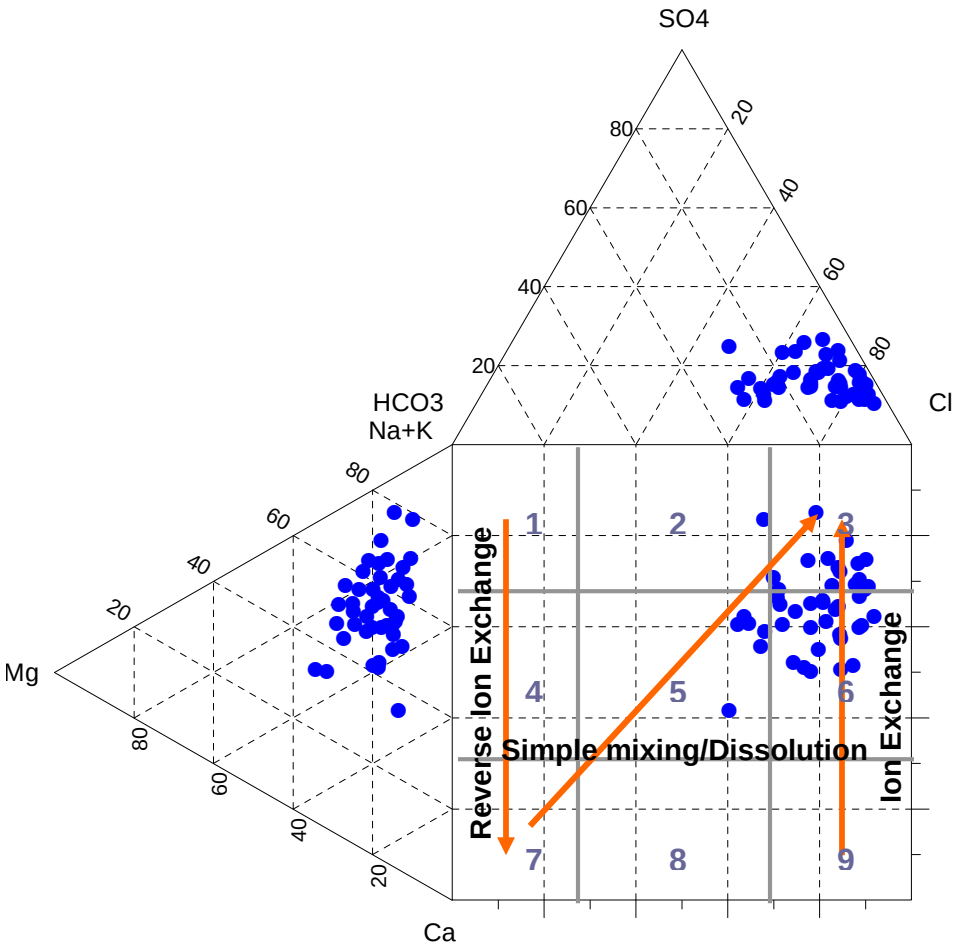


Fig. 6.2: Durov plot of the groundwater samples showing geochemical evolution trend.

The Durove plot (Fig. 6.2) reveal geochemical processes that are taking place in the fractured basement aquifers in the area. The groundwater of both catchments plot in fields 3, 5 and 6 in the Expanded Durov diagram (Fig 6.2). The fields are explained by (Lloyed and Heathcote, 1985) as follows:

- "3. HCO_3^- and Na^+ dominant often indicates ion exchanged waters,
- 5. No dominant anions or cations, indicates water resulting from dissolution or mixing, and
- 6. SO_4^{2-} (or anion indiscriminate) and Na^+ dominant, is a water type not frequently found and may be due to mixing influences"

The above explanations may also be seen in the groundwater type below (Table 6.1)

Table 6.1: Groundwater Type presentation of the study area catchment D82B (yellow), F30A (green) and the control samples (orange).

Sample ID	Water Type of the Area	Sample ID	Water Type of the Area
JL 07/01	Na-Ca-Cl	JL 07/49	Na-Cl
JL 07/02	Na-Cl	JL 07/51	Na-Ca-Cl
JL 07/09	Ca-Na-Cl-SO_4	JL 08/01	Na-Ca-Cl
JL 07/11	Na-Ca-Cl-SO_4	JL 08/03	Na-Ca-Cl
JL 07/13	Na-Ca-Cl-SO_4	JL 08/05	Na-Ca-Cl-HCO_3
JL 07/15	Na-Ca-Cl	JL 08/07	Na-Ca-Cl
JL 07/17	Na-Ca-Cl-HCO_3	JL 08/09	Na-Ca-Mg-Cl
JL 07/19	Na-Ca-Cl-SO_4	JL 08/11	Na-Ca-Cl
JL 07/21	Na-Ca-Cl	JL 08/19	Na-Ca-Cl
JL 07/23	Na-Cl-SO_4	JL 09/07	Na-Ca -Cl
JL 07/25	Na-Ca-Cl	JL 09/09	Na-Ca-Cl
JL 07/27	Na-Ca-Cl	JL 09/11	Na-Cl
JL07/29	Na-Ca-Cl-SO_4	JL 09/13	Na-Ca-Mg-Cl-SO4
JL 07/41	Na-Ca-Mg-Cl-HCO_3	JL 09/15	Na-Ca -Cl
JL 07/47	Na-Ca-Mg-Cl	JL 08/25	Na-Mg-Cl
JL 07/31	Na-Cl-HCO_3	JL 08/27	Na-Mg-Cl
JL 07/33	Na-Mg-Ca-Cl	JL 08/29	Na-Mg-Cl
JL 07/35	Na-Cl	JL 08/31	Na-Ca-Mg-Cl
JL 07/37	Na-Cl	JL 08/33	Ca-Na-Mg-Cl
JL 07/39	Na-Mg-Cl-HCO_3	JL 08/37	Mg-Na-Ca-Cl
JL 08/13	Na-Ca-Mg-Cl-HCO_3	JL 09/17	Na-Ca-Cl-HCO3
JL 08/21	Na-Ca-Mg-Cl-HCO_3	JL 09/23	Na-Ca-Cl
JL 07/03	Na-Ca-Cl-HCO_3	JL 09/01	Na-Ca-Cl-SO4
JL 07/04	Na-Mg-Ca-Cl-SO_4	JL 09/03	Na-Cl
JL 07/43	Na-Mg-Ca-Cl-HCO_3	JL 09/05	Na-Cl
JL 07/45	Na-Mg-Cl-HCO3	JL 09/19	Na-Cl
JL 08/23	Na-Cl	JL 09/21	Na-Ca-Mg-Cl
JL 08/35	Ca-Na-Cl-HCO_3-SO_4		

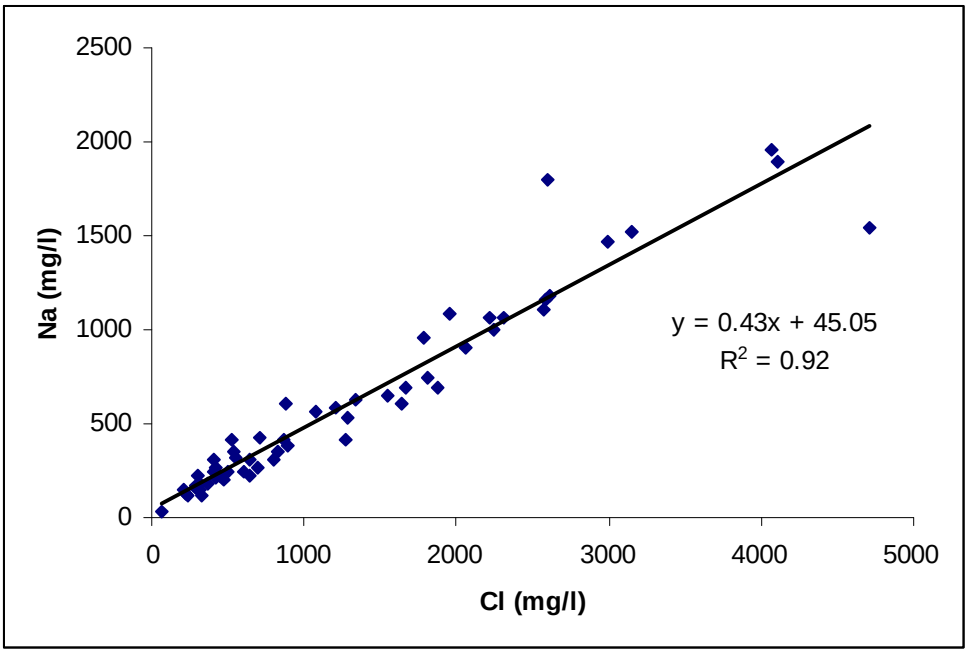
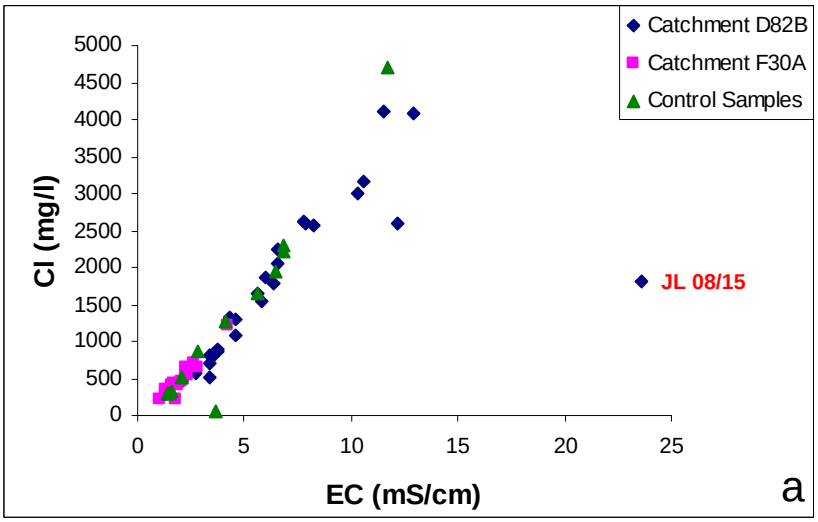
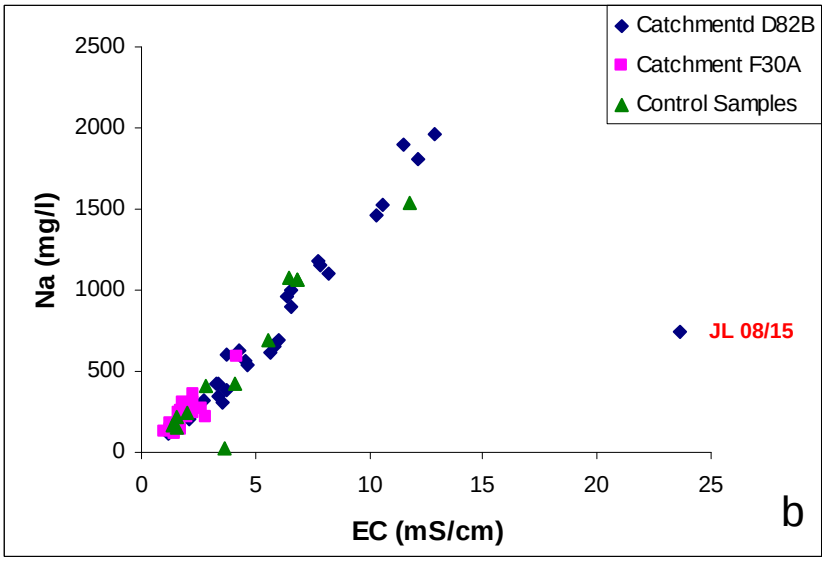
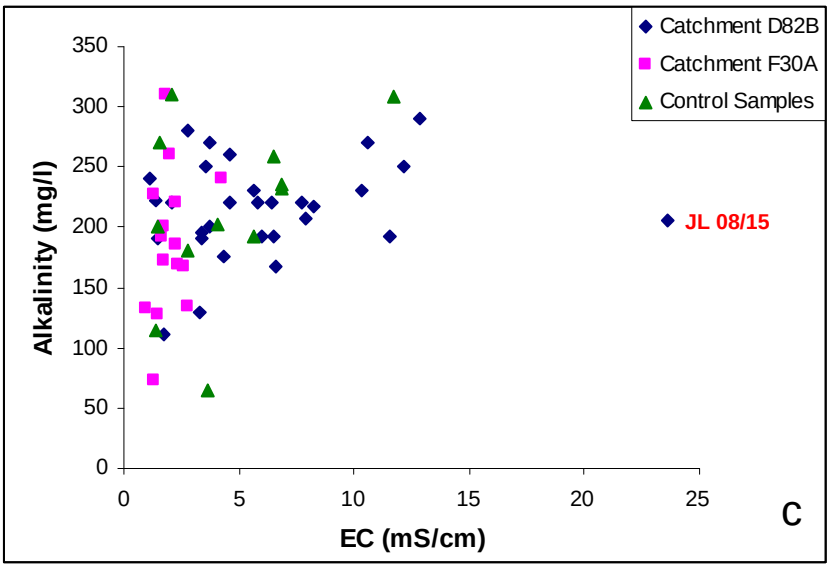


Fig. 6.3: Na/Cl relationship in the study area

The above scatter diagram (Fig. 6.3) shows that the relationship between sodium and chloride is directly proportional, which support mixing process (Fig 6.3, 6.2 and 6.1). The strong correlation between these two ions indicates that the most salinity in the groundwater of the area is due to salt (leaching of evaporitic deposits where NaCl, $CaSO_4$, $CaSO_4.H_2O$ are abundant) or sea water intrusion, evaporation or mixing processes (Nencetti et al., 2005; Rabemanana et al., 2005; Portugal et al., 2006; Kalisperi et al., 2010). This diagram also shows perfect mixing line and similarity of groundwater in two basins where there is a continuous flow from one catchment (F30A) to the other (D82B).


Catchment D82B
Catchment F30A
Control Samples
JL 08/15
Cl (mg/l)
EC (mS/cm)
a


Catchmentd D82B
Catchment F30A
Control Samples
JL 08/15
Na (mg/l)
EC (mS/cm)
b


Catchment D82B
Catchment F30A
Control Samples
JL 08/15
Alkalinity (mg/l)
EC (mS/cm)
c

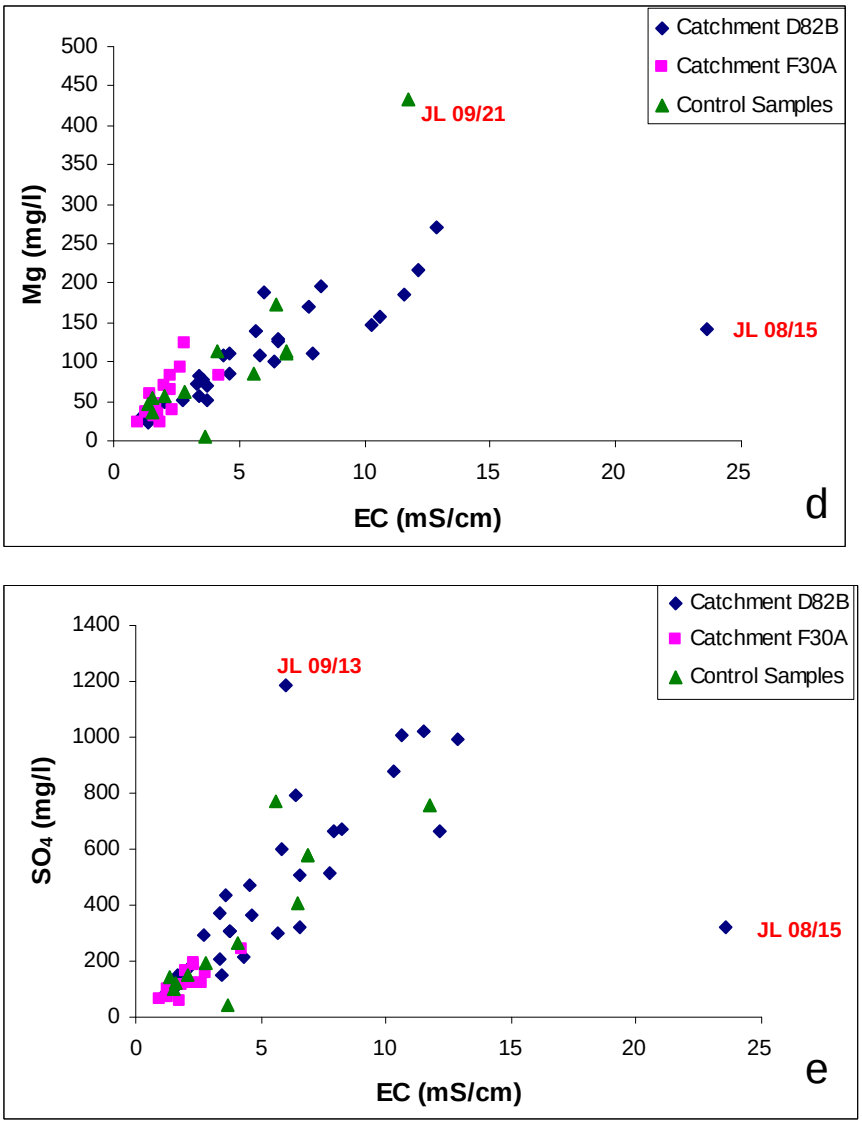


Fig. 6.4: The control of ions over EC.

The strong correlation between various major elements and EC indicate that there are several possible sources of salinity. The good linear correlation of EC and Cl (Fig 6.4a) implies that the increase in EC is directly related to salinity source from rocks (Hasan et al., 2009). In Fig 6.4a, some samples show a domination of Cl indicating an additional source like evaporation over rock weathering. Figure 6.4(c), suggests carbonate and/or soil CO_2 as a source of alkalinity.

Sample JL08/15 (from D82B catchment), show higher EC value and low concentration of the other constituencies (Cl, Na, alkalinity, Mg and SO_4) (Fig 6.4a, b, c, d and e). This borehole is the only one that is located in the burtons puts granite. Thus the results outline a completely different chemical composition of the granite compared to the surrounding lithologies.

In Fig. 6.4d, sample JL09/21 show elevated Mg concentration; this sample is located in the hytkoras formation. The high Mg concentration is from the lithology which is coarse grained cordierite-hypersthene-biotie gneisses, which according to Agenbacht (2007) contain concentrations of the rare magnesium-aluminium silicates sapphirine and kornepine. Sample JL09/13 in Fig. 6.4e shows high sulphate concentration suggesting additional source of sulphate.

The area has noticeably high nitrate concentrations ranging from 4.37mg/l to 448.86 mg/l. There is no clear source of the nitrate in the area, therefore, the high nitrate concentration is presumed to be natural. This observation needs to be confirmed through ^{15}N. Nitrite was not detected in the water samples to indicate bacterial induced.

The only source of Nitrate in the area may be igneous rocks or clays since there are no agricultural activities or sewage facility and the area is sparsely populated (no developments in the area). Salts, sodium and potassium nitrates are the main N-bearing minerals (Jordana and Batista, 2004). In addition Jordana and Batista, (2004) stated that in very arid regions nitrate/nitrogen may be found in concentration more than the recommended limit of 50 mg/l nitrate (WHO, 2006) due to natural fixation (e.g. fixation by leguminous plants or micro-organisms).

Nitrate was plotted against sulphate and chlorite, and sulphate against chlorite to understand if the anions are from the same source and also to understand the groundwater flow path (Fig. 6.5a, Fig. 6.5b and Fig. 6.5c respectively).

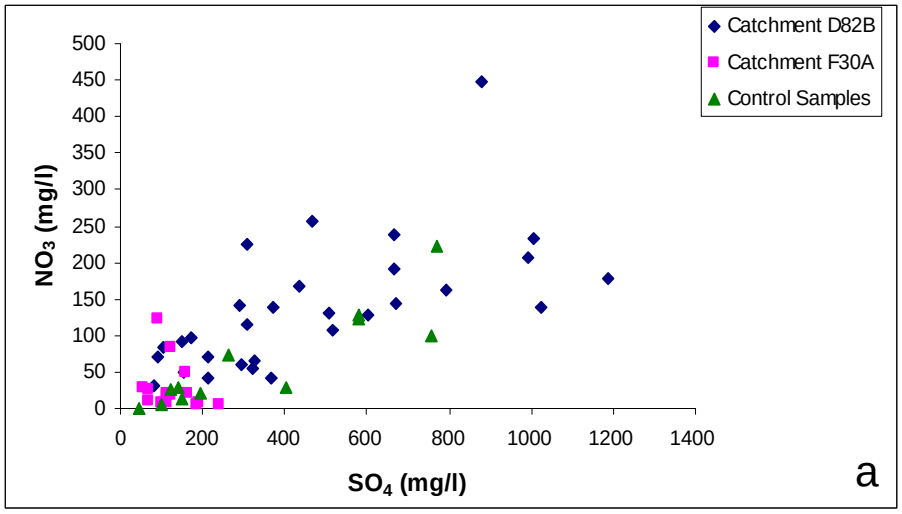


Figure 6.5a: Nitrate vs. sulphate diagram.

The above diagram (Fig 6.5a) show dispersed points with no clear correlation between nitrate versus sulphate; these suggest a possibility of different sources.

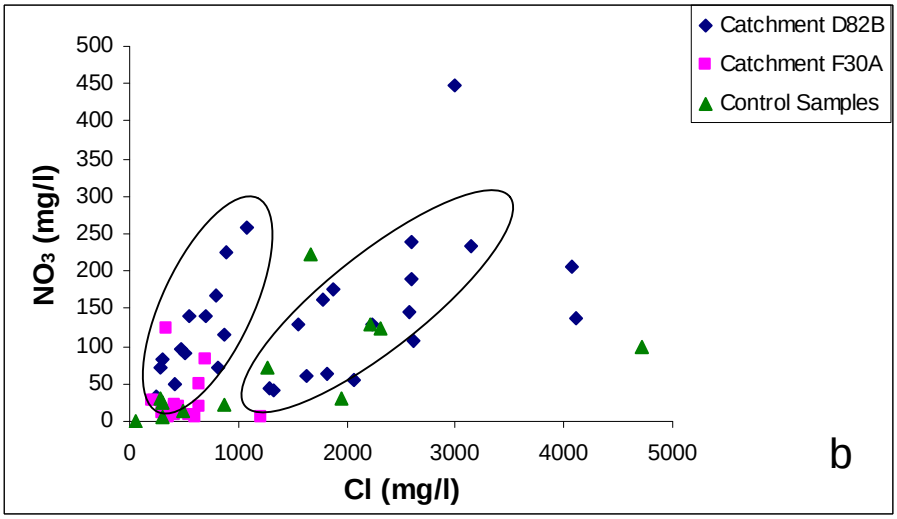


Fig. 6.5b: Nitrate vs. chloride diagram.

The above diagrams (Fig 6.5b) shows disperse points with no clear correlation between nitrate versus chloride in catchment F30A and the control samples. In catchment D82B the samples points show two groupings which suggests a possibility of two different groundwater flow path.

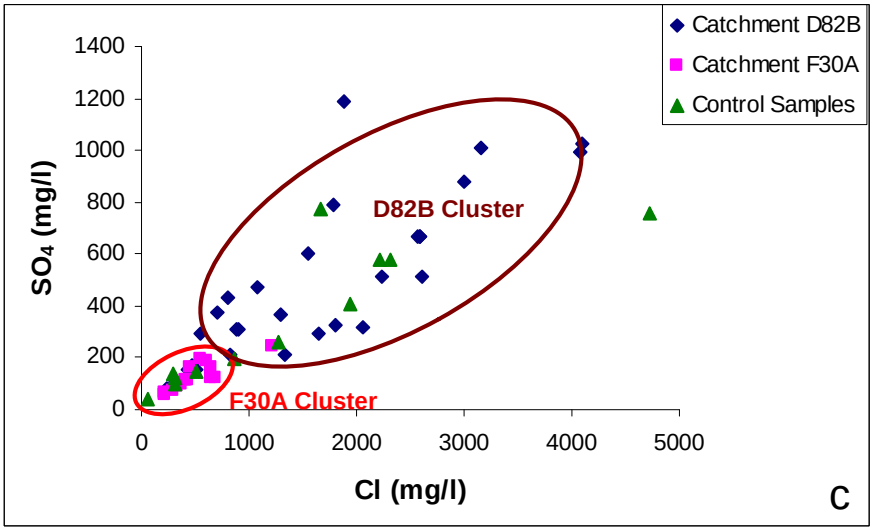


Fig. 6.5c: Sulphate vs. chloride diagram.

The plot for sulphate versus chloride (Fig. 6.5c) shows a good correlation suggesting that they both results from a common source or processes e.g. dissolution of secondary evaporate minerals or evaporates (Fig. 6.5c), especially in F30A catchment. The most likely source of sulphate is from the dissolution of gypsum, oxidation of pyrite and weathering of pegmatites in the study area. The diagram also shows two distinct pathways in catchment D82B. This means two different flow path in the aquifer, (i.e.) deep and shallow groundwater flow.

Fig. 6.5c shows two trends. The recharging area (F30A) has similar Cl versus SO_4 while both anions follow different evolution trend as groundwater flow to catchment D82B. In this catchment (D82B) there could be strong pyrite oxidation process than in catchment F30A.

A Gibbs diagram was plotted to understand the processes that are controlling the water chemistry in the study area (Fig. 6.6).

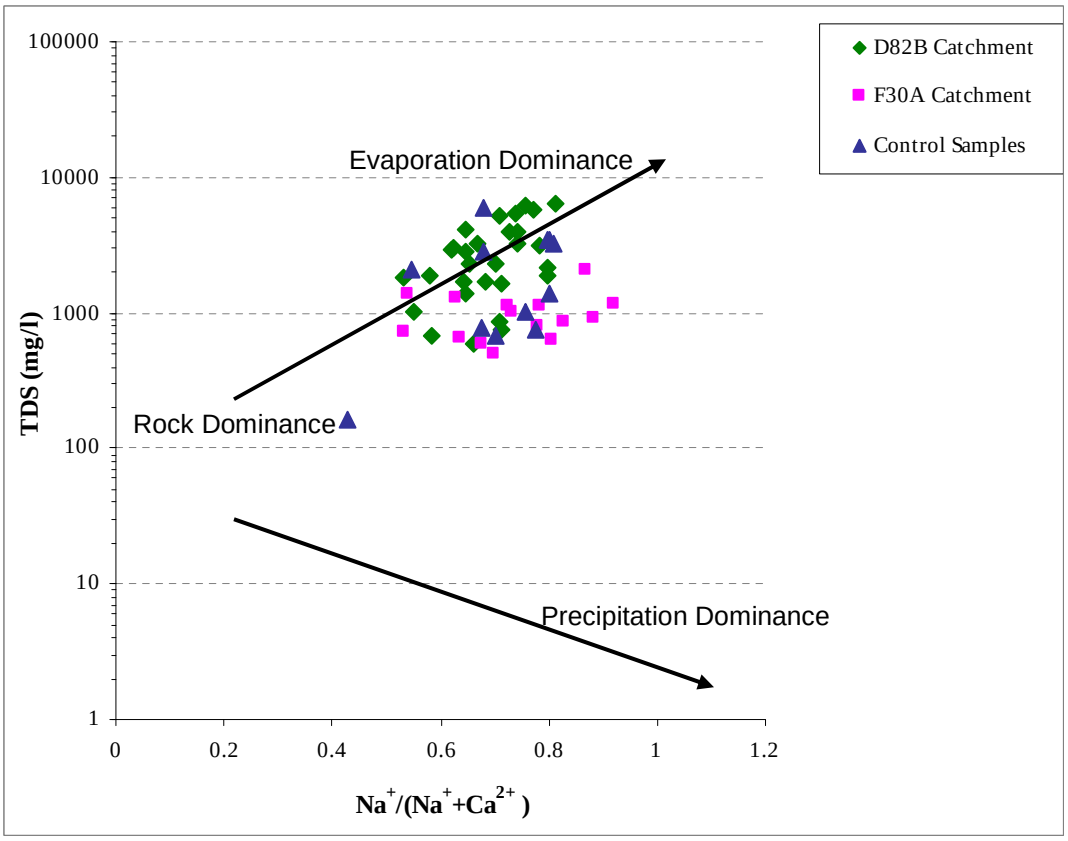


Fig. 6.6: Plot that depicts processes controlling water chemistry (based on Gibbs, 1970).

Trabelsi et.al, (2007) define salinity as the total amount of inorganic solid material dissolved in any natural water and is expressed as TDS (Total Dissolved Solids). The Gibbs diagram show that all the groundwater samples of the area plots in the evaporation field except one sample (JL 08/35) from the control samples which plots in the rock dominance field (Fig. 6.6). This means that the samples are affected by evaporation either before or during recharge and the groundwater chemistry of sample JL 08/35 is characterised by rock-water interaction. The sample shows no direct infiltration from precipitation.

Bromide and chloride are conservative elements and, therefore, can be used to define physical processes such as mixing, evaporation among others. Bromide concentration in groundwater is generally low, but high concentrations of this

element sometimes occur in groundwater by pollution, interaction with seawater or reaction with evaporite deposits (Mokrik et al., 2005).

Br^- vs. Cl^- diagrams were plotted to establish the source of salinity in the groundwater samples (Fig 6.7a and b).

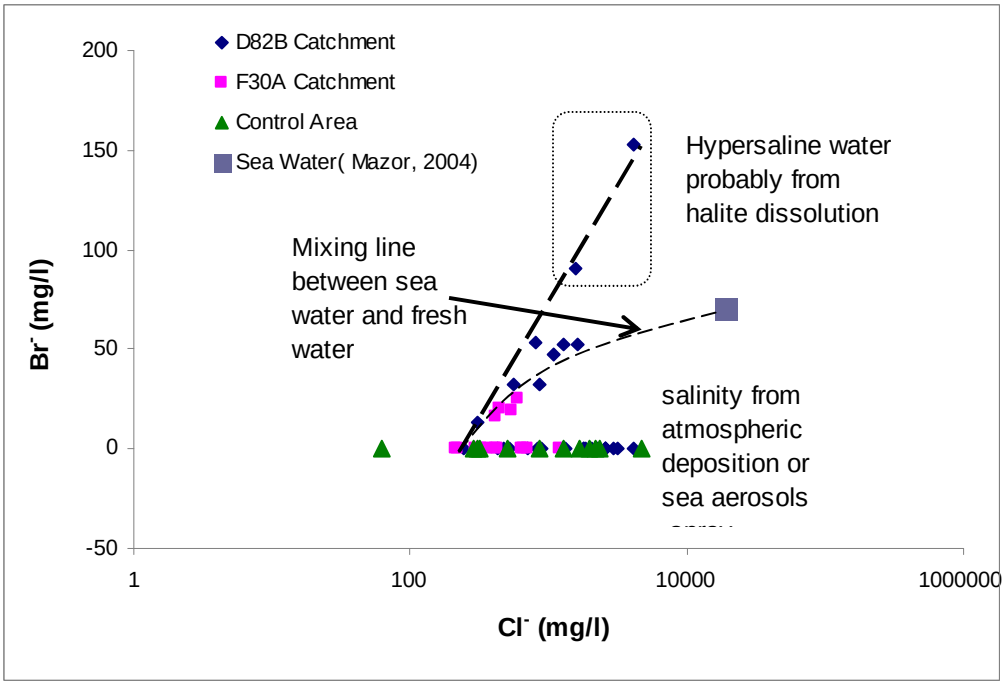


Fig. 6.7a: Br^- vs. Cl^- diagram

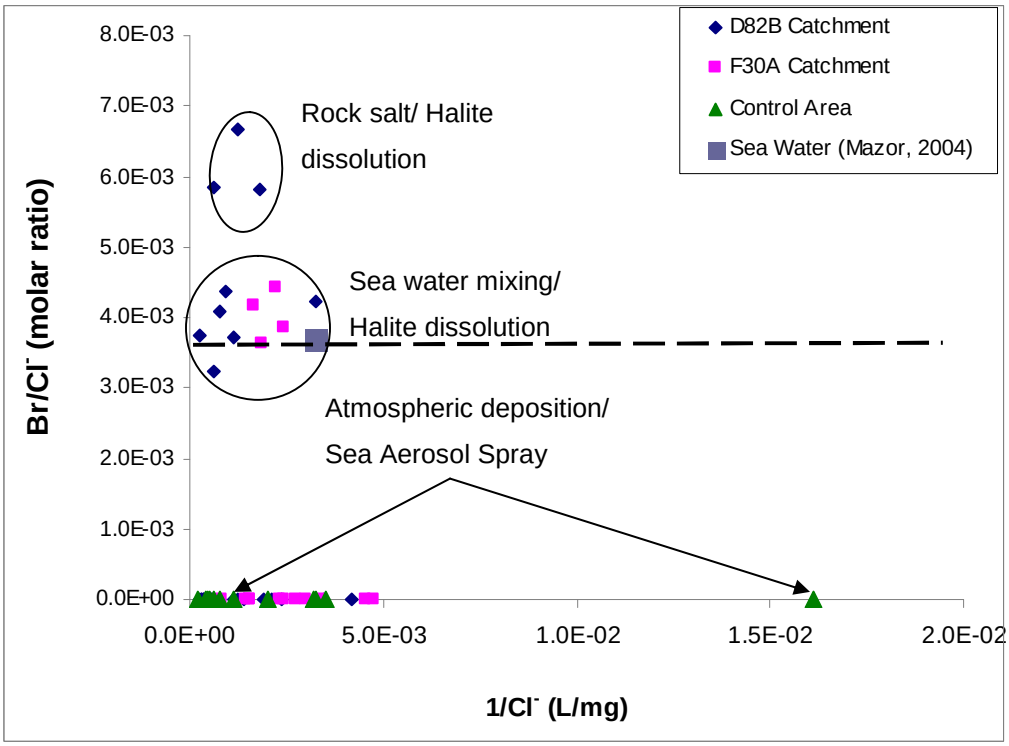


Fig.6.7b: Br^-/Cl^- ratio vs. $1/Cl^-$ diagram

The Br/Cl ratio for the samples exceed the marine ratio of 0.0035 (Fig. 6.7a) and this means that the groundwater could originate from marine formations (Edmunds et al., 2006). The occurrence of high chloride concentrations in the F30A catchment which has high recharge (freshwater) indicate evolution by evaporation and/or that the rainfall of the area has high Cl concentration (NaCl) (Edmund et al., 2006)

The above Br vs Cl graphs (Figs. 6.7a and b) show that the salinity in the area results from sea water mixing, halite dissolution and atmospheric deposition/ sea aerosol spray. Under excessive evaporative regimes, as experience in arid environments some of the groundwater is heading towards hypersaline waters especially that of D82B catchment (Figs. 6.7a and b). The F30A catchment seems to have its Cl and Br ions from atmospheric deposition/sea aerosol spray, with some of the samples showing salinity from seawater intrusion/halite

dissolution (Figs. 6.7a and b). The control area show that the groundwater salinity is from atmospheric deposition/sea aerosol spray (Figs. 6.7a and b).

The presence of fluoride in the groundwater of the two catchments presumably results from local rock composition. The local lithology of the area is mainly granites and gneiss which is covered by alluvium, calcareous, gypsiferous soil, e.t.c. Sanexa and Ahmed (2001) concluded that interaction of fluoride-enriched minerals with water and residence time are important factors controlling the fluoride dissolution process. Other factors which are favourable for fluoride dissolution are conditions like alkaline and high EC between 750–1750 µS/m (Sanexa and Ahmed, 2003).

6.2. Stable Isotopes

Ten groundwater isotope data from catchment F30A and ten isotope data from catchment D82B were plotted to assess possible source of recharge and groundwater circulation in the area. Data interpretation was undertaken using Windhoek Meteoric Water Line, global meteoric water line and local evaporation line as references.

Regarding the stable isotope of groundwater Mook, (2006) describes that pluvial or fossil groundwater tends to plot on or below the GMWL (Fig. 6.8). The same work also deems the correlation of groundwater and precipitation in semi arid/arid region as complicated process. The stable isotope analyses indicate that the samples have undergone fractionation due to evaporation before infiltration because they plot below the WLMWL. Groundwater samples (Group 1) from catchment D82B plots away from the GMWL showing isotope enrichment due to evaporation which has been supported by major ion results and high salinity occurrence. Group 2 samples (F30A) show infiltration from local precipitation with signs of infiltration after evaporation, plotted below but close to the local meteoric water line

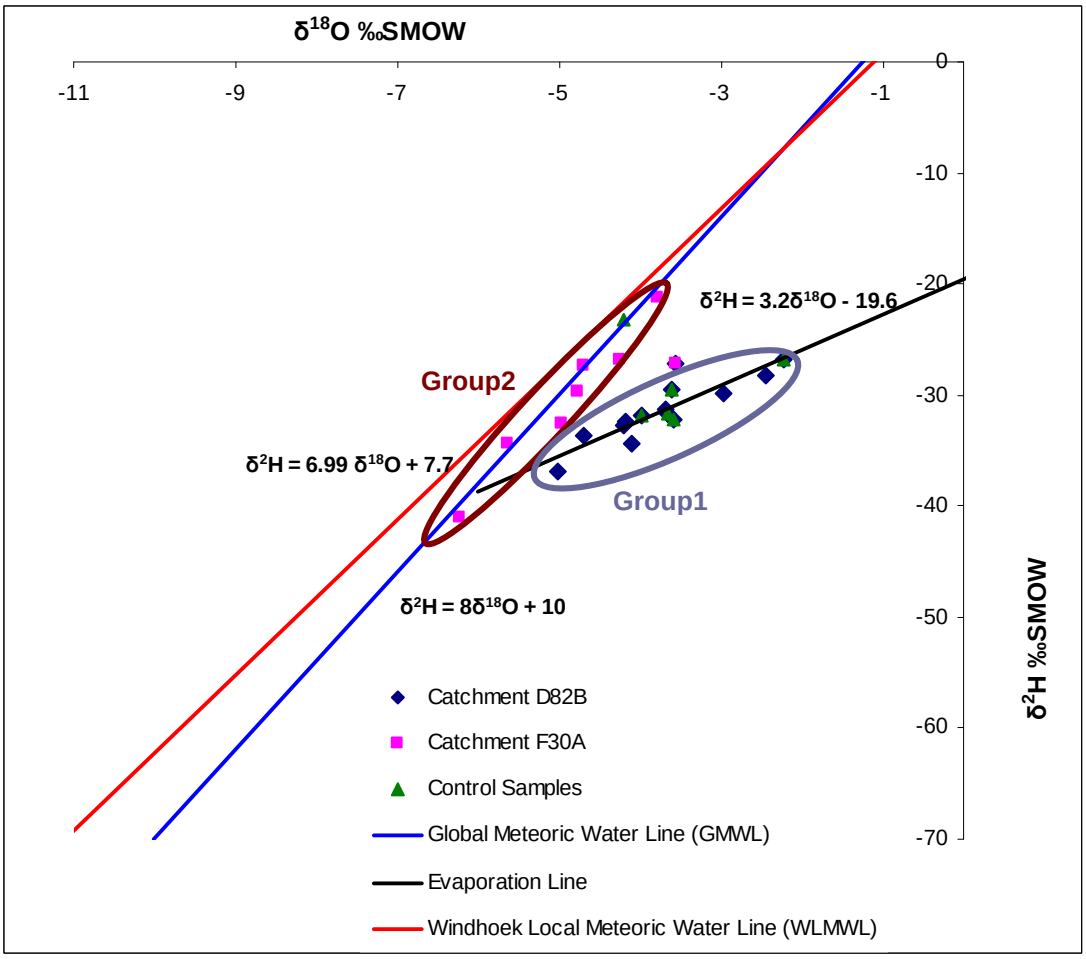


Fig. 6.8: Stable isotope plot relative to Global Meteoric Water Line (Craig, 1961) and Windhoek Local Meteoric Water Line.

The displacement of the samples from the GMWL and WLMWL show that the groundwater has been affected by evaporation, mixing of saline water (connate) from the aquifer, or increasing $\delta^{18}O$ values with increasing Cl^- concentration which is observed in Figs. 6.8 and 6.9b (Currel et al. 2010).

The strong variations in the stable isotope values are mainly due to seasonal variation in precipitation and altitude effects (Nordstrom et al., 1992). Sulphate, nitrate and chloride were plotted against $\delta^{18}O$ in the following diagrams to understand the occurrence of salinity and evaporation in the area Fig. 6.9.a, Fig. 6.9.b and Fig. 6.9.c.

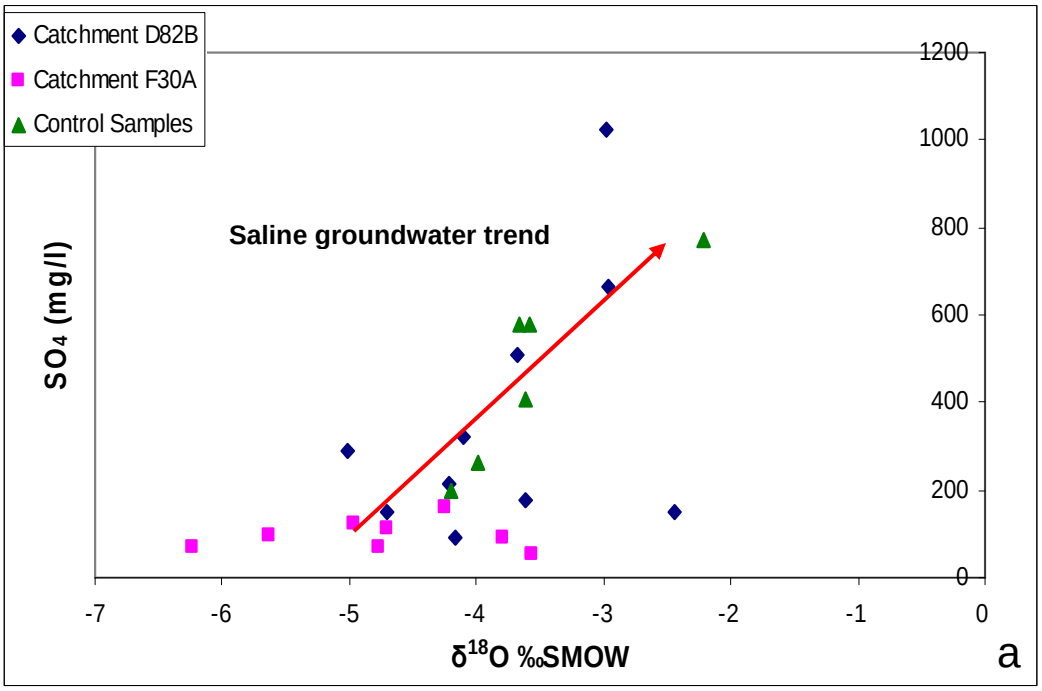


Fig. 6.9a: $\delta^{18}O$ vs. Sulphate.

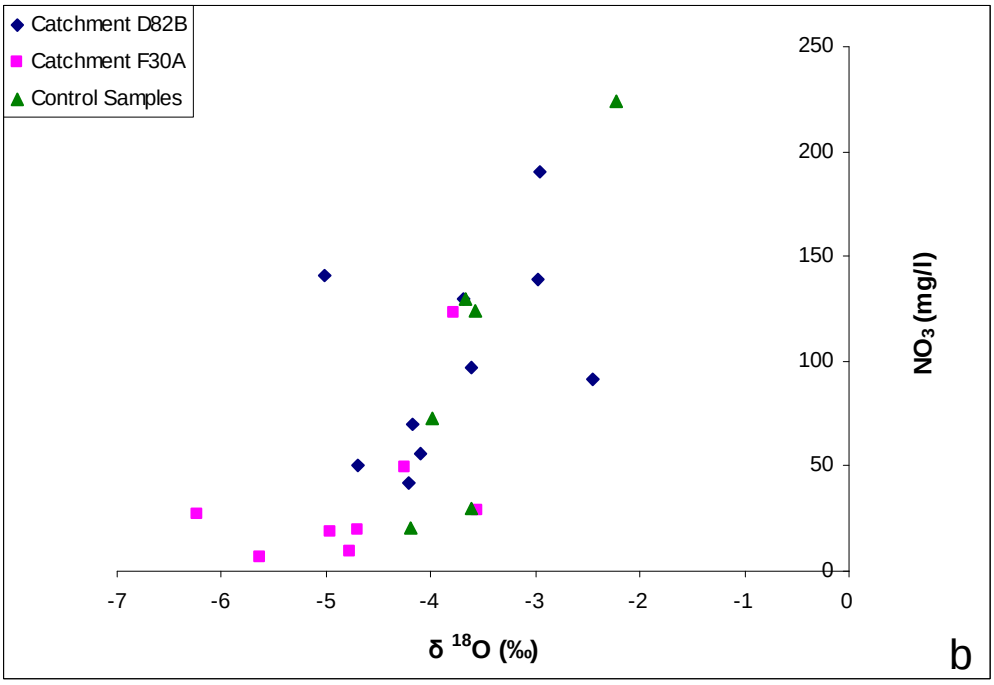


Fig. 6.9b: $\delta^{18}O$ vs. NO_3.

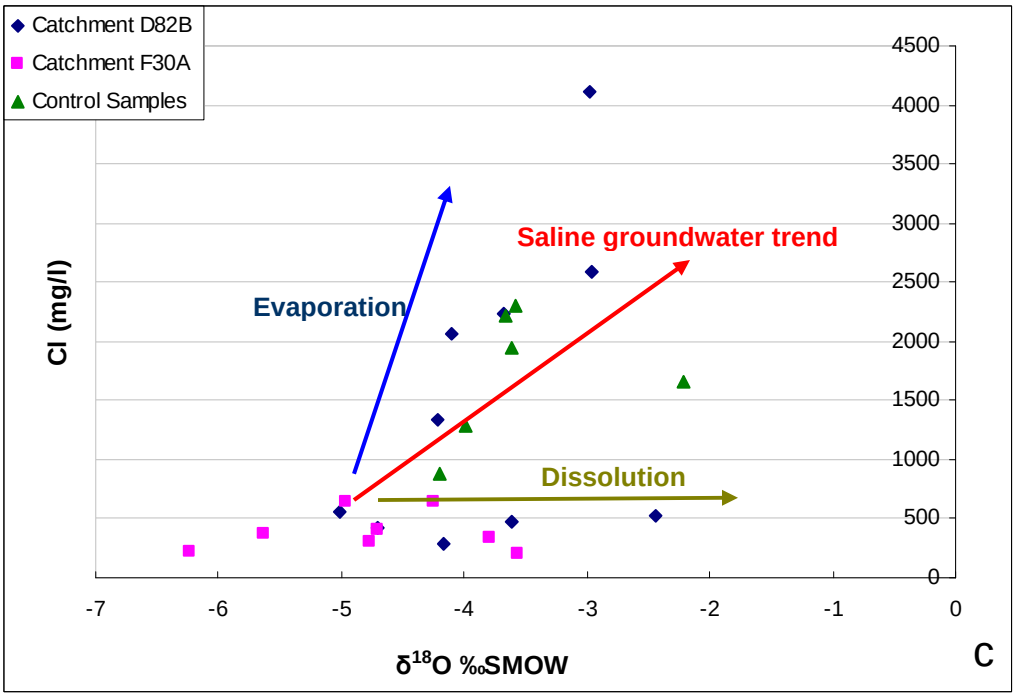


Fig. 6.9c: δ ^{18}O vs. Chloride

According to Gonfiantini et al. (1998), the high salinity and chloride contents of these groundwaters in the area (EC 12.88 mS/cm and Cl 4716mg/l) could indicate high evaporation rates from the recharge area and the dissolution of evaporites in the area. The above diagrams (Figs 6.9a, b and c) show almost similar trend of chloride, nitrate and sulphate in the groundwater as plotted against $\delta^{18}O$. These diagrams show that salinity and evaporation occur in the groundwater of the study area. Fig. 6.9a and b show enrichment of oxygen isotope with increasing SO_4 and NO_3 respectively. This means that the water receives oxygen isotopes from the sulphate and nitrate oxygen.

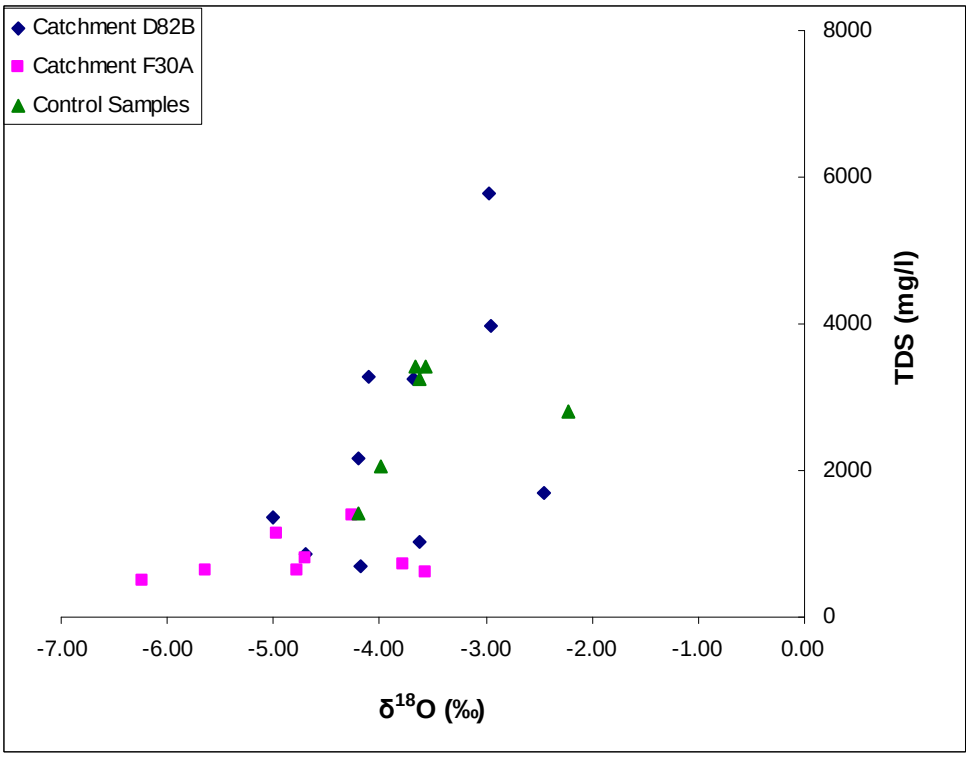


Fig. 6.10: TDS vs. $\delta^{18}O$

Also Fig. 6.10 shows $\delta^{18}O$ depleted groundwater with low TDS and the water become enriched through groundwater evolution along flow path (Gastmans et al., 2010). The isotope enrichment with increasing TDS indicates that the groundwater of the area in addition to evaporation and altitude effect it is also characterized by rock-water interaction.

6.3. Tritium Data

A total of 18 tritium data and six control samples were plotted against Cl to depict the groundwater flow path. The highest TU value analysed in the groundwater samples in the area is 2 TU. The age of the groundwater calculated from average tritium of the local rainfall (Windhoek) of 28.32 TU, ranges from 87.01 to 174.02 years.

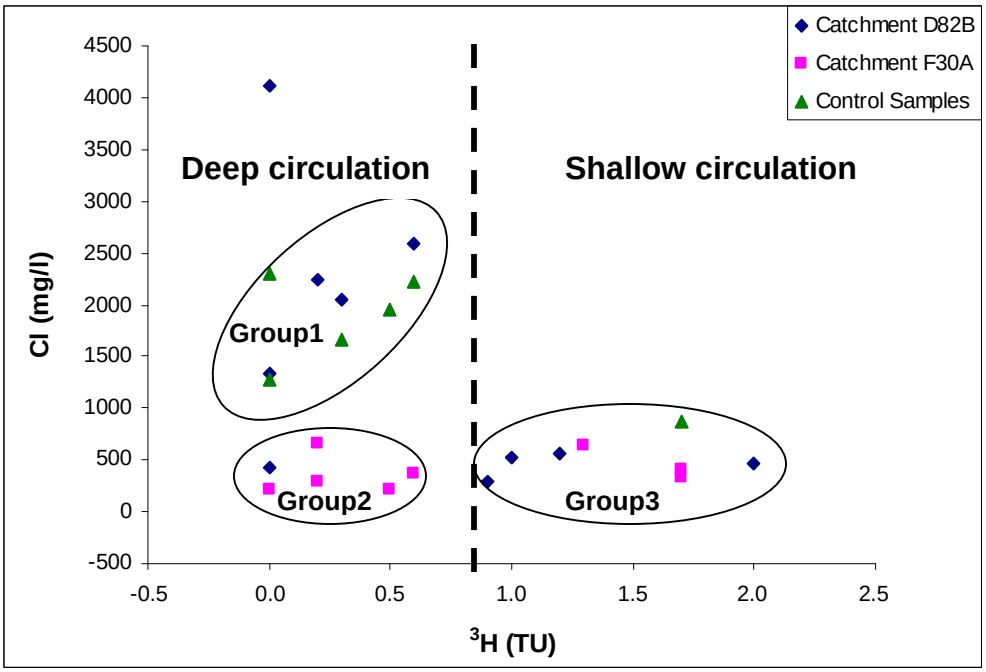


Figure 6.11: Tritium vs. Cl^-

The highly distributed TU values (0–2 TU) in catchment F30A implies comparatively higher level of recharge than the D82B catchment (Fig. 6.11). The older groundwaters of 0.0 TU in the area may result from upwelling of old groundwater from within the granites and/or metamorphic bodies. Moreover, the variation in tritium values may be attributed to flow direction and velocities within faults and fractures in the area. Fracturing and faulting may lead to mixing of waters from different aquifer units.

Mixing between high salinity or brine with modern meteoric water in the area is demonstrated by the decrease in salinity in most boreholes (Clark and Fritz, 1997). Fig. 6.11 shows three distinct groundwaters in the area:

1. Group 1 – is deep circulating water which is characterised by higher Cl values >1000 m/l and lower tritium values of less than 0.8 TU (Fig. 6.11). The groundwater with low tritium units and higher Chloride concentration is from the low lying or flat areas of the study area Indicating groundwater which underwent sever evaporation before and/or during recharge.

2. Group 2 –is a deep circulating groundwater which is characterised by Cl values less than 1000 mg/l and a range of tritium values of less than 0.8 TU) These samples are mostly from F30A catchment.
3. Group 3 – a shallow circulating groundwater which is characterised by low chloride and low tritium content. The group 2 and group 3 water samples show almost similar signature of chloride which indicate the same recharge source (Fig 6.11).

6.4. Salinity and Recharge/discharge Area Delineation

The spatial distributions patterns for TDS (mg/l), EC (mS/cm) and Na (mg/l) of the two catchments (Figs. 13, 14 and 15) has been developed using a GIS software ARC Info 9.1 version and it shows almost similar patterns. The Figs.6.13, 6.14 and 6.15 show that major recharge occur in catchment F30A which is characterised by fractures and faults and in the D82B catchment recharge takes place in the higher areas and where the fractured basement aquifers are exposed consistent with stable isotope and tritium data.

The recharge in catchment F30A maybe due to the faults, fractures and lineaments that extends throughout the catchment (Fig. 4.10). The recharge in catchment F30A is probably from the adjacent catchments or the Kamiesburg Mountains in the eastern side of the catchment. The isotopes results show no direct infiltration of precipitation in the area.

In catchment D82B recharge takes place in the higher lying areas where the fractured basement aquifers are exposed (Fig 4.11). Recharge water flow through preferential flow to the low lying areas of the catchment (shown by arrows in Figs. 6.13, 6.14 and 6.15).

High values of Na, TDS and EC which resulted poor water quality cold be derived from the salts that are dissolved by precipitation and subsequent evaporation in

the study area. During precipitation the fast dissolving salts could be washed away by run-off and shallow groundwater flow to the low lying (flat) areas. Under direct sun water evaporates and leaves the salts concentrating on the surface (Fig 6.12), this lead to accumulation of salts and also account for the several salt pans found in the study area especially, catchment D82B (Fig 4.11; P1, P2, P3 and P4).



Fig. 6.12: Salt found on the surface in the Bitterputs se Pan (P3 in Fig 4.11).

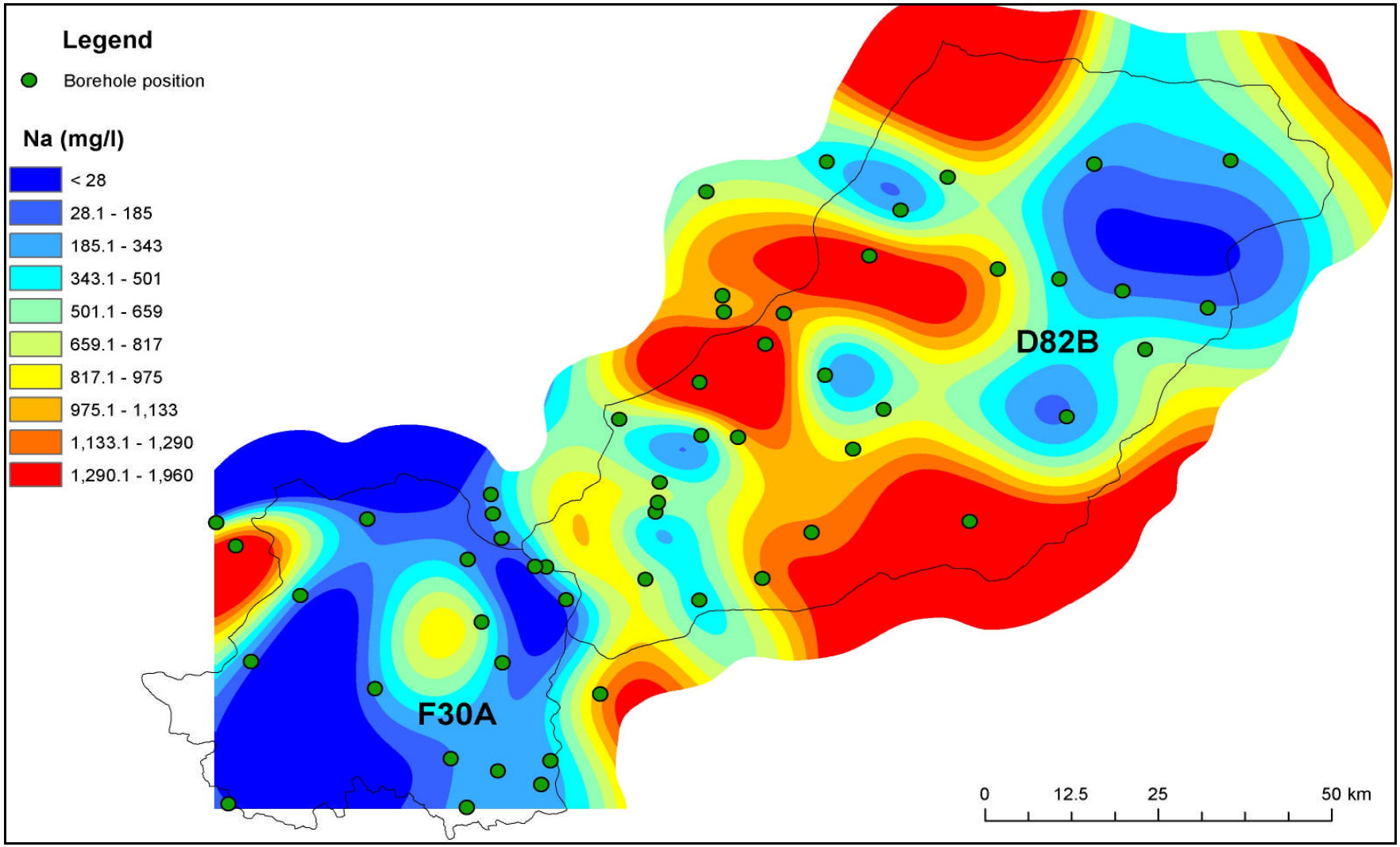


Fig. 6.13: Spatial distribution of Sodium (Na) in the area.

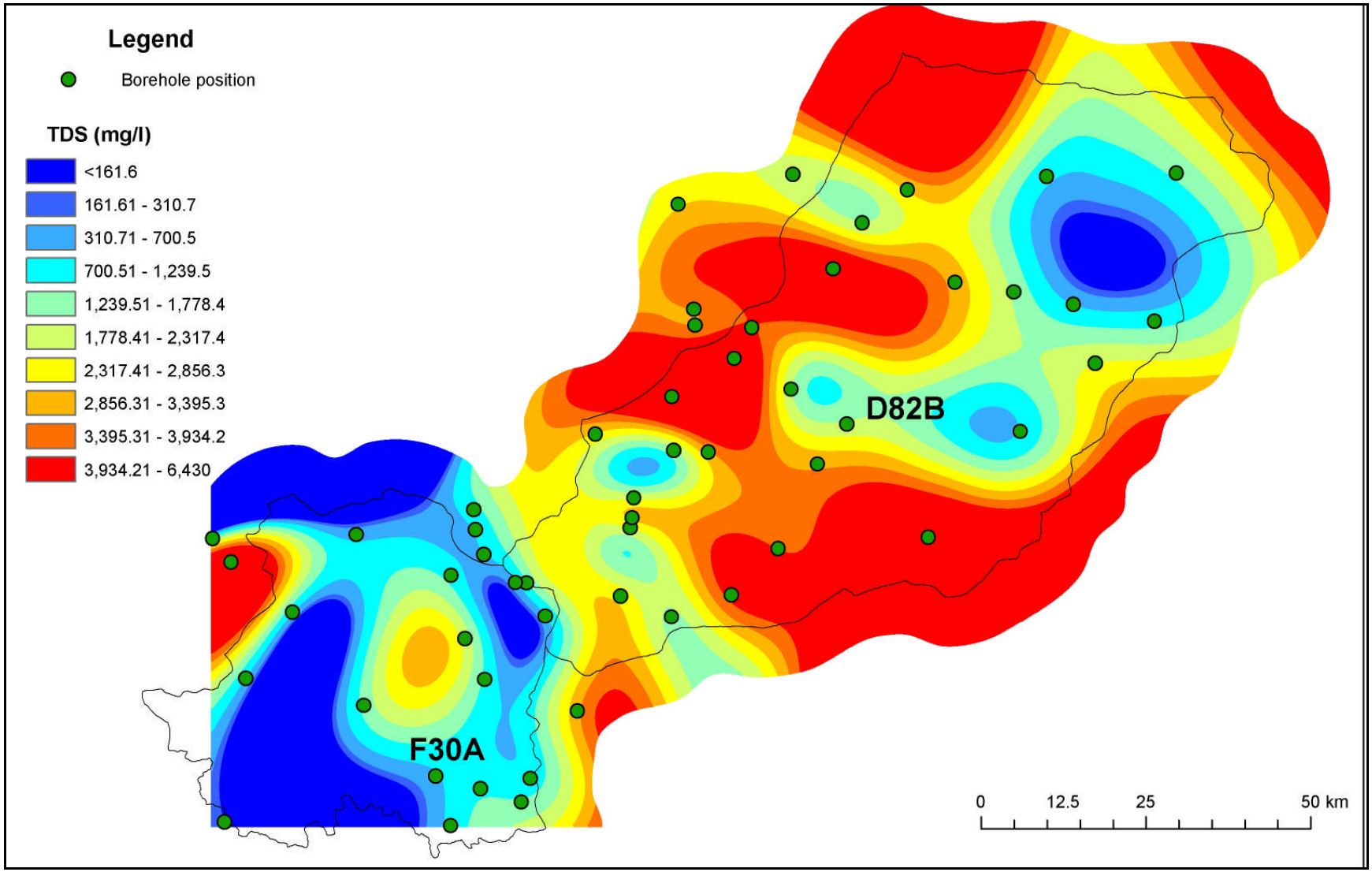


Fig. 6.14: Spatial distribution of the Total Dissolved Solids (TDS).

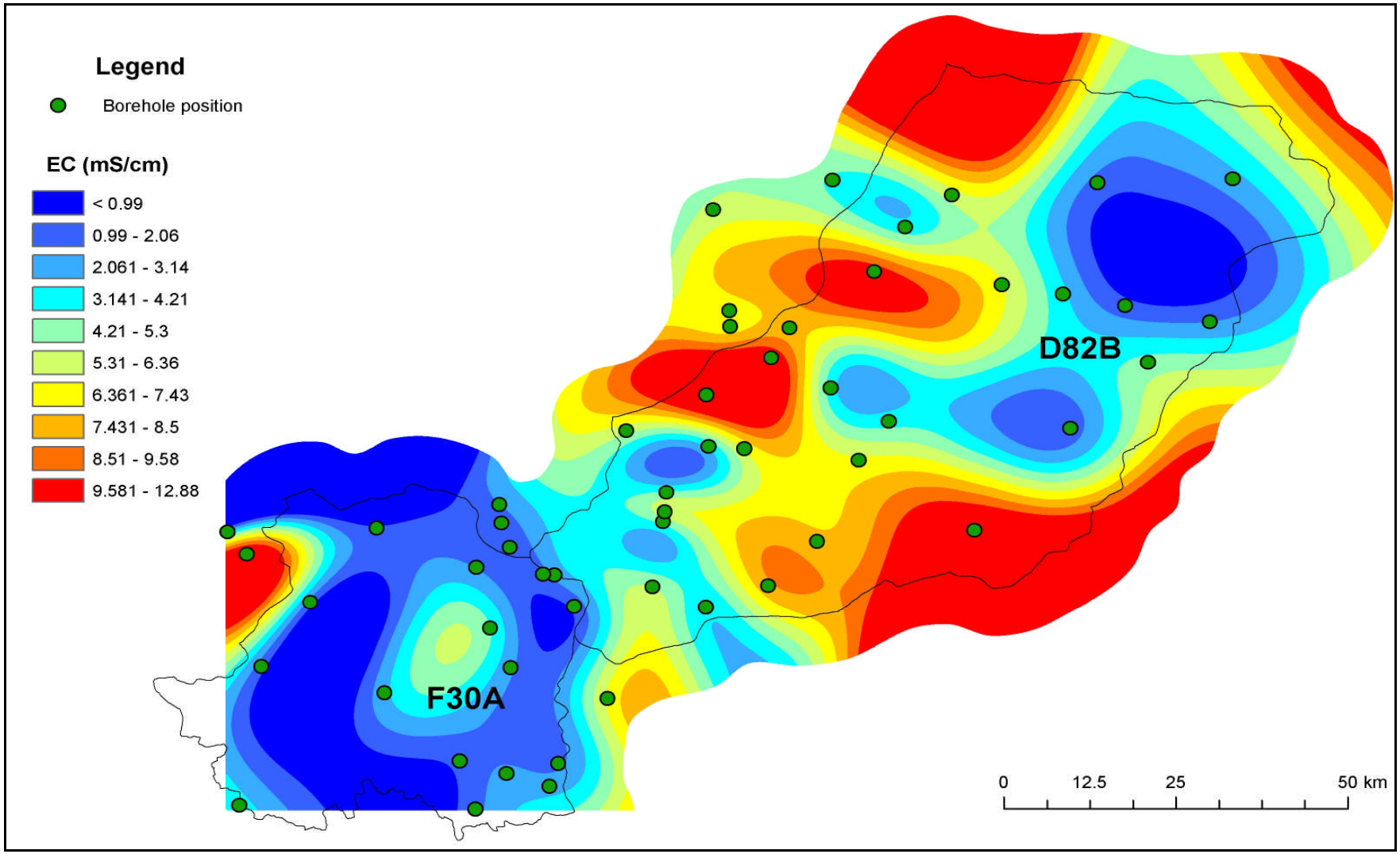


Fig. 6.15: Spatial distribution of the Electrical Conductivity (EC).

Salt deposits may also be formed by evaporation of the infiltrated water in the vadose zone and evapotranspiration. When the saline water move up to the surface during evapotranspiration and water is taken up by the plant roots the salt remain in the soil and increase salt accumulation in the subsurface.

Based on the topographic configuration, relation of hydrochemistry and environmental isotope cross catchment boundary groundwater interaction is taking place between the two quaternary catchments where water flows from catchment F30A to D82B and other surrounding catchments.

6.5. Uranium

Uranium in the area occurs naturally in the metamorphic and igneous rocks of the study area. The presents of the uranium bearing rocks such as pegmatite, lekkerdrink gneiss, mesklip gneiss etc. and the mineralization and mining of uranium, sulphur (in pyrite), diamonds (in alluvial), etc. in the study area increases the availability of these elements in the groundwater.

The influxes of oxidant (e.g., nitrate), and the presence of reductants (e.g., organic carbon, sulfide, Fe(II) will likely influence the rate and extent of U(IV) oxidation; also the concentration of fluoride, sulphate, calcium, potassium and phosphate with which to form complexes. The presents of uranium in high concentration in the groundwater of the area may be related to the slightly oxidation nature of the groundwater and the presents of carbonates and other reactants that keeps uranium in solution (nitrate, fluoride, sulphate, phosphate, etc.).

The redox potential data of the groundwater samples showed positive values, which indicate the presence of oxygen, which increases uranium solubility. Oxygen in the aquifers maybe from the fractures and faults in the study area

or/and from other complexing lignands (e.g. SO_4, NO_3, PO_4, etc.). Groundwater pH also plays a role in the solubility of uranium.

The pH of groundwater in the area stayed closed to neutral despite the presence of SO_4 in high concentration, this shows that there is a buffering agent that is keeping the pH higher. In this case, the buffering agent is thought to be bicarbonate and H^+ that is released during the oxidation of sulphide and iron reactions. The pH and Eh of water affect U-speciation as well as adsorption and precipitation rates.

Due to the mineralization of uranium and uranium mining in the area, some boreholes have high uranium concentration. The highest concentration measured was detected in borehole JL07/09 (146 µg/l), JL07/19 (104 µg/l), JL08/11 (88 µg/l) and JL 08/23 (77 µg/l) respectively.

The uranium in the groundwater is above the drinking water guidelines proposed by WHO (2006) of 0.015 mg/l (15 µg/l). This guideline addresses only the chemical aspects of uranium toxicity. WHO 2006, also suggested a Tolerable Daily Intake (TDI) of 0.6 µg/kg of body weight per day, which assumes a 60 kg adult consumes 2 litres of drinking water per day. The South African Water Quality Guidelines do not have a specific guideline for Uranium.

The radioactivity data analysed in both liquid and colloids (from filters) show that uranium in the groundwater is present in solution and not adsorbed to colloids. This means that uranium is not transported as mineral particles or colloids but it is dissolved, possibly formed complexes with other complexing agents. This outlined the complex geochemical evolution and processes that takes place in the area.

Higher uranium concentrations are found in the discharging area (Fig 6.17). A spatial distribution plot of uranium reveal that the groundwater in catchment F30A

has low uranium concentrations (mostly, less than 15.1 µg/l), while high uranium concentration is evident in catchment D82B of up to 146 µg/l (Fig 6.17).

A spatial distribution of uranium was plotted in the diagram below to show the distribution of uranium in the groundwater of the area and to compare the concentrations between the two catchments (Fig 6.17).

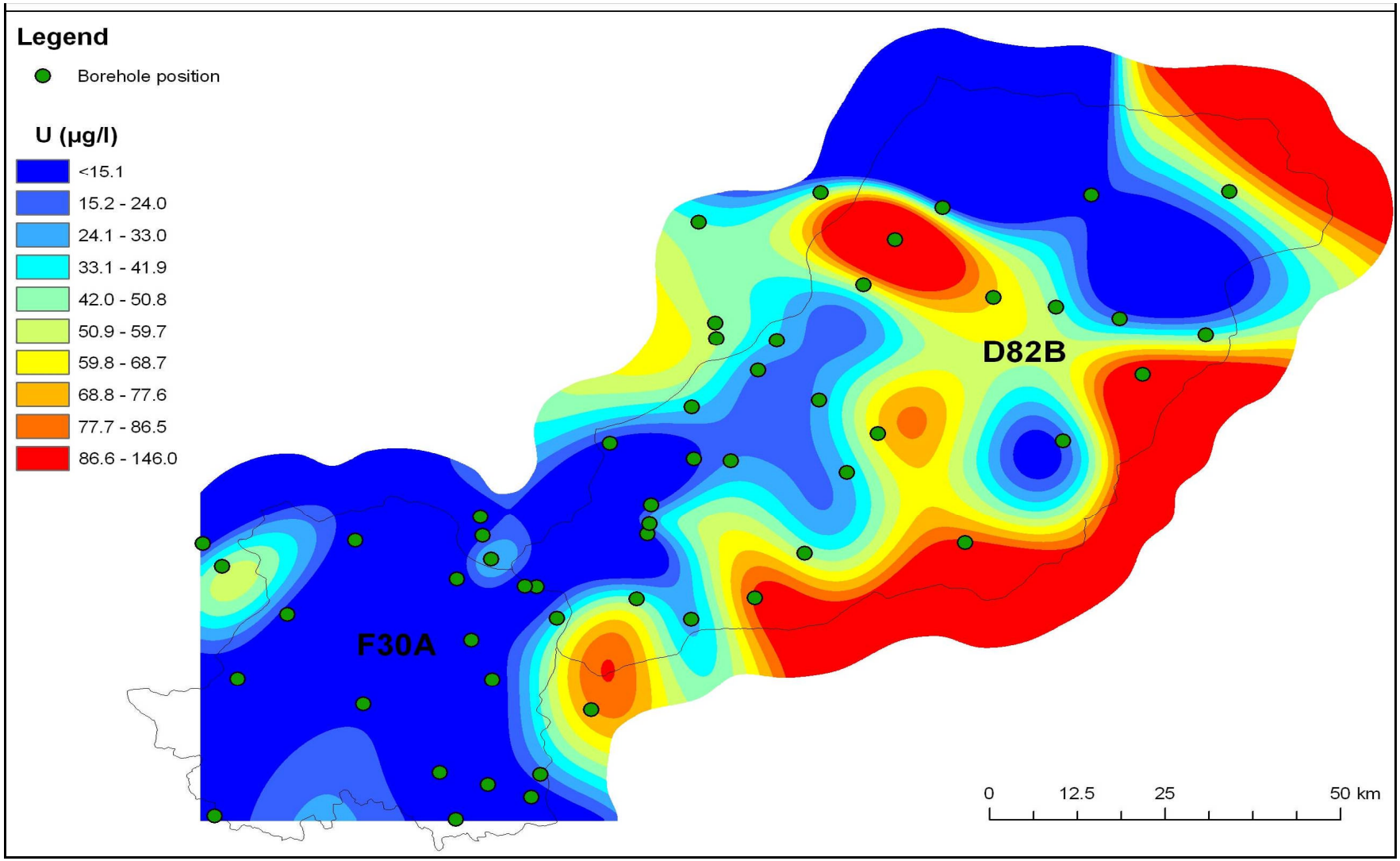


Fig. 6.17: Spatial distribution of uranium (U).

7. CONCLUSIONS

Groundwater quality in the two quaternary catchments (F30A and D82B) aquifers is variable with groundwater ranging from fresh to very saline water. Salty water occurs locally in these aquifers, which is mostly the result of natural processes. The geochemical composition of groundwater on either catchment is generally similar.

The process that might cause salinity in the groundwater is ion exchange, evaporation and the long residence time of the water, which promote rock-water interaction. The geochemistry of the water samples in the area indicate that groundwater evolution is taking place and dissolution, ion exchange and mixing processes are the driving processes. These processes are responsible for the diverse water chemistry or water type. The mixing influence is depicted by the linear relationship of most of ions and TDS.

The area, generally, has poor water quality due to geogenic sources of chemical constituents and uranium from the host rock. The range of groundwater compositions in the aquifer suggests varying influences of evaporite dissolution, carbonate or silicate weathering. Sulphate and chloride dominated groundwater compositions are attributable to pyrite oxidation, gypsum and halite dissolution.

The chemical constituents show good correlation with the sampled soils in the area. Therefore, it can be concluded that the high total dissolved solids results from the aquifers. Br^-/Cl^- ratios show that the salinity in the area results from sea water mixing, halite dissolution and atmospheric deposition/sea aerosol spray. Under excessive evaporative regimes, the groundwater in the area is heading towards hypersaline water.

The stable isotope analyses indicate that the samples have undergone fractionation due to evaporation before infiltration. Groundwater samples (Group

1) from catchment D82B plots away from the GMWL showing isotope enrichment due to excessive evaporation. An enrichment of oxygen isotope with increasing SO_4 and NO_3 was noticed which may be caused by the oxygen from the two constituencies. The isotopes clearly showed that there are two groundwater flow types that characterize the area. There is a deep and shallow groundwater flow system. The isotope also revealed that there is a mixing process of groundwater in the aquifer (deep circulating and shallow groundwater). The groundwater data plotted below the WLMWL, the shift may be explained by evaporation prior to or during infiltration (Catchment F30A).

No direct infiltration observed from the isotope data, therefore, it is concluded that recharge in the area results from cross flow from the neighboring formations or catchments. The age of the groundwater calculated from average tritium of the local rainfall of 28.32, ranges from 87.01 to 174.02 years. The groundwater becomes mineralized along the flow path within the fractured basement aquifer, mainly through dissolution, ion exchange and mixing processes.

The Gross Alpha/Beta-activity of residual liquids show that uranium is found in lower quantities in the recharging catchment (F30A) which is within the WHO drinking water standard than the discharging catchment (D82B), which is found in high quantities, more than the WHO drinking water standard.

The presence of uranium in high concentration in the groundwater of the area may be related to the oxidizing nature of the groundwater and the presents of carbonates and other reactants that keep uranium in solution (nitrate, fluoride, sulphate, phosphate, etc.).

8. RECOMMENDATIONS

In rural areas drinking waters are collected exclusively from wells and natural springs. More work needs to be done in South Africa in monitoring drinking waters and/or groundwater used by villagers in order to assess the health impact of radioactivity pollution and heavy metals pollution (whether through anthropogenic activities or geogenic sources).

Knowledge of the radionuclides (Uranium) contamination and behaviour (source-pathway-receptor) will assist in finding methods and techniques for radionuclides remediation. Further study on the health impact of the radionuclides and chromate on the population exposed to radionuclides in groundwater-dependent communities, is needed.

Further studies on the isotopes of sulphate are necessary to determine the source(s) of sulphate in the groundwater of the area. Chromate was detected in high concentrations. This raise a health concern as chromate (hexavalent) is one of the toxic elements (carcinogenic element).

Sulphate isotopes need to be analysed in order to determine its source(s).

9. REFERENCES

Adams, S., Titus, R., Pietersen, K., Tredoux, G. and Harris, C. 2001. Hydrochemical characteristics of aquifers near Sutherland in the Western Karoo, South Africa. Journal of Hydrology, Vol. 241, pp 91–103.

Agenbacht, A.L.D. 2007. The geology of the Pofadder area. Explanation Sheet 2918, 1:250 000.

Agenbacht, A.L.D. 2007. Geological series, 2918 Pofadder. 1:250 000. Council for Geoscience, Pretoria.

Ainslie, L.C. 2003. Influence of waste disposal operations on the radiological environment at Vaalputs. South African Nuclear Energy Coperation (NECSA), Document number: GEA-1638.

Albat, H.M. 1984. The Proterozoic granulite facies terrane around Kliprand, Namaqualand Metamorphic Complex. Ph.D. Thesis, Dept. of Geology, University of Cape Town, South Africa. In: Chamber of Mines Precambrian Research Unit. Bulletin 33.

Allard, B. 1995, Groundwater. In “Trace elements in natural waters: Ann Arbor “. Brit, S. and Eiliv, S. (Editors), Michigan, CRC Press, pp 302.

Allard, T., Ildefonse, P., Beaucaire, C. and Calas, G. 1999. Structural chemistry of Uranium associated with Si, Al, Fe gels in a granitic uranium mine. Chemical Geology, Vol. 158, Issue 81, pp 103.

Allen, N.M. and Suchy M. 2001. Geochemical evolution of groundwater on Saturna Island, British Colombia. Canadian Journal of Earth Science. Vol. 38, pp 1059–1080.

Andreoli, M.A.G., Smith, C.B., Watkeys, M., Moore, J.M., Ashwal, L.D. and Hart, R.J. 2004. The geology of the Steenkampskraal monazite deposit, South Africa: implications for REE-Th-Cu mineralization in charnockite-granulite terranes. Economic Geology, Vol. 89, No. 5, pp 994–1016.

Andreoli, M.A.G., Hart, R.J., Ashwal, L.D. and Coetzee, H. 2006. Correlation between U, Th content and metamorphic grade in the western Namaqualand belt, South Africa, with implications for radioactive heating of the crust. Journal of Petrology. pp 1–24.

Bajjali, W., Clark, I.D. and Fritz, P. 1997. The artesian thermal groundwaters of northern Jordan: Insights into their recharge history and age. Journal of Hydrology, Vol.192, Issues 14, pp 355–382.

Boronina, A., Balderer, W., Renard, P. and Stichler, W. 2005. Study of stable isotopes in the Kouris catchment (Cyprus) for the description of the regional groundwater flow. Journal of Hydrology, Vol. 308, pp 214–226.

Bourg, A.C.M. 1988. Metals in aquatic and terrestrial systems: Sorption, speciation and mobilisation, In: Salomons, W and Forstner, U, eds., Chemistry and biology of solid waste dredged material and mine tailings. Springer–Verlag: Berlin, Germay.

Brickler, O.P., and Jones, B.F. 1995. Main facts affecting the compositions of natural waters, in: Salbu, Brit, and Steinnes, Eiliv, eds., Trace elements in natural waters: Ann Arbor, Michigan, CRC Press, pp 302

Bucur, C., Olteanu, M. and Pavelescu, M. 2006. Radionuclides diffusion in geological media. Romania Journal of Physics, Vol. 51, No. 3–4, pp 469–478.

Burns, P.C. and Finch, R. (Editors). 1999. Uranium: Mineralogy, Geochemistry and the Environment. Reviews in Mineralogy. Volume 38. Mineralogical Society of America, Washington, D.C.

Chilton, P.J. and Foster, S.S.D. 1995. Hydrogeological characterisation and water-supply potential of basement aquifers in Tropical Africa. Hydrologeology Journal, Vol. 3, No. 1, pp 36–49.

Clark, I and Fritz, P. 1997. Environmental isotopes in hydrogeology. Lewis Publishers. New York, pp 328

Cole, D. I. 1998. Uranium. In: “The Mineral Resources of South Africa”. Wilson, M.G.C. and Anhaeusser, C.R. (Editors), Handbook, Council for Geoscience, Vol. 16, pp 642-658.

Conrad, J. and Adams, S. 2003. GIS based assessment of groundwater recharge in the fractured rocks of Namaqualand, South Africa. In “Groundwater in fractured rocks”. Krásný, J. and Sharp, J.M. (Editors). International Association of Hydrogeologists Selected Papers. Taylor and Francis, pp 203–217.

Craig, H. 1961. Isotopic variations in meteoric waters. Science, 133, pp 1702–1703.

Crançon, P. and van der Lee, J. 2003. Speciation and mobility of uranium (VI) in humic-containing soils. Radiochimica Acta, Vol. 91, pp 673–679.

Currell, M.J., Cartwright, I., Bradley, D.C. and Han, D. 2010. Recharge history and controls on groundwater quality in the Yuncheng Basin North China. Journal of Hydrology, Vol. 385, pp 216–229.

DWAF (Department of Water Affairs and Forestry). 1996. South African Water Quality Guidelines, Domestic Use, 2nd edition, Vol.1, Issue 1, pp 197.

DWAF (Department of Water Affairs and Forestry). 2002. Lower Orange Water Management Area: Water resources situation assessment. Compiled by V3 Consulting Engineers, assisted by Water Resource Planning and Conservation. South Africa, Report number 14000/00/0101.

DWAF (Department of Water Affairs and Forestry). 2003. Lower Orange Water Management Area: Overview of water resources availability and utilisation. South Africa, Report number P WMA 14000/00/0203.

Edmunds, W.M., Ma, J., Aeschbach-Hertig, W., Kipfer, R. and Darbyshire, D.P.F. 2006. Groundwater recharge history and hydrogeochemical evolution in the Minqin Basin, North West China. Applied Geochemistry, Vol. 21, pp. 2148–2170.

EPA (U.S. Environmental Protection Agency). 1999a. Understanding variation in partition coefficient, kd, values: Volume II, Review of geochemistry and available kd values for cadmium, cesium, chromiun, lead, plutonium, radon, strontium, thorium, tritium (^{3}H), and uranium. EPA 402-R-99-004B, prepared for the U.S. environmental Protection Agency, Washington, D.C. by Pacific Northwest National Laboratory, Richard, Washington.

EPA (U.S. Environmental Protection Agency). 1999b. Understanding variation in partition coefficient, kd, values: Volume II. Review of geochemistry and available kd values for cadmium, cesium, chromium, lead, plutonium, radon, strontium, thorium, tritium (^{3}H), and uranium. EPA 402-R-99-004B, prepared for the U.S. Environmental Protection Agency,

Washington, D.C. by Pacific Northwest National Laboratory, Richland, Washington.

Frick, C. 1986. The Behaviour of uranium, thorium and tin during leaching from a coarse grained porphyritic granite in arid environment. Journal of Geochemical Exploration, Vol. 25, Issue 3, pp 261–282.

Gastmans, D., Chang, H.K. and Hutcheon, I. 2010. Groundwater geochemical evolution in the northern portion of the Guarani Aquifer System (Brazil) and its relationship to diagenetic features. Applied Geochemistry, Vol. 25, Issue 1, pp 16-33.

Ghomshei, M.M. and Allen, D.M. 2000. Potential application of oxygen-18 and deuterium in mining effluent and acid rock drainage studies. Environmental Geology Journal, Vol. 39, No. 7, pp 767–773.

Giammar, D. 2001. Geochemistry of uranium at mineral-water interface: Rates of sorption-desorption and dissolution-precipitation reactions. PhD Thesis (Unpublished), California Institute of Technology, Pasadena, California, pp 277.

Gibbs, R. J. 1970. Mechanisms controlling world water chemistry. Science, Vol. 170, pp 1088–1090.

Gonfiantini, R., Fröhlich, K., Araguás- Araguás, L. and Rozanski, K. 1998. Isotopes in groundwater hydrology. In: Kendall, C. and McDonnell, J.J. (Eds), Isotope tracers in Catchment hydrology. Elsevier Science B.V., Amsterdam, pp 203–246.

Grainger, L. 1958. Uranium and Thorium. London, George Newnes Ltd.

Grenthe, I., Fuger, J., Konings, R.J.M., Lemire, R.J., Muller, A.B., Nguyen-Trung, C. and Wanner, H. 1992. Chemical thermodynamics 1: Chemical thermodynamics of uranium. North-Holland, Elsevier Science Publishing Company, Inc., New York, New York.

Grenthe, I., Puigdomenech, I., Sandino, M.C.A. and Rand, M.H. 1995. Appendix D–chemical thermodynamics of uranium. In “Chemical Thermodynamics 2: Chemical Thermodynamics of Americium”. North-Holland, Elsevier Science Publishing Company, Inc., New York. pp 347–374.

Gueniot, B., Munier-Lamy, C., and Berthelin, J. 1988. Geochemical behaviour of uranium in soils, part II. Distribution of uranium in hydromorphic soils and soil sequences. Applications for surficial prospecting. Journal of Geochemical Exploration, Vol. 31, Issue 1, pp 39–55.

Gustafson G. and Krásný J. 1994. Crystalline rock aquifers: Their occurrences, use and importance. Applied Hydrogeology, Vol. 2, Issue 2, pp 64–75.

Guthrie, V.A., and Kleeman, J.D. 1986. Changing uranium distribution during weathering of granite. Chemical Geology, Vol. 54, Issues 1–2, pp 113–126.

Hasan, M.A., Bhattacharya, P., Sracek, O., Ahmed, K.M., von Brömssen, M. and Jacks, G. 2009. Geological controls on groundwater chemistry and arsenic mobilization: Hydrogeochemical study along an E–W transect in the Meghna, Bangladesh. Journal of Hydrology, Vol. 378, pp 105–118.

Hem, J.D. 1989. Study and Interpretation of the chemical characteristics of natural water [3rd Ed]: U.S. Geological Survey Water Supply Paper 2254, pp 263.

Hsi, C-K.D., and Langmuir, D. 1985. Adsorption of uranyl onto ferric oxyhydroxides: Application of the surface complexation site-binding model. Geochimica et Cosmochimica Acta, Vol. 49, pp 1931–1941.

Jerden, J.L. and Sinha, A.K. 2003. Phosphate based immobilization of uranium in an oxidizing bedrock aquifer. Applied Geochemistry, Vol. 18, No. 6, pp 823–843.

Jordana, S. and Batista, E. 2004. Natural groundwater quality and health. Geologica Acta: An International Earth Science Journal, Vol. 2, Issue 2, pp 175–188.

Kalisperi, D., Parisi, S., Collins, P., Kershaw, S., Lydakis-Samantiris, N., Mongelli, G. Paternoster, M., Sdao, F. and Soupios, P. 2010. Groundwater resource quality in the North-central coastal aquifer of Crete, Greece, from hydrochemical and isotopic analysis. Proceeding GIRED3D Conference, AGADIR 24-26 March, Morocco. Pp 1–8.

Katz, B.G., Catches, J.S., Bullen, T.D. and Michel, R.L. 1998. Changes in the isotopic and chemical composition of ground water resulting from a recharge pulse from a sinking stream. Journal of Hydrology Vol. 211, pp. 178–207.

Křepelová, A., Sachs, S. and Bernhard, G. 2006. Uranium(VI) sorption onto kaolinite in the presence and absence of humic acid. Radiochimica Acta, Vol. 94, pp 825–833.

Krupka, K.M. and Serne, R.J. 2002. Geochemical factors affecting the behaviour of antimony, cobalt, europium, technetium, and uranium in vadose sediments. A report prepared for CH2M HILL Hanford Group, Inc., and

the U.S. Department of Energy under contract DE-AC06-76RL01830, USA.

Langmuir, D.1978. “Uranium solution-mineral equilibria at low temperatures with applications to sedimentary ore deposits.” Geochimica et Cosmochimica Acta, Vol. 42, pp 547–569.

Langmuir D. 1997. Aqueous environmental geochemistry. Prentice Hall, Upper Saddle River, New Jersey.

Lekhov, A.V. and Shvarov, Y.V. 2002. On the rate of radionuclide migration in groundwater. Water Resources, Vol. 29, No. 3, pp 244–251.

Lenhart, J.J., Cabaniss, S.E., MacCarthy, P. and Honeyman, B.D. 2000. Uranium (VI) complexaion with citric, humic and fluvic acids. Radiochimicha Acta, Vol. 88, pp 345–353.

Lloyd, J.W. and Heathcote, J.A. 1985. Natural inorganic hydrochemistry in relation to groundwater. An introduction. Claredon Press, Oxford.

Mazor, E. 2004. Chemical and isotopic groundwater hydrology: 3rd Edtion, Marcel Dekker, Inc. New York USA, pp 451.

Meinrath, G. 1998. Chemometric analysis: Uranium (VI) hydrolysis by UV-Vis spectroscopy. Journal of Alloys and Compounds, Vols. 275–277, pp 777–781.

Meinrath, G., Volke, P., Dudel, E.G. and Merckel, B.J. 1999. Determination and interpretation of environmental water samples contaminated by uranium mining activities. Frensenius Journal of Analytical Chemistry. Springler-Verlag. Vol. 364, pp 191–202.

Milton, G.M. and Brown, R.M. 1987. Adsorption of uranium from groundwater by common fracture secondary minerals. Canadian Journal of Earth Sciences, Vol. 24, pp 1321–1351.

Mokrik, R., Savitskaja, L. and Savitski, L. 2005. Aqueous geochemistry of the Cambian-Vendian aquifer system in the Tallinn intake, northern Estonia. Geologija, No. 51, pp 50–56. Available on line: http://www.ebiblioteka.lt/resursai/LMA/Geologija/0503_08_Geol_050_056.pdf

Mook, W.G. 2006. Introduction of isotope hydrology and radioactive isotopes of hydrogen, oxygen and carbon. Taylor & Francis, pp. 226.

Motalane, M.P. and Strydom, C.A. 2004. Potential groundwater contamination by fluoride from two South African phosphogypsums. Water SA, Vol. 30, No. 4, pp. 465–468. Available online: http://www.wrc.org.za

Mukhopadhyay, B., Sundquist, J. and Schmitz, R. 2007. Removal of Cr(VI) from Cr-contaminated groundwater through electrochemical addition of Fe(II). Journal of Environmental Management, Vol. 82, Issue 1, pp. 66–76.

Ncube, E.J. and Schutte, C.F. 2005. The occurrence of fluoride in South African groundwater: A water quality and health problem. Water SA, Vol. 31, No. 1, pp. 35–40. Available online: http://www.wrc.org.za

Nencetti, A., Tassi, F., Vaselli, O., Macías, J.L., Magro, G., Capaccioni, B., Minissale, A. and Mora, J.C. 2005. Chemical and isotopic study of thermal springs and gas discharges from Sierra de Chiapas, Mexico. Geofisica International, Vol. 44, No. 1, pp 39–48. Available online:

Nordstrom, D.K., McNutt, R.H., Puigdomènech, I., Smellie, J.A.T. and Wolf, M. 1992. Ground Water chemistry and geochemical modelling of water-rock

interactions at the Osamu Utsumi mine and Morro do Ferro analogue study sites, Poços de Caldas. Minas Gerais, Brazil. Journal of Geochemical Exploration, Vol. 45, pp 249–287.

Price, R.M., Top, Z., Happell, J.D. and Swart, P.K. 2003. Use of tritium and helium to define groundwater flow conditions in Everglades National Park. Water Resources Research, Vol. 39, No. 9, 1267, doi: 10.1029/2002WR001929.

Portugal, E., Álvarez, J. and Romero, B.I. 2006. Hydrochemical and isotopical tracers in the lacustrine aquifer of the Cerro Prieto area, Baja Califonia, México. Journal of Geochemical Exploration, Vol.88, pp 139–143.

Rabemanana, V., Violette, S., de Marsily, G., Robain, H., Deffontaines, B., Andrieux, P., Bensimon, M. and Parriaux, A. 2005. Origin of the high variability of water mineral content in the bedrock aquifer of Souther Madagascar. Journal of Hydrology, Vol. 301, pp 143–156.

Raith, J.G., Cornell, D.H., Frimmel, H.E., and De Beer, C.H., 2003. New insight into the geology of the Namaqua TectonicProvince, South Africa, from Ion Probe dating of ditrital and metamorphic zircon. The Journal of Geology, Vol. III, No. 3, pp 347–366.

Read D, Lawless, T.A., Sims, R.J. and Butter, K.R. 1993. “Uranium migration through intact sandstone cores.” Journal of Contaminant Hydrology, Vol.13, pp 277–289.

Rebouças, A.D.C., 1993. Groundwater development in Precambrian shield of South America and West side Africa. . IAH Congress. Hydrogeology of Hard Rocks, Banks S. B. and Banks D. (eds). ISBN 82-7385-093-5.

Reynolds, B.C., Wasserburg, G.J. and Baskaran, M. 2003. The transport of U- and Th-series nuclides in sandy confined aquifers. Geochimica et Cosmochimica Acta, Vol, 67, No. 11, pp 1955–1972.

Robertson, D.E., Cataldo, D.A., Napier, B.A., Krupka, K.M. and Sasser, L.B. 2003. Literature review and assessment of plant and animal transfer factors used in performance assessment modelling. Prepared for division of systems analysis and regulatory effectiveness; Office of Nuclear Regulatory research; US Nuclear Regulatory Commission; Washington, DC 20555 – 0001; and NRC Job Code Y6469.

Salameh, E. 2004. Using environmental isotopes in the study of the recharge-discharge mechanisms of the Yarmouk catchment area in Jordan. Hydrogeology Journal Vol. 12, No. 4, pp 451– 463.

Sanexa, V.K and Ahmed, S. 2001. Dissolution of fluoride in groundwater: A Water–rock Interaction Study. Environmental Geology. Vol. 40, No. 9, pp 1084–1087.

Sanexa, V.K and Ahmed, S. 2003. Inferring the chemical parameters for the dissolution of fluid in groundwater. Environmental Geology. Vol. 43, No. 6, pp 731–736.

Senior, L.A., 1998. Radon-222 in the ground water of Chester County, Pennsylvania. Water-Resources Investigations Report 98-4169. U.S. Department of the Interior.U.S. Geological Survey.

Siegel, M. D. and Bryan, C. R. 2004. Environmental geochemistry of radioactive contamination. Treatise on geochemistry, Environmental Geochemistry, Vol. 9, pp 205 – 250.

Sayko, S.P., Daniels, W.F., Passmore, R.J. 2004. Using major ions data to support the demonstration of hydraulic containment in a fractured bedrock aquifer. (Presentation for the 2004 USEPA Fractured Rock Conference, Portland, Maine). Unpublished.
From:http://www.cluin.org/products/siteprof/2004fracrockconf/cdr_pdfs/indexed/group1/100.pdf

Tankard, A. J., Jackson, M. P., Eriksson, K. A., Hobday, D. K., Hunter, D. R. and Minter, W. E. L. 1982. Crustal Evolution of South Africa: 3.8 Billion Years of Earth History. Springer-Verlag, New York.

Tantawi, M.A., El-Sated, E. and Awad, M.A. 1998. Hydrochemical and stable isotope study of groundwater in the Saint Catherine-Wadi Feiran area, south Sinai, Egypt. Journal of African Earth Sciences. Vol. 26, No. 2, pp 227–284

Tieh, T.T., Ledger, E.B. and Rowe, M.W. 1980. Release of uranium from granitic rocks during in situ weathering and initial erosion (Central Texas). Chemical Geology, Vol. 29, pp 227 – 248.

Titus, R. 2003. Personal Communication.

Titus, R., Xu, Y., Adams, S. and Beekman, H. 2009. A tectonic and geomorphic framework for the development of basement aquifers of Namaqualand – A Review. In “The Basement Aquifers of Southern Africa”. Titus R., Beekman R., Adams, S. and Strachan, L. (Editors). WRC Report TT 428/09. ISBN 978-1-77005-898-9.

Toens, P.D., Stadler, W. and Wullschleger, N.J. 1998. The association of groundwater chemistry and geology with atypical lymphocytes (as a

biological indicator) in the Pofadder Area, North Western Cape, South Africa. WRC Report 839/1/98, Water Research Commission, Pretoria.

Trabelsi, R., Zairi, M. and Dhhia, H.B. 2007. Groundwater sainization of the superficial aquifer, Tunisia. Hydrogeology Journal, Vol. 15, pp 1341–1355.

Tricca, A., Wasserburg, G.J., Porcelli, D., Baskaran, M. 2001. The transport of U- and Th-series nuclides in a sandy unconfined aquifer. Geochimica et Cosmochimica Acta, Vol. 65, pp 1187–1210.

Visser, D. J. L. (Ed). 1989. Explanation of the 1:1.000.000 geological map, fourth edition, 1984. Department of Mineral and Energy Affairs, Government Printer. ISBN 0-621-12516-4.

Vorster, C.J. and Cole, D.I. 2007. Uranium deposits – South Africa, Lesotho and Swaziland. Council for Geoscience. Available on line: http://www.geoscience.org.za

Waite, T.D., Davis, J.A., Payne, T.E., Waychunas, G.A. and Xu, N. 1994. “Uranium (VI) adsorption to ferrihydrite: Application of a surface complexation model.” Geochimica et Cosmochimica Acta, Vol. 58, No. 24, pp 5465-5478.

Weaver, J.M.C., Cavè, L. and Talma, A.S. 2007. Groundwater sampling. Second edition. Water Research Commission Report, TT 303/07.

WHO (World Health Organization). 2006. Guidelines for drinking-water quality. Third edition. Volume 1, Recommendations. Geneva, ISBN 92 4 154696 4

Wright, E.P. and Burgess, W.G. 1992. The hydrogeology of crystalline basement aquifers in Africa. Geological Society Special Bulletin No. 66. The Geological Society, London.

Yeliseyeva, O.P., and Omel'Yanenko, B.O. 1988. Behaviour of uranium during weathering-crust formation at the Alek Seyevka Kaolinite Deposit, North Kazakhstan. Geochemistry International, Vol. 25, No. 1–4, pp 83–97.

Yuan, F. and Miyamoto, S. 2008. Characteristics of oxygen-18 and deuterium composition in waters from the Pecos River in American Southwest. Chemical Geology, Vol. 255, Issues 1-2, pp.220–230.

Zapecza, O.S., and Szabo, Z. 1986. Natural radioactivity in ground water- a review. U.S. Geological Survey National Water Summary 1986, Ground-Water Quality: Hydrologic Conditions and Events, U. S. Geological Survey Water Supply Paper 2325. pp. 50–57.

ANNEXTURE A